1957

The rare earth-carbon systems

Karl Albert Gschneidner Jr.
Iowa State College

THE RARE EARTH-CARBON SYSTEMS

by

Karl Albert Gschneidner, Jr.

A Dissertation Submitted to the
Graduate Faculty in Partial Fulfillment of
The Requirements for the Degree of
DOCTOR OF PHILOSOPHY

Major Subject: Physical Chemistry

Approved:

Signature was redacted for privacy.

Signature was redacted for privacy.
In Charge of Major Work

Signature was redacted for privacy.
Head of Major Department

Signature was redacted for privacy.
Dean of Graduate College

Iowa State College
1957

TABLE OF CONTENTS

INTRODUCTION

Before the beginning of the nineteenth century the foundations of the present day concepts of the elements were being established. During the first two-thirds of the nineteenth century the discovery and classification of new elements led to some confusion until Mendelejeff and Meyer, independently, established their periodic tables of the known elements. In the next 45 years, the discovery of new elements indicated that the periodic tables of Mendelejeff and Meyer were incomplete. This was especially true concerning the rare-earth elements. The presence of a series of elements similar to yttrium and scandium could not be explained, nor could the exact number of elements in this series be predicted by the atomic theory of that age. Around 1910, the relationship of the rare earths with the other elements was clarified, unveiling the true nature of the periodic classification of the elements. The work of Moseley on the x-ray spectra of the elements and Bohr's theory of atomic structure finally convinced even the most skeptical, that there could only be fourteen rare earths. Furthermore, it finally established their true position in the periodic table. Although all of the rare earths except promethium were discovered before 1910, the real beginning of our understanding of the fundamental nature of the rare earth elements started about this time.

Although this series of elements is called "the rare earths", it is interesting to note that cerium is the twenty-seventh most abundant element (or nineteenth most abundant metal). And for this reason many feel the word "rare" to be a misnomer. But if one considers this series of elements as unique, then the word "rare" is quite appropriate. Other synonyms for this group of metals are "the lanthanides" and "the lanthanons". The lanthanides are generally divided into two groups: the light rare earths, lanthanum to gadolinium and the heavy rare earths, terbium to lutetium. Yttrium, though not a rare earth, is generally included in the latter group for reasons described later.

A complete study of the nature of the rare earths offers an opportunity to add much to the atomic theory of the elements. The lanthanides are a series of elements which in general differ from one another by the number of $4f$ electrons while maintaining the same number of valence electrons, three. This change is used to study the variation of chemical and physical properties and relate them to atomic theory. The change in the number of $4f$ electrons can explain the valence, magnetic susceptibility, the "lanthanide contraction", the decrease in basicity, and the increase of ease of complex formation within this group. Because of the occurrence of the rare earths in the fission products of the actinides used in nuclear reactors, a better understanding

of the chemical and physical properties of the rare earths is quite important. New information on these elements might lead to a quicker and more economical means of removing these contaminants from the fissionable material. Lanthanum is not a true rare earth since it possesses no 4 f electron, but since it does have chemical and physical properties similar to the rare earths, it is therefore considered a member of this series of elements. The change in the number of 4 f electrons as one moves along this series can best be appreciated by examining the electronic configuration of the trivalent ionic lanthanon species. For this case lanthanum has no 4 f electrons, cerium--one, praseodymium--two, and so forth until the series is completed at lutetium with all fourteen 4 f electrons. This regular change is most apparent in the ionic radii of these elements (Table 1). The radii of these ions decrease in a normal fashion from lanthanum (1.04 Å) to lutetium (0.84 Å); this phenomenon is known as the lanthanide contraction. Other valence states of the lanthanons do indeed exist. The ions Ce^{+4}, Pr^{+4}, Sm^{+2}, Eu^{+2}, Tb^{+4}, Tm^{+2}, and Yb^{+2} have been shown to exist in some compounds. From elementary quantum mechanics the observation that filled and half-filled quantum levels are more stable than partially-filled ones, easily explains the existence of Ce^{+4}, Eu^{+2}, Tb^{+4}, and Yb^{+2}. No such simple explanation is known for the Pr^{+4}, Sm^{+2}, and Tm^{+2} states.

Table 1. The ionic and metallic radii and the melting and boiling points of the lanthanides

Rare earth	Atomic number	Ionic radii[a] +2 (Å)	Ionic radii[a] +3 (Å)	Ionic radii[a] +4 (Å)	Metallic radii[b] (Å)	Melting point[c] (°C)	Boiling point[c] (°C)
yttrium	39		0.93		1.797	1552	3200
lanthanum	57		1.04		1.871	920	4250
cerium	58		1.02	0.92	1.818	804	3330
praseodymium	59		1.00	0.90	1.824	935	3180
neodymium	60		0.99		1.818	1024	3030
promethium	61		(0.98)		(1.81)		
samarium	62	1.11	0.97		1.798[d]	1052	1650
europium	63	1.09	0.96		2.084	826[e]	1490[e]
gadolinium	64		0.94		1.795	1350	2700
terbium	65		0.92	0.84	1.773	1360	2500
dysprosium	66		0.91		1.770	1375-1425	2330
holmium	67		0.89		1.761	1475-1525	2400
erbium	68		0.87		1.748	1500-1550	2300
thulium	69		0.86		1.743	1550-1650	1730[f]

[a] Fried and Zachariasen (1956)

[b] Pauling (1947), CN = 12

[c] Spedding et al. (1957)

[d] Calculated from data by Daane et al. (1954)

[e] Hanak (1957)

[f] Barton (1956)

Table 1. (Continued)

Rare earth	Atomic number	Ionic radii[a] +2 (Å)	+3 (Å)	+4 (Å)	Metallic radii[b] (Å)	Melting point[c] (°C)	Boiling point[c] (°C)
ytterbium	70	0.93	0.85		1.933	824	1500
lutetium	71		0.84		1.738	1650-1750	3200

Unlike the trivalent rare earth ions, the electronic structure of these metals cannot be obtained directly from spectroscopic data. Examination of some of the physical properties of the metals, metallic radii, melting and boiling points (Table 1) and magnetic properties may help in determining the electronic configuration of the metallic state. The general trend in the observed values of the radii and boiling and melting points indicate that the rare earth metals behave in an almost predictable manner, except for europium and ytterbium. This indicates that the electronic configurations of the metallic atoms should have the same $4f$ electron distribution as the trivalent ions except for europium and ytterbium. Magnetic data (Spedding et al., 1957) observed in a study of these metals support this view. The abnormally low melting and boiling points of europium and ytterbium, and the fact that the metallic radii of the above two metals lie on a straight line with barium when plotted against the atomic number (Figure 1), indicate that they are divalent.

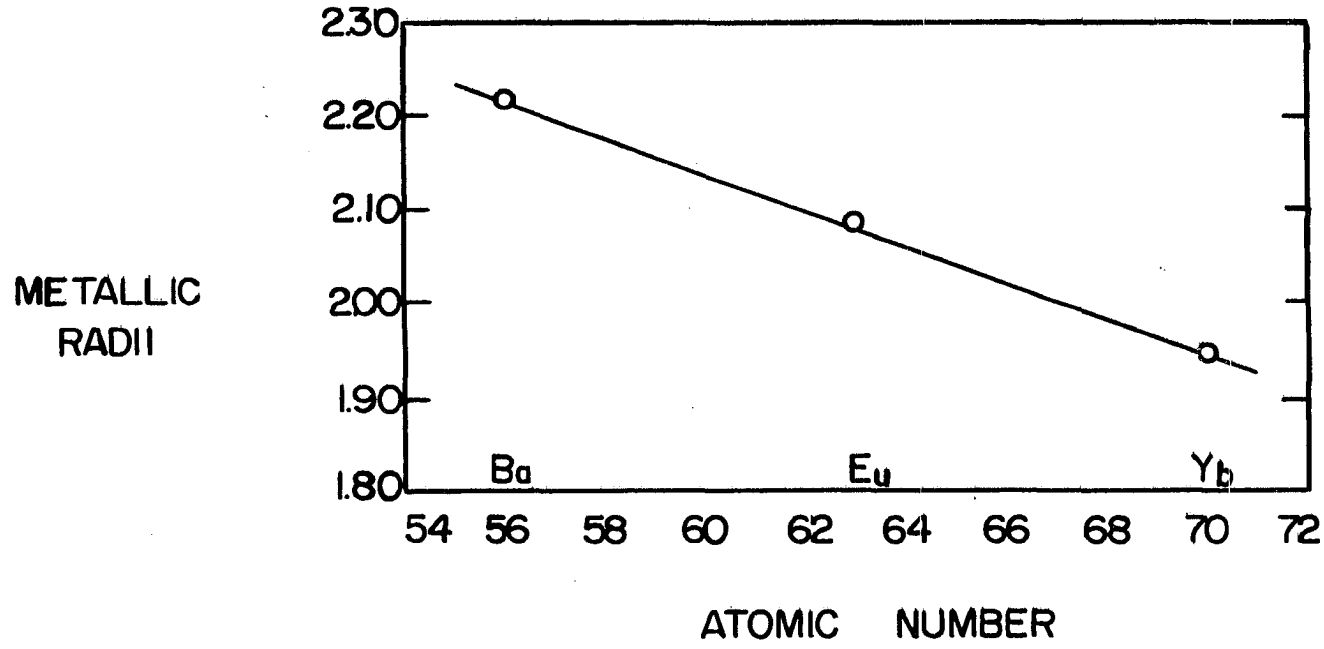

Figure 1. Metallic radii of barium, europium and ytterbium versus atomic number.

From magnetic susceptibility measurements Lock (1957) has shown that ytterbium metal has only 1/260th of the atoms in ^2F 7/2 (trivalent) state. In the case of cerium, the metallic radius is somewhat smaller than would be expected from its neighbors, lanthanum and praseodymium. According to Pauling's (1947) resonating-valence bond theory, the valence electrons should affect bond distances; the greater the interatomic distance, the smaller the number of valence electrons. Therefore, from this and magnetic measurements, Pauling has concluded that the valence of cerium should be 3.2. The quadrivalent state for cerium metal has been attained either by cooling the metal below -188°C or by placing it under 15,000 atmospheres of pressure.

Yttrium, a co-member of the group III A elements, is often studied with the rare earths since its size is such that it falls within the range from gadolinium to holmium. In some compounds the lattice parameter appears to be close to gadolinium, in others near to holmium. This indicates that the yttrium atom (or ion) is being polarized to a different degree than the lanthanons. Most of the chemical and physical properties of this element characterize it as being a typical heavy lanthanide.

A phase of research that will contribute much to the understanding of the rare earth series, is the study of crystal structures of compounds of the lanthanides with other

elements whether ionic or metallic in nature. This field of research was somewhat neglected in the past but since World War II studies in this area have gained much momentum. Studies of the trichlorides, trifluorides, oxychlorides, oxides and nitrides have been reported and these are summarized in Table 2. It is interesting to note that the rare earth nitrides in contrast to the other type compounds cited form a completely isostructural series from lanthanum to lutetium, including yttrium. However, there is one anomaly; the lattice parameter of cerium lies approximately mid-way between those of samarium and europium, which might indicate tetravalence for cerium in this case. The partially completed studies of the borides and oxyfluorides have progressed sufficiently to permit some conclusions to be drawn. The rare earth oxyfluorides crystallize in several forms: cubic, tetragonal and rhombohedral, and several of them are dimorphic (Zachariasen, 1951 and Baenziger et al., 1954). The hexaborides of the rare earths appear to behave similarly to the nitrides (Post et al., 1956 and Bertaut and Blum, 1952). However, slight differences are noted in that the lattice parameter of ytterbium hexaboride appears to be abnormally large and parameter of cerium compound appears normal. This indicates that ytterbium probably exhibits divalence in this compound, while the other lanthanides are trivalent. Di-

Table 2. Review of structure types reported for the rare earth trichlorides, trifluorides, oxychlorides, sesquioxides and nitrides

Lanthanide	RCl_3	RF_3[a]	ROCl[b]	R_2O_3	RN[c]
lanthanum	UCl_3[d]	LaF_3	PbFCl	A[e]; C[f]	NaCl
cerium	↓	↓	↓	A[e]; C[g]	↓ h
praseodymium	↓	↓	↓	A[e]; C[g]	↓ h
neodymium	↓	↓	↓	A[e]; C[f]	↓
samarium	↓	LaF_3;YF_3	↓	B[i]; C[j]	↓
europium	↓	LaF_3;YF_3	↓	C[j]	↓
gadolinium	↓	YF_3	↓	B[k]; C[j]	↓
yttrium	YCl_3[l]	↓	↓	C[j]	↓ m
terbium	YCl_3;$TbCl_3$[l]	↓	↓	↓	↓

[a] Zalkin and Templeton (1953).

[b] Templeton and Dauben (1953).

[c] Klemm and Winkelmann (1956).

[d] Zachariasen (1948).

[e] Zachariasen (1926), the A form has a hexagonal structure.

[f] Lohberg (1935), the C form has body-centered cubic structure.

[g] Bommer (1939).

[h] Iandelli and Botti (1938).

[i] Cromer (1957), the B form has a monoclinic structure.

[j] Pauling and Shapell (1930).

[k] Vickery (1953).

[l] Templeton and Carter (1954).

[m] Smidt (1957).

Table 2. (Continued)

Lanthanide	RCl_3	RF_3[a]	ROCl[b]	R_2O_3	RN[c]
dysprosium	YCl_3;$TbCl_3$[1]	YF_3	PbFCl	C[j]	NaCl
holmium	YCl_3[1]	LaF_3;YF_3	↓	↓	↓
erbium	↓	YF_3	PbFCl;TmOCl	↓	↓
thulium	↓	LaF_3;YF_3	TmOCl	↓	↓
ytterbium	↓	YF_3	↓	↓	↓
lutetium	↓	↓	↓	↓	↓

valence in this type compound is not unusual, since the alkaline earth metals also form isostructural hexaborides.

While working on ionic materials, Goldschmidt (1954) observed that there are three important factors that influenced the relationship between the chemical composition and crystal structure. These are: (1) the ratio of the components, (2) the ratio of the radii of the components and (3) the influence of polarization. Of these three the first is constant and the third is nearly constant for the rare earth elements, and therefore the size effect should be the governing factor in determining which structure will be stable. If the size factor or the radius ratio R_{Ln}/R_x is the determining factor, it must be quite critical since neighboring rare earths differ from one another by about 0.02 Å in their radii. However in most of these series, one or two of the rare earths in the critical region exhibit dimorphism. This

would mean that a difference of 0.06 ± 0.02 Å would be the governing factor in choosing one structure rather than another; which is still quite small, since deviations as large as 0.35 Å [1] have been observed in size dependent type structures. Of course in cases where such a difference is observed, polarization must play quite an important role. Some workers (Zalkin and Templeton, 1953, and Vickery, 1953) have suggested that type structures of light rare earths are isomorphic with the high temperature forms of the heavy lanthanides. This has been verified to some extent by Dennison (1957), who has observed solid state transitions for several of the heavy lanthanon trifluorides, while determining the melting points of the rare earth fluorides. This would seem quite reasonable, because upon heating, expansion of the lattice might cause the radius ratio to change. This could be brought about by a greater increase of the effective radius of the rare earth cation as compared to the smaller increase of effective radius of the anion, thus changing the radius ratio with increasing temperature. When the critical ratio is reached, the material may transform into the struc-

---

[1] The radius ratios of sodium and lithium iodides are 0.44 and 0.28, respectively. And since the ratio for sodium iodide is nearly equal to the lower limit for the sodium chloride type structure (0.414), the value (0.35 Å) is the difference between the ionic radii of sodium and lithium.

ture type of the light lanthanides. Inversely, upon cooling a light rare earth, the compound might undergo a transformation to the structure type of the heavy lanthanon. A complete study of the variation in transition temperatures for a series of rare earth compounds, along with an x-ray study of these compounds above and below the transitions might add much to the knowledge of the size criterion of atoms in compounds possessing the same structure type.

To date no complete study of an alloy system of a non-rare earth metal with each of the lanthanides has been made. The most complete study to date is that of the uranium-lanthanide systems. Haefling (1957) has examined the solubility of all the rare earth metals in uranium and the solubility of uranium in the seven lowest melting rare earths (Table 1). All the rare earths behave similarly, showing liquid immiscibility with low terminal solubility on each side of the diagram. The only significant difference in this series is that the terminal solubilities of the cerium-uranium system are about twice as high as that of the other rare earths. The alloying properties of the first four light rare earths with many other metals have been completely or partially studied. No notable differences have been reported in the phase diagrams between these four rare earths and a given metal. Haefling (1957) in preliminary examinations of the lanthanum-, yttrium-, and neodymium-iron systems has

found some interesting differences; the lanthanum-iron system shows no compound formation and low terminal solid solubility on either side of the equilibrium diagram. Cerium, however, forms two compounds, $CeFe_2$ and $CeFe_5$ (Jepson and Duwez, 1955). The yttrium- and neodymium-iron systems are at least similar to that of cerium, in that compound formation has been observed. A complete study of the rare earth alloy equilibrium diagrams should add much information to the present day concepts of alloying theory and intermediate metallic phases. There are at present some rare earth-metalloid systems nearly completed which should also contribute some information along these lines. The borides have already been mentioned. The rare earth-hydrogen systems have been investigated sufficiently to note that there are some differences among them. The systems of lanthanum through samarium with hydrogen are identical (Holley et al., 1955 and Mulford and Holley, 1955). The gadolinium system is different in that a second hydride is formed GdH_3 (Sturdy and Mulford, 1956); whether the heavy lanthanides form systems similar to gadolinium is not known. The europium and ytterbium dideuterides have been prepared and found to be isostructural with the alkaline earth dihydrides (Korst and Warf, 1956). In conclusion it can be said that unlike the other rare earth metals, europium and ytterbium behave toward hydrogen as divalent metals.

Within the decade immediately following World War II, Spedding and Powell (1954) have shown that the individual rare earths of very high purity (99.9%) could be produced in kilogram quantities by ion exchange techniques. Also, within this period, new methods were developed for producing high quality rare earth metals in large quantities from the oxides (Spedding and Daane, 1954). With the increasing availability of these metals a study of the rare earth carbon systems was undertaken. The major impurities in these metals are oxygen (100-2000 ppm) and carbon (50-500 ppm). An investigation of a rare earth-carbon system could explain what effect carbon has on the physical, mechanical and chemical properties of this rare earth metal. Secondly, the addition of carbon might be a feasible method for reducing the oxygen content in the metal without adversely affecting the properties of the pure metal. Although some of the lanthanon dicarbides and two lower cerium carbides have been reported, a study of these phase diagrams might reveal the existence of new crystallographic species.

Because of the availability and low melting points of cerium and lanthanum, these metals are the logical elements for the study of a complete phase diagram. Lanthanum was chosen rather than cerium, because lanthanum should be more typically a rare earth than cerium from the stand-point of their valences. Secondly, cerium is much more difficult to

prepare for microscopic examination because of its tendency to stain and tarnish when being etched.

HISTORICAL

The first attempt to prepare a rare earth carbide was reported by Mosander (1827) who obtained a black powder by the decomposition of cerium oxalate in the absence of air. The inertness of this material to acids indicates that it was not cerium carbide. Similarly Delafontaine (1865) claimed to have prepared the carbide by decomposition of various organic salts, but likewise it is doubtful that he prepared the carbide. Bühring (1875) repeated the experiments of Mosander and Delafontaine and obtained only a mixture of carbon, and ceric and cerous oxides. Sterba (1904) concluded as the result of a critical study of this method of preparing the carbides, that the decomposition of organic salts could not lead to the formation of definite carbides.

Pettersson (1895) was apparently the first to prepare a rare earth carbide. He prepared the dicarbide of both yttrium and lanthanum, by heating the respective oxides with carbon in an electric furnace, and showed that their formulas corresponded to RC_2. These carbides were described as crystalline, brittle and yellow in color with densities of 4.186 and 4.716 gm/cm^3. They were reported to react with water with the evolution of hydrogen and hydrocarbons and the formation of the hydrated oxide. At approximately the same time, Moisson prepared lanthanum and other rare earth dicarbides using the same method as Pettersson. He studied the

dicarbides of cerium (Moisson, 1896a), lanthanum (Moisson, 1896b, c, d), praseodymium, neodymium (Moisson, 1900a) and samarium (Moisson, 1900b, 1901). Moisson made a complete study of the hydrolytic properties of these compounds, the results of which are summarized below. At room temperature the amount of acetylenic hydrocarbons liberated when the dicarbide reacted with water at room temperature varied between a maximum of 75 per cent for cerium and a minimum of 66 per cent for neodymium. The amount of ethylenic homologs and saturated hydrocarbons liberated varied from 2 to 8 per cent and 20 to 30 per cent, respectively for these dicarbides. He found that the percentage of acetylenic compounds liberated varied inversely with the temperature at which hydrolysis took place. Moisson also reported that nitric acid yields a larger amount of acetylenic homologs than water, while hydrochloric acid showed a decrease as compared to water. In 1902, Muthmann et al. (1902) in an attempt to prepare cerium metal by reacting equimolar amounts of cerium dioxide and cerium dicarbide obtained a red brown mixture still containing carbon and partially soluble in hydrochloric acid. From the gas evolved when the mixture was treated with hydrochloric acid, they believed they might have prepared a lower carbide. In a further investigation of cerium dicarbide, Sterba (1902) while characterizing some of the chemical properties of this compound found that it reacts with fluorine

and chlorine gas at 150°C with incandescence yielding the corresponding cerium halide. Hydrogen sulfide and sulfur both yield cerium sulfide.

Since this seven year period, 1895 to 1902, very little has been reported on the preparation or properties of these carbides. Although several researchers have studied the hydrolytic properties of these carbides, the results are quite varied, especially with regard to the amount of hydrogen liberated (0 to 25 per cent). It is interesting to point out that Damiens (1918) showed that the amount of acetylene liberated is increased considerably (from 68 to 94 per cent) when a solution of hydrochloric acid and ferric chloride is used to attack the dicarbide. At the same time the hydrogen content is reduced from 13 to 2 per cent. This seems to indicate that acetylene is initially formed along with free hydrogen, and that the other hydrocarbons are formed by a subsequent reaction of free hydrogen and acetylene. Mott (1918), reporting on the volatilities of refractory materials, listed the boiling point of yttrium dicarbide as 4600°C. von Stackelberg's (1930) investigation of the crystal structure of the MC_2 carbides showed that the rare earth dicarbides, lanthanum to neodymium, are of the calcium dicarbide type, the Strukturbericht notation is $C11_a$. He found the space group to be $I\frac{4}{m}mm$ (D_{4h}^{17}). In the following year von Stackelberg (1931) gave the lattice parameters for samarium and yt-

trium dicarbides, and he believed that the latter has a different structure. The results are given in Table 3. In 1944, Trombe (1944) investigated the magnetic properties of gadalinium dicarbide; he prepared this compound by Pettersson's method. Trombe found that gadolinium dicarbide has a

Table 3. The lattice constants for the rare earth dicarbides[a]

Compound	a_o[b,c] (Å)	c_o[c] (Å)	Density (gm/cm^3) x-ray	Density (gm/cm^3) pycnometric[d]
LaC_2	3.92	6.56	5.35	5.02
CeC_2	3.88	6.49	5.56	5.23
PrC_2	3.85	6.42	5.73	
NdC_2	3.82	6.37	6.00	
SmC_2	3.76	6.29	6.50	
YC_2[e]	3.80	6.57	4.58	

[a]von Stackelberg (1931).

[b]Converted to the body-centered tetragonal lattice to conform with space group given in the International Tables for X-Ray Crystallography, Vol. 1. ($a_{bct} = 0.7071\ a_{fct}$).

[c]Converted from kX units to Angstrom Units (1kX = 1.00203 Å).

[d]von Stackelberg (1930).

[e]von Stackelberg stated that YC_2 was probably hexagonal, two molecules per unit cell.

magnetic moment corresponding to seven unpaired electrons, that it obeys the Curie-Weiss law, and that its paramagnetic Curie point should be -6.5°K. He lists the pycnometric density as 6.20 gm/cm^3 at 21°C. A high temperature x-ray investigation of lanthanum dicarbide (Bredig, 1953) showed that at 1750°C, the tetragonal structure transforms to a face-centered cubic structure, as 6.0 ± 0.1 Å. Bredig stated that it is probably of the pyrite, FeS_2 type. Brewer and Krikorian (1956) in their research on reactions of refractory silicides with carbon found two new types of cerium carbides, the mono- and sesqui-carbides. The carbides were prepared by sintering cerium with approximately 60 per cent graphite at 1400°C. The x-ray analysis of the sintered mass indicated the presence of the three carbides plus several unidentified phases. The monocarbide was of the sodium chloride type, a = 5.130 Å, the sesquicarbide was of the body-centered plutonium sesquicarbide type, a = 8.455 Å, and the dicarbide was the same as reported by von Stackelberg (1930). Warf (1956) reported the preparation of a cerium monocarbide, silvery in color and a golden cerium tricarbide. Both react with water forming a mixture of hydrocarbons. Warf prepared the carbides by reacting the cerium hydride with graphite in an electric furnace. The existence of this gold colored tricarbide seems contradictory to the results reported by other investigators. It is possible that the presence of

hydrogen in this method of preparation may be the cause of this difference.

The evidence for the existence of lower carbides suggests that the rare earth-carbon phase diagrams might be analogous to those of the actinide series. A study of the uranium-carbon system (Mallett et al., 1952) revealed the existence of the uranium mono-, sesqui- and di-carbides, all of which are isostructural with the corresponding cerium compounds which have been reported. The structure details of the uranium mono- and di-carbides were published independently by Rundle et al. (1948) and Litz et al. (1948). The structure details of the uranium sesquicarbide were reported by Mallet et al. (1951). They found it to be of the plutonium sesquicarbide type, the Strukturbericht notation is $D5_c$ (Zachariasen, 1952). The only other published actinide-carbon phase diagram is that of thorium (Wilhelm and Chiotti, 1950). In this system only the mono- and di-carbides exist. The monocarbide is of the sodium chloride type. The structure of the thorium dicarbide was at first believed to be tetragonal and similar to calcium carbide, except that the C_2 groups were rotated so that they lay in the AB plane, instead of being perpendicular to this plane (von Stackelberg, 1930). Hunt and Rundle (1951) have shown by single crystal methods that the lattice is C-centered mono-

clinic and by neutron diffraction they were able to determine the carbon positions.

The relationship between the carbides of the elements in the periodic table has been discussed by many authors. In general, they have divided these compounds into four general types, covalent, ionic, interstitial and metallic. The covalent carbides are those of hydrogen, boron, nitrogen, the chalkogens, the halogens and silicon. The compounds formed by inserting metal atoms between layers of graphite, such as RC_8 and RC_{16} (where R is potassium, rubidium and cesium), are also classified as being covalent carbides.

The ionic (or salt-like) carbides are mainly formed by the group I, II and III elements. These carbides are characterized by their transparency, lack of electrical conductivity and reactivity with water or dilute acids. These ionic carbides are divided into subgroups according to the number of carbon atoms in the anion, i.e., one, two or three. The first have the carbon atoms far apart, and on hydrolysis, yield primarily methane. Be_2C, which has an anti-fluoride structure, and Al_4C_3, which has a complex structure but with the carbon atoms 3.16 Å apart, are considered methanides. Those crystals that have carbon atoms in pairs, forming the $C_2^=$ anion, comprise the largest group of salt-like carbides. Examples of these acetylides are: the alka-

line and coinage metal carbides, R_2C_2; the group II metal carbides, RC_2; the group III metal carbides, Al_2C_6, the rare earth dicarbides and the actinide dicarbides; and the vanadium dicarbide. The existence of the acetylenic anion in some of these compounds has not been proved by x-ray methods, but hydrolytic studies indicate that they probably contain a $C_2^{=}$ anion. The carbide, Mg_2C_3, is the only compound known to have a C_3^{-4} anion. There is no proof, however, that the C_3^{-4} ion exists in this compound, but since it yields chiefly allylene, $CH_3-C\equiv CH$, on hydrolysis suggests the presence of this anion.

Interstitial carbides are formed primarily by the transition metals of the IVth, Vth and VIth groups of the periodic table. The general formulas are RC and R_2C. The RC compounds are generally face-centered cubic (sodium chloride structure) with the metal atoms occupying the corners and face centers, while the carbon atoms occupy the octahedral holes. The R_2C carbides are generally hexagonal with the metal atoms occupying the positions of the hexagonal closest packed structure, while the carbon atoms randomly occupy the half the octahedral holes. These carbides are very hard, metallic in appearance, and have high melting points. They are extremely stable to water and dilute acids. Hagg (1931) has pointed out that these carbides have a radius ratio,

R_c/R_m, less than 0.59; and those metals which have a ratio greater than 0.59 generally form the metallic type carbides.

The metallic carbides of the metals of groups VII and VIII are not nearly as well defined as the other types. Their properties lie mid-way between that of the salt-like and interstitial carbides. They are similar to the interstitial carbides in hardness and their metallic appearance. They are related to the salt-like compounds by their behavior toward acids and water. The metallic carbides have complicated formulas and structures, and in many cases there is still much doubt to the exact stoichiometry of the various compounds. Some of the compounds reported are: (1) the Fe_3C type, cementite (also Ni, Co, Mn compounds); (2) the Cr_7C_3 type (also the Mn compound); (3) Cr_2C_3; (4) the $Cr_{23}C_6$ type (also Mn); (5) $Fe_{20}C_9$; and (6) the Fe_2C type (also formed by Co).

The classification of some of the carbides as outlined above may be changed as more information concerning these compounds becomes available. The case of thorium dicarbide is a good example. Originally it was classified as a salt-like carbide, but recent data (Hunt and Rundle, 1951 and Wilhelm and Chiotti, 1950) indicate it might best be classified as a metallic carbide.

SOURCE OF MATERIALS AND METHODS OF CHEMICAL ANALYSIS

Yttrium and the Rare Earth Metals

High purity rare earth (except for samarium, europium and ytterbium) and yttrium metals were prepared at the Ames Laboratory by metallothermic reduction of the corresponding fluoride with triply distilled calcium. The details of the method are described by Spedding and Daane (1954). Samarium, europium and ytterbium were prepared by distillation of these metals from a mixture of the respective oxides and lanthanum turnings (Daane et al., 1953). The analyses of the metals used in preparing the carbides are listed in Table 4. In general the metals were used in the form of filings or finely divided chips. It was found that it was easier to achieve homogeneous alloys by arc melting compressed packets of the metal filings and carbon powder.

Carbon

The carbon used was of two types, (1) "National Special Graphite Spectroscopic Electrodes", and (2) high purity Acheson graphite, ATZ. The analysis of the Acheson material is shown in Table 5. The carbon dust (powder) was prepared by turning spectroscopic electrodes on a lathe. The Acheson graphite was used to prepare large quantities of master alloys and for crucibles for the determination of liquidus points.

Table 4. Chemical and spectroscopic analysis of yttrium and the rare earth metals[a,b]

Impurity	Rare earth						
	Y	La	Ce	Pr	Nd	Sm	Gd
Ce		--	xxx	--	--		
Dy	<0.01						
Er							
Eu							--
Gd						--	xxx
Ho							
La	0.01	xxx	0.01	--	--		
Lu							
Nd		--	--	--	xxx		--
Pr		--	--	xxx	--		
Sm			--		0.2	xxx	0.1
Tb	<0.1						<0.01
Tm							
Yb						<0.01	
Y	xxx	0.01	--				0.05
C[c]		230	210	220			
N[c]		115	47	62			
Al	0.01	0.01			--		--
Ca	<0.01	0.02	0.01	<0.01	<0.03	0.04	<0.04
Cu		0.01				<0.01	
Fe	0.01	0.01	--	<0.01	<0.004	<0.01	<0.005
Mg		0.02			<0.007		--
Si	0.01	0.01	0.01	--	<0.02	<0.02	--
Ta	0.1	--	--	--	--	*	--

Impurity	Tb	Dy	Ho	Er	Tm	Yb	Lu
Ce							
Dy	--	xxx	--	--	--		

[a]The symbols used in the above table having the following significance: --, not detected; *, interference; > greater than; < less than.

[b]Values are reported in per cent, unless otherwise stated.

[c]Values for carbon and nitrogen are reported in parts per million.

Table 4. (Continued)

Impurity	Rare earth						
	Tb	Dy	Ho	Er	Tm	Yb	Lu
Er	--	--	<0.01	xxx	<0.01	<0.01	
Eu						--	
Gd	--						
Ho		--	xxx	<0.01	--		
La		<0.01				--	
Lu					0.1	<0.01	xxx
Nd							
Pr							
Sm							
Tb	xxx	--			--		
Tm				<0.01	xxx	--	
Yb		--			<0.02	xxx	<0.01
Y	<0.01	--	0.02		<0.02		
C[c]		231	367				
N[c]		60	423				
Al	--		--				
Ca	--	<0.02	--	<0.05	0.02	0.05	<0.02
Cu	--	--	0.01	*	*		0.01
Fe	--		0.01	<0.01	0.02	<0.01	<0.015
Mg		--	<0.01	--	0.02	--	
Si	--			<0.05	<0.02	<0.02	<0.02
Ta	--	--	0.1	--	>1.0	--	--

Table 5. Spectroscopic analysis of Acheson graphite

Element	Per cent present
Calcium	<0.01
Magnesium	<0.01
Silicon	<0.01
No other elements detected	

Chemical Analyses

The analysis of all the minor constituents except carbon and nitrogen were carried out by the spectrochemistry group of the Ames Laboratory. Of the metals used in preparing the carbides, only thulium had a large amount of an impurity, tantalum. Examination of x-ray patterns of various thulium carbides did not show any tantalum or Ta_2C or TaC lines. The analysis of carbon (by method I, see below) and nitrogen were performed by the analytical chemistry group. All chemical compositions are reported in weight percentages, unless otherwise indicated.

Two different methods were used for determining carbon in the lanthanum-carbon alloys. The low carbon alloys, up to 1.5 per cent carbon, were analyzed by igniting the alloy by induction heating in a stream of oxygen, and collecting the carbon dioxide gas in a barium hydroxide solution. The change in the conductivity of the barium hydroxide solution is proportional to the carbon dioxide formed from the carbon in the alloy. This procedure will be called method I. Method II was used for determining the amount of carbon in alloys above 1.5 per cent. This procedure consisted of igniting the weighed alloy in air at 850 to 900°C. From the weight of the oxide, the percentage lanthanum in the alloy is calculated directly and the amount of carbon is obtained by dif-

ference. Below 1.5 per cent carbon, method I is undoubtedly more reliable than method II.

Although method II appears to be inferior to method I, even above 1.5 per cent, the following arguments are presented to show that this is not true. First of all, it should be pointed out that the rate of oxidation in air at room temperature of alloys containing carbon varies directly with the carbon content, i.e. the higher the carbon content the more rapid the rate of oxidation (Figure 2). This will affect the accuracy of either method by the same amount. However, the manner in which oxidation takes place will affect the two methods differently. These alloys react with water to form volatile hydrocarbons and the corresponding hydrated rare earth oxide. Therefore, any oxidation will affect method I in two ways, (1) the weight of the alloy and (2) the loss of carbon. Both of these are additive and will lead to low carbon values. Method II is only affected by the change in weight of the alloy, since the carbon is obtained by difference; and this error in weighing gives a high value for the carbon content. Another important consideration is that method I requires that the volume of the carbon dioxide obtained from the carbon in an alloy is between 0.1 and 1.0 cc. This means that the weight of an alloy decreases with increasing carbon content (1.0 gm for a pure metal sample to 1.3 mg for a 15 per cent carbon - 85 per cent rare earth al-

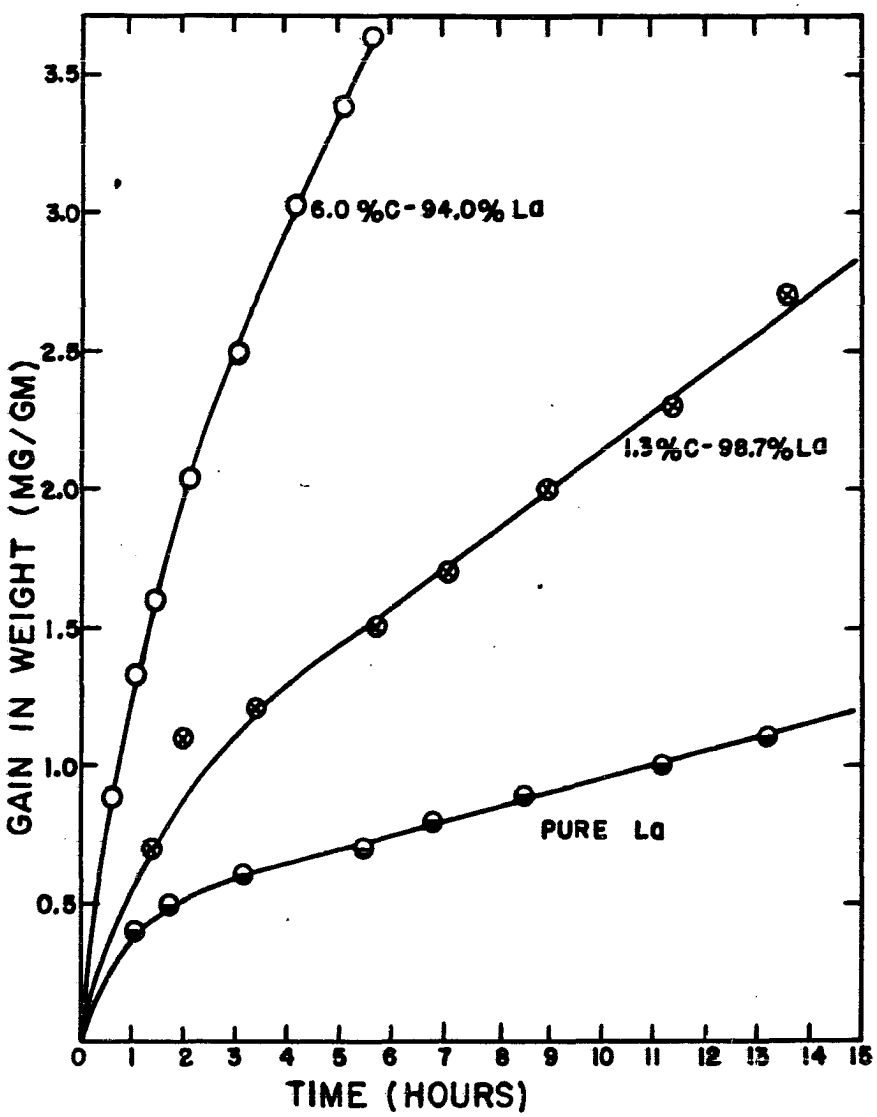

Figure 2. Rate of oxidation of lanthanum and some carbon-lanthanum alloys in air at room temperature.

loy). Thus, it is obvious, that as the carbon concentration increases, the reliability in the procedure is lessened because of the increased weighing error. Method II, however, does not require that the weight of the alloy decrease with increasing carbon content, and therefore the weighing error is essentially constant.

The impurities in the lanthanum metal probably cause the largest error in method II. The effect of these impurities on an analysis is shown in Table 6. Examination of Table 6 indicates that the major concern is oxygen especially if more than 0.05 per cent is present. However, the addition of carbon does reduce the oxygen content (discussed later under

Table 6. Effect of impurities on the results of analytical method II

Impurities	Deviation from the true value of lanthanum
Metals	+0.003
Nitrogen	-0.014
Oxygen	
max., 0.100%	-0.10
mean, 0.05	-0.05
min., 0.02	-0.02
Combined Effect	
Metals; N; $O_{max.}$	-0.11
Metals; N; O_{mean}	-0.06
Metals; N; $O_{min.}$	-0.03

the lanthanum-carbon phase diagram) and the error introduced by the residual oxygen in the metal is less than that indicated in Table 6. Secondly, as higher carbon content alloys are analyzed the error introduced by impurities is reduced because the amount of lanthanum in the alloy is decreased. When alloys are analyzed by both methods (Table 7), it is noted the agreement is excellent, the largest deviation

Table 7. Comparison of the results of carbon analyses by method I and II

Alloys as prepared[a]		Carbon as analyzed		Difference
		Method I	Method II	
%La	%C	%C	%C	
100.00	--	0.033	0.02	-0.013
99.90	0.10	0.089	0.08	-0.009
99.76	0.24	0.28	0.26	-0.02
99.51	0.49	0.52	0.48	-0.04
99.25	0.75	0.72	0.73	+0.01

[a]In the process of preparing these carbon-rare earth metal alloys the composition may vary considerably because of the loss of either carbon or metal due to volatilization or spattering during arc melting; and therefore, the composition of the alloy as prepared is not reliable and may be in error as much as ± 2 per cent carbon from the true value.

observed was 0.03 per cent carbon. From this it is concluded that carbon analyses obtained by method II are accurate within ± 0.05 per cent carbon.

The free carbon content in alloys was determined according to the standard procedure used for uncombined carbon

in steels and other iron-carbon alloys. The rare earth-carbon alloy was treated with small amounts of water in a sintered glass crucible until the reaction subsided. Dilute nitric or hydrochloric acid is added to dissolve the hydrated rare earth oxide. The solution is filtered and the carbon residue is washed several times with dilute acid, water and finally alcohol. The material is dried at 100-110°C to constant weight. These analytical results indicate that lanthanum dicarbide does not have the stoichiometric composition of LaC_2 with respect to the combined carbon. The maximum amount of combined carbon found in lanthanum-carbon alloys by subtracting the free carbon from the total carbon was 14.43 per cent carbon, compared to the theoretical composition of 14.75 per cent.

CRYSTAL STRUCTURES OF THE GROUP IIIA ELEMENT CARBIDES

Equipment and Techniques

A 114.59 mm diameter Debye-Scherrer camera, obtained from Philips Electronics, Inc. (formally North American Philips Co.), was used for the structure determinations, and in some cases it was also used for determining lattice parameters. A symmetrical focusing back reflection camera, 120 mm in diameter, was used to obtain patterns for a more accurate lattice constant. A constant flow of helium through the back reflection camera served to reduce air scattering of x-rays and to reduce the rate of corrosion of the sample. All of the carbides were examined with both cameras but in many cases, the patterns obtained using the Debye-Scherrer camera were much sharper and therefore the lattice parameters were determined from the Debye-Scherrer pattern rather than the back-reflection pattern. Both cameras were checked for accuracy using fused sodium chloride and tantalum filings.

Copper K_α radiation was used in conjunction with a Philips Electronics basic x-ray diffraction unit. The values used for $K_{\alpha_{avg.}}$, K_{α_1}, K_{α_2} radiation were 1.54178, 1.54050 and 1.54433 Å, respectively. For some of the lanthanum, cerium and praseodymium samples, a 0.5 mil sheet of aluminum foil was placed between the sample and film to reduce the background due to the x-ray fluorescence of these rare earths.

Exposure times, except for intensity studies, were about twelve hours for alloys of lanthanum to neodymium, ten hours for those of samarium to holmium, eight hours for the carbides of erbium to lutetium, and four to six hours for the yttrium compounds. Kodak "No-Screen" x-ray film was employed and the recommended procedures for developing and fixing using General Electric chemicals were followed. When films were used for intensity determinations, they were developed simultaneously to maintain uniformity. The lines of a diffraction pattern were measured on a General Electric Illuminator, Model 5-17, employing a vernier scale enabling the operator to read line positions within 0.05 mm.

Preparation of Samples

The samples were prepared by two techniques. The first method was employed for the rare earth metals which have a boiling point above 2200°C (see Table 1). Approximately 200 mg of the metal were weighed out to an accuracy of $\pm$ 0.2 mg. Carbon was weighed (accurate to $\pm$ 0.2 mg) and added to the metal to give the desired composition. The metal and carbon were mixed and compressed in a 3/16 inch diameter die under a pressure of 25-40 tons/sq in. Because of the reactivity of cerium and lanthanum in air, the filings of these metals were prepared in a vacuum dry box and only removed for weighing and compressing. The weighed compacts were placed on a

water cooled copper plate. The copper plate served as the positive electrode during arc-melting. A tungsten or a coreless carbon rod was used as the negative electrode. The system was evacuated to a pressure of one to ten microns of mercury and then filled with helium or argon. The residual nitrogen and oxygen were removed by melting zirconium metal. The samples were arc-melted and inverted and remelted. This procedure was repeated two or three times to insure complete reaction in the center of the specimens. Analyses of the samples showed no detectable tungsten pick up in the melting and a maximum amount of 0.01 per cent of copper. An attempt was made to prepare the thulium carbides by this method, but because of the high volatility of the metal, it was discarded in favor of the second method.

The second method was used for samarium, europium, thulium and ytterbium. This method consisted of placing the weighed metal and carbon in a tantalum bomb. The bombs were constructed by welding in a helium atmosphere a five mil bottom to a piece of tubing, 3/4 inch high, 3/8 inch diameter, and having a 20 mil wall. The contents were sealed in the bomb under 2/3 atmosphere of helium by welding on a five mil top. A second size bomb was also used. This was constructed of one inch high, 1/8 inch diameter, 15 mil wall tantalum tubing. The bomb was sealed by welding the pinched ends. The bombs were heated at 1200 to 2000°C for 2 to 24 hours,

using either an induction furnace or a tantalum tube furnace to obtain the desired temperatures.

The carbides are quite unstable in air. The powdered material will be completely converted to the hydrated oxide and hydrocarbons within a minute or two, while bulk samples are attacked much slower. For this reason x-ray samples must be prepared in an inert atmosphere. The alloys were placed in a vacuum dry box and the system evacuated to a pressure of 20-30 microns mercury. A positive pressure of argon or helium was maintained on the dry box while working with the specimens. Any oxide coating was first removed from the alloy by scraping it clean with a razor blade. The carbide was crushed in a hardened tool steel mortar and then ground to approximately 350 mesh with an agate mortar and pestle. The powdered material was loaded into a thin walled pyrex capillary tubing, whose inside diameter varied between 0.2 and 0.4 mm. After the pyrex capillary tubes were filled, the system was opened and the tubes were sealed by fusion of the open end. In the short space of time that the sample is exposed to the atmosphere, no reaction between the sample and the atmospheric gases was detected because of the inert atmosphere in the capillary tube. While the capillary tubes were being filled, back reflection samples of the alloy were prepared by spreading a thin layer of the alloy over the adhesive side of a cellophane tape. A second piece of this

tape was fastened back to back to the first, sealing the alloy between them. No appreciable oxidation of the sealed specimens was detected after ten hours exposure to air. Samples with low carbon contents (those with less carbon than that equivalent to the theoretical composition RC, i.e. 8 per cent carbon for lanthanum to 6.5 per cent carbon for lutetium and 11 per cent for yttrium) were prepared in the manner described above, except that the samples were filed instead of crushed. The mesh size of the filings ranged between 200 and 300. X-ray patterns of these filed samples were taken without annealing. If the back reflection lines were diffuse, the samples were then annealed at 400 ± 25°C for 20 to 100 hours before taking a second pattern.

Pycnometric Density Measurements

Pycnometric density measurements are quite important in any crystal structure determination. If the density is known within reasonable accuracy, then the number of molecules in a unit cell can be calculated, provided that the lattice constants are known. The density measurements were made by weighing the carbide in air and then in absolute alcohol, the difference in weight divided by the measured density of the alcohol gives the volume of the specimen. The density is then calculated from the weight in air and the volume. The results of these measurements and the number of molecules

per unit cell are reported in Table 8. The number of molecules per unit cell (formula units, f.u.) was calculated by using the following formula

$$\text{f.u.} = \frac{d\ V\ N \times 10^{-24}}{M} \quad , \qquad (1)$$

where d is the density, V is the volume of the unit cell, N is Avogadro's number (6.0235×10^{23}), and M is the molecular weight.

Table 8. Pycnometric density of some rare earth carbides

Compound	Density (gm/cm^3)	Atomic volume ($Å^3$)	Molecular weight	# Molecules per unit cell
La_2C_3	5.992	685.5	313.8	$7.89 \approx 8$
LaC_2	5.297	101.7	162.9	$1.99 \approx 2$
$YC_{0.4}$	4.73	132.8	93.72	$4.02 \approx 4$

Determination of Crystal Structures

Lanthanum sesquicarbide

Although Brewer and Krikorian (1956) reported cerium sesquicarbide as being isostructural with plutonium sesquicarbide, they did not undertake any intensity studies to determine the cerium positions in this compound. Zachariasen (1952) found the plutonium atoms to occupy the 16(c) posi-

tions of the space group $I\bar{4}3d$ (T_d^6) with the x parameter equal to 0.050 ± 0.003. Mallett et al. (1951) reported that the uranium atoms also occupy the 16(c) positions with the x parameter for uranium sesquicarbide equal to 0.20. This apparent discrepancy can be resolved by shifting the unit cell $\frac{1}{4}$ the distance along the body diagonal, i.e., the symmetry of this structure repeats itself every quarter of a unit cell along the body diagonal.

The lanthanum sesquicarbide was the first rare earth sesquicarbide to be examined in this study. The x-ray diffraction pattern of this material was indexed to be body-centered cubic with a lattice constant of approximately 8.82 Å. The systematic absences were categorized as:

A. h,k,l is absent if $h + k + l = 2n + 1$

B. h,h,l is absent if $2h + l = 4n + 2$

C. h,k,l is absent if h,k,l are all even and $h + k + l = 4n + 2$.

The absences listed under A are characteristic of a body-centered lattice and those under B uniquely determine the space group as $I\bar{4}3d$ (T_d^6). The last set of absences corresponds to the sixteen-fold positions of the space group, 16(c). These positions are:

$$(000);\ (\tfrac{1}{2}\ \tfrac{1}{2}\ \tfrac{1}{2})\ \text{plus}$$

$$(xxx);\ (x + \tfrac{1}{4},\ x + \tfrac{1}{4},\ x + \tfrac{1}{4});\ (\tfrac{1}{2} + x,\ \tfrac{1}{2} - x,\ x)\circlearrowright;$$
$$3/4 + x,\ \tfrac{1}{4} - x,\ 3/4 - x)\circlearrowright.$$

The atomic scattering factor of an atom depends on the atomic number of the element. Therefore, in the case of lanthanum sesquicarbide, there is little hope of determining the carbon positions by x-ray methods. Density measurement (Table 8) reveals that there must be 16 lanthanum atoms per unit cell and thus the lanthanum atoms must occupy the 16(c) positions. Examination of these positions shows that there is only one parameter to be determined; the value for this parameter can be calculated by a trial and error method. The intensity data for the lanthanum sesquicarbide were obtained by visual comparison of the lines on four Debye-Scherrer patterns of different time exposures (i.e., two, four, eight and sixteen hours). The data are given in Table 9. The intensities were calculated according to the following equation:

$$I_{hkl} \approx |F_{hkl}|^2 \, p \, L \, , \qquad (2)$$

where I_{hkl} is the intensity of the diffracted line (hkl), p is the multiplicity, L is the combined Lorentz and polarization factor, and F_{hkl} is the structure factor for the (hkl) plane. The form for the structure factor is given as:

$$|F_{hkl}|^2 = \left[\sum_r f_r A_r\right]^2 + \left[\sum_r f_r B_r\right]^2 , \qquad (3)$$

where f_r is the atomic scattering factor for the r^{th} atom, and A_r and B_r are the geometrical scattering factor for the r^{th} atom in a given space group. The values of A_r and B_r for

Table 9. Diffraction data for lanthanum sesquicarbide, $a_o = 8.8173$ Å

$\sin^2\theta_{obs.}$ for $K_{\alpha}{}_{avg.}$ [a]	hkl	I_o	I_c
0.04625	211	518	576
0.06141	220	622	814
0.07675	310	622	704
0.10803	321	415	369
0.12306	400	10	22
0.16843	332	207	200
0.18322	422	124	131
0.19859	510, 431	622	172 + 345
0.22945	521	207	245
0.24410	440	1	1
0.25998	530	26	25
0.29048	611, 532	93	37 + 74
0.30609	620	42	38
0.32193	541	166	154
0.35204	631	73	54
0.36708	444	83	76
0.38247	710, 543	47	13 + 26
0.41296	721, 633	135	94 + 47
0.42838	642	93	125
0.44253	730	47	46
0.47426	732, 651	83	3 + 73
0.49009	800	36	34
0.50488	741	26	17
0.53633	653	31	30
0.55141	822, 660	47	52 + 2
0.56522	831, 750, 743	207	72 + 22 + 72
0.59593	752	26	29
0.61151	840	5	6
0.62913	910	5	8
0.65676[a]	921, 761, 655	83	3 + 62 + 1

[a]All values of $\sin^2\theta$ greater than 0.65 are $K_{\alpha 1}$ lines

Table 9. (Continued)

$\sin^2\theta_{obs.}$ for $K\alpha_{avg.}$ [a]	hkl	I_o	I_c
0.67274	664	104	99
0.68709	930, 851, 754	135	21 + 72 + 43
0.71725	932, 763	62	63 + 3
0.73366	844	31	30
0.74887	941, 853	26	17 + 17
0.77786	10.11, 772	47	16 + 42
0.79361	10.20, 862	218	106 + 53
0.80852	950, 943	93	42 + 51
0.83933	10.31, 952, 765	218	38 + 100 + 38
0.87036	871	5	24
0.90005	10.33, 961	36	52 + 6
0.91551	10.42	21	27
0.93090	11.10, 954, 873	415	45 + 150 + 150
0.96154	11.21, 10.51, 963	415	10 + 180 + 180
0.97675	880	93	174
0.99204	11.30, 970	--not determined--	

the space group $I\bar{4}3d$ are given in the International Tables for X-Ray Crystallography (1952). The simplified equations of $|F_{hkl}|^2$ for the 16-fold positions are:

(1) hkl all even; $h + k + l = 4n$

$$|F_{hkl}|^2 = (16f_{hkl})^2\left[\left\{\prod_i \cos 2\pi h_i x\right\}^2 + \left[\left\{\prod_i \sin 2\pi h_i x\right\}^2\right]\right] \quad (4a)$$

(2) one index even, two odd; $h + k + l = 4n$

$$|F_{hkl}|^2 = (8f_{hkl})^2\left\{\sin 2\pi x(\text{sum of odd indices})\right\}^2 \quad (4b)$$

(3) one index even, two odd; $h + k + l = 4n + 2$

$$|F_{hkl}|^2 = (8f_{hkl})^2\{\sin 2\pi x(|\text{difference between odd indices}|)\}^2 \qquad (4c)$$

Examination of Equations 4a to 4c reveals that the periodicity depends on the indices hkl; if the indices are small, the frequency is also small. A plot of $|F_{220}|^2$ versus x shows the minimum number of cycles in which a given value of $|F_{220}|^2$ is repeated (Figure 3). From these symmetry conditions the x parameter must lie in a given $1/8^{th}$ interval (i.e., between 0 and 1/8, or 1/8 to 1/4, etc.). The range in which x varies from zero to 1/8 was chosen. The comparison of the observed intensities of the (220), (332), (440), (530) and (800) with the values of $|F_{hkl}|^2$ plotted as a function of x over the range zero to 1/8 (Figure 4) shows that the value of the x parameter is limited to the range between 0.05 and 0.06. The last 13 lines in the back reflection region ($\sin^2\theta > 0.70$) were used to determine the x parameter more accurately because absorption errors are at a minimum in this region. The value of x which gave the best (lowest) result for the reliability index was chosen as the correct parameter. The reliability index, R, is given by the following equation:

$$R = \frac{\Sigma\,|\,|F_o| - |F_c|\,|}{\Sigma\,|F_o|} \quad , \qquad (5)$$

where F_o and F_c are the observed and calculated structure

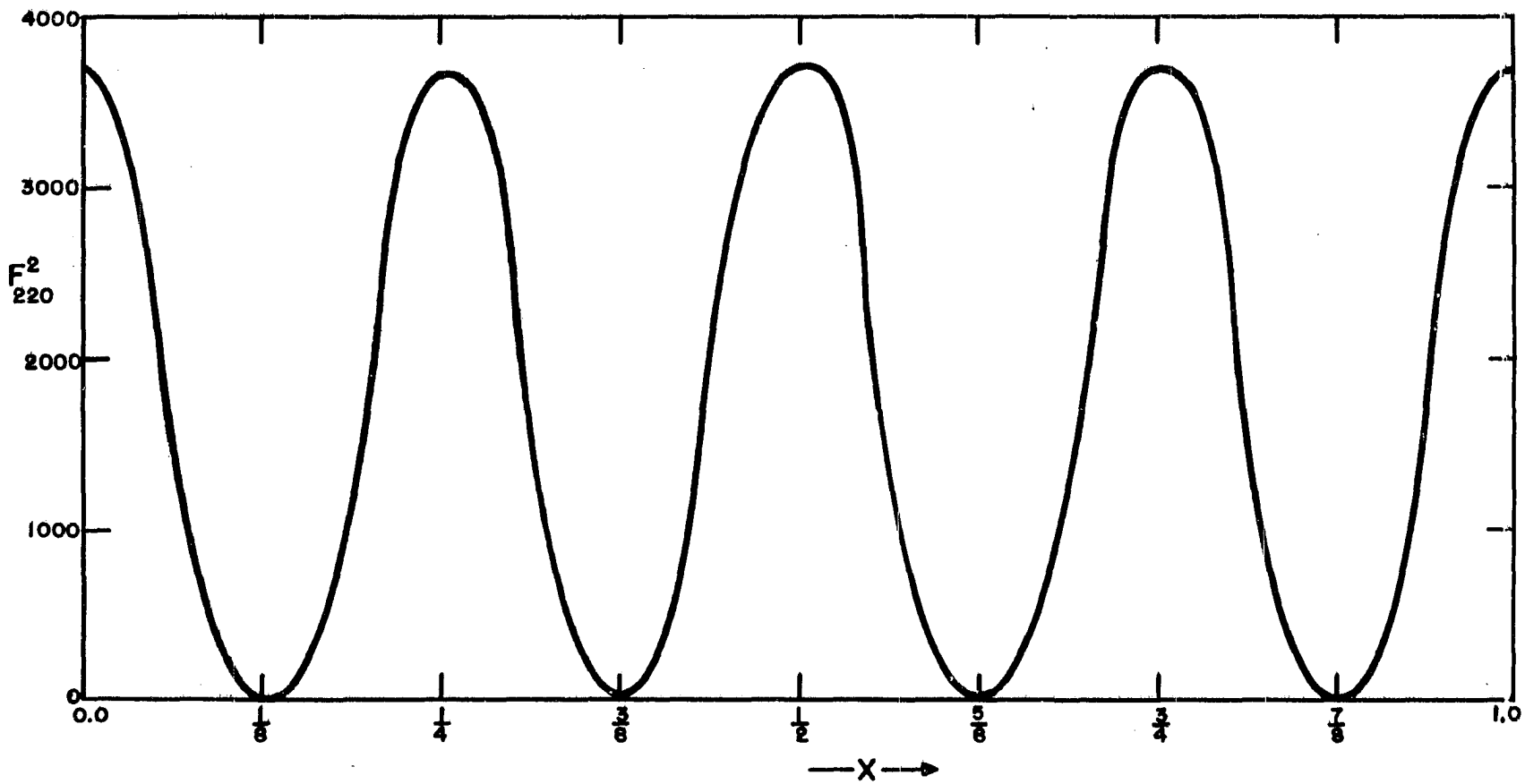

Figure 3. The symmetry of F_{220}^2 as a function of x.

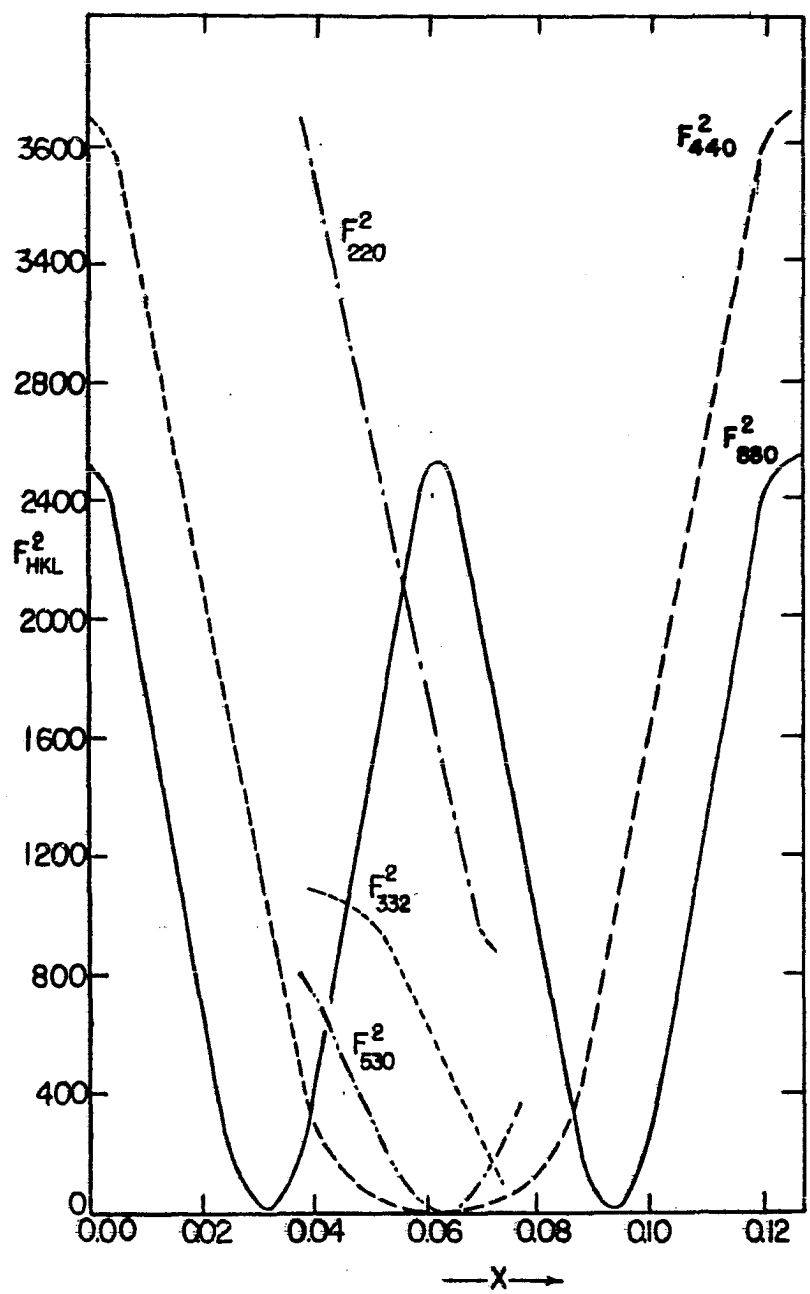

Figure 4. Some calculated F_{hkl}^2 values as a function of x, from $0 \leq x \leq 1/8$.

factors respectively. The R values for x equal to 0.050, 0.053 and 0.056 are 0.141, 0.107 and 0.158, respectively. Since R for all three values of x are considered acceptable, the final choice of x is 0.053 ± 0.003. If all the reflections are considered, the reliability index is 0.165 for $x = 0.053$.

In joint work with Dr. M. Atoji, of the Ames Laboratory, neutron diffraction was used to locate the carbon atoms in this compound and lanthanum dicarbide. The carbon to carbon bond distances are 1.32 Å and 1.28 Å for the lanthanum sesqui- and di-carbides, respectively (Atoji et al., 1957).

Triyttrium carbide

A new rare earth carbide was found to exist. It was first observed while investigating some low carbon yttrium alloys. Initially it was believed to be Y_2C, but microscopic examination of some alloys ranging from 1.0 to 9.0 per cent carbon indicated that this could not be correct, and that the composition of this lower carbide varied from $YC_{0.25}(Y_4C)$ to $YC_{0.40}(Y_5C_2)$. Photomicrographs of some of these alloys are shown in Figures 5 to 7. The lower carbide of yttrium will be called "triyttrium carbide", Y_3C, since this composition lies approximately half way between the two limits. Indexing of the triyttrium carbide pattern showed only face-centered cubic lines. A density measurement of an alloy of

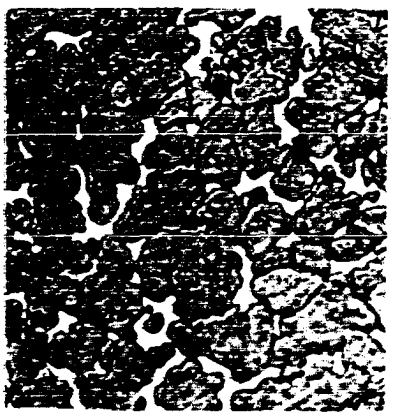

Figure 5. 3 per cent C - 97 per cent Y alloy, X500 unetched. Light area Y, dark areas Y_3C.

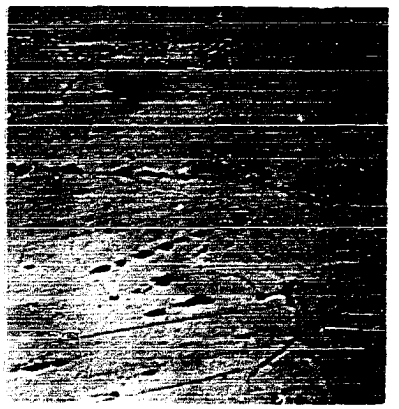

Figure 6. 5.16 per cent C - 94.84 per cent Y alloy, X200 unetched. Light area Y_3C, second phase - Y_2C_3.

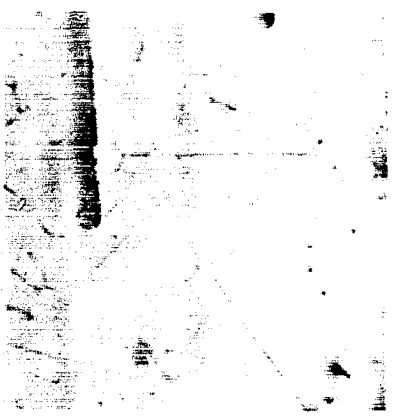

Figure 7. 4.3 per cent C, 95.7 per cent Y, approximately of the Y_3C composition, as arc melted. X200.

the composition $YC_{0.40}$ (Table 8) indicates that there are four yttrium and 1.6 carbon atoms per unit cell. The intensity measurements were taken from this sample, and therefore, all calculations are based on this ratio of yttrium to carbon atoms. The films used for the intensity study were prepared in the same manner as previously described. Since the atomic numbers of yttrium and carbon lie much closer together than in the case of lanthanum and carbon, it should be possible to determine the carbon positions. For a face-centered cubic lattice with the heavy metal atoms at the origin and in the face-centered positions [i.e. (000); $(\frac{11}{22}0)$ ↻], the carbon atoms can occupy two possible sets of positions. These are the random filling of 1.6 of (1) the four octahedral holes or (2) the eight tetrahedral holes. There is the possibility of an order structure, but since no extra lines were observed this possibility was discarded. The coordinates for the octahedral holes are:

$$(\tfrac{1}{2}\ \tfrac{1}{2}\ \tfrac{1}{2});\ (00\tfrac{1}{2})\ ↻.$$

Those for the tetrahedral holes are:

$$(\tfrac{1}{4}\ \tfrac{1}{4}\ \tfrac{1}{4});\ (\tfrac{3}{4}\ \tfrac{3}{4}\ \tfrac{3}{4});\ (\tfrac{3}{4}\ \tfrac{3}{4}\ \tfrac{1}{4})↻;\ (\tfrac{1}{4}\ \tfrac{1}{4}\ \tfrac{3}{4})\ ↻.$$

The former requires the space group to be Fm3m (O_h^5), the sodium chloride type. The second possibility requires the space

group to be $F\bar{4}3m$ (T_d^2), the sphalerite (ZnS) type. The approximate intensities were calculated using Equation 2. The structure factors, $|F_{hkl}|^2$, for the two space groups were simplified for the above conditions from the equations given in the International Tables for X-Ray Crystallography (1952). For the space group Fm3m, $|F_{hkl}|^2$ is given as:

(1) if hkl are all even

$$|F_{hkl}|^2 = (4f_y + 1.6f_c)^2 , \qquad (6a)$$

(2) if hkl are all odd

$$|F_{hkl}|^2 = (4f_y - 1.6f_c)^2 . \qquad (6b)$$

For the space group $F\bar{4}3m$, $|F_{hkl}|^2$ is given as:

(1) if hkl are all even; $h + k + l = 4n$

$$|F_{hkl}|^2 = (4f_y + 1.6f_c)^2 , \qquad (7a)$$

(2) if hkl are all even; $h + k + l = 4n + 2$

$$|F_{hkl}|^2 = (4f_y - 1.6f_c)^2 , \qquad (7b)$$

(3) if hkl are all odd

$$|F_{hkl}|^2 = (4f_y)^2 + (1.6f_c)^2 . \qquad (7c)$$

The calculated intensities for the space groups Fm3m (using Equations 6a and 6b) and $F\bar{4}3m$ (using Equations 7a to 7c);

the observed intensities based on arbitrarily assigning the (111) as 1000 ; and the calculated intensities for pure yttrium metal (if it were face-centered cubic) are listed in Table 10. Also shown in Table 10 are the intensity ratios of various reflections. Of these ratios, I_{331}/I_{420} is the most critical with regard to the anion position. From these ratios it is obvious that the 1.6 carbon atoms per unit cell must randomly occupy the four octahedral holes. Comparing the observed intensities with the calculated intensities of the space Fm3m, it is noted that at low angles the observed intensities are larger than the calculated intensities, but in the back reflection region the reverse occurs. This indicates that a temperature correction should be applied to the calculated intensities. The effect of temperature on the intensities can be taken into account using the following equation:

$$|F_o| = |F_c| \exp\left[(-B \sin^2\theta)/\lambda^2\right] . \qquad (8)$$

In general B is not known, but an approximation to its value can be found if $\ln \frac{|F_o|}{|F_c|}$ is plotted against $\sin^2\theta$. The slope of this plot is equal to $-B/\lambda^2$. Applying this correction the new calculated structure factors for the space group Fm3m is shown in Table 11 along with the observed structure factors

Table 10. Calculated and observed intensities for the Y_3C structure

hkl	I_o	I_c		
		$Fm3m$[a]	$F\bar{4}3m$[b]	Pure yttrium[c]
111	1000	421.5	475.6	474.1
200	667	278.4	222.6	249.7
220	468	211.7	211.7	192.0
311	444	203.4	223.7	223.3
222	158	70.0	58.8	64.3
400	70	30.8	30.8	28.5
331	156	76.3	82.3	82.2
420	240	80.2	69.4	74.7
422	111	60.9	60.9	56.8
511, 333	111	62.8	67.2	67.1
440	49	25.0	25.0	23.4
531	117	92.6	99.4	99.4
600, 442	101	70.3	61.1	65.6
620	59	72.9	72.9	67.7
533	83	114.1	123.7	123.7
$\frac{I_{111}}{I_{200}}$	1.50	1.51	2.14	1.90
$\frac{I_{220}}{I_{311}}$	1.05	1.04	0.95	0.86
$\frac{I_{331}}{I_{420}}$	0.65	0.95	1.19	1.10

[a]Carbon atoms occupy the octahedral holes.

[b]Carbon atoms occupy the tetrahedral holes.

[c]If yttrium were face-centered cubic.

Table 11. Calculated structure factors (including temperature correction) and the observed structure factors (normalized) for the Y_3C structure

hkl	$\|F_o\|$	$\|F_c\|$
111	19.7	18.0
200	15.7	14.6
220	12.9	12.3
311	12.3	12.0
222	7.1	7.2
400	4.5	4.7
331	6.7	7.1
420	6.8	8.8
422	5.6	5.9
511, 333	5.5	5.9
440	3.2	4.0
531	6.0	6.1
600, 442	5.1	5.7
620	4.9	4.4
533	5.9	5.2

(normalized to the same scale as the calculated values). The reliability index (Equation 5) for this structure is 0.08.

Determination of Lattice Constants

The accurate lattice parameters for the rare earth sesquicarbides were determined by Bradley and Jay's (1932) extrapolation method. Since $\sin^2\theta$ values were used in calculating lattice constants and $\sin^2\theta = 1 - \cos^2\theta$, the method was modified by plotting "a" against $\sin^2\theta$ and extrapolating "a" to $\sin^2\theta = 1$.

The lattice parameters of the trilanthanon carbides and β-lanthanum metal were obtained by using Nelson and Riley's (1945) method. This technique involves an extrapolation of "a" against $(\cos^2\theta/\sin\theta) + (\cos^2\theta/\theta)$. Nelson and Riley have shown that this function has a linear relationship with "a" down to θ values as low as 30°, while the $\cos^2\theta$ function is only linear between 60 and 90°. The sesquicarbides generally have between eight and twelve possible α_1, and α_2 pairs in the region between 60 and 90°, so that there are a sufficient number of points for a good extrapolation. But the trilanthanon carbides have at the most, three possible pairs and in some cases the pairs are not distinguishable. Therefore, a more reliable extrapolation can be made using the Nelson and Riley function.

The standard error for a given lattice constant as determined by either extrapolation method was calculated from the following equations:

(1) for the precision back reflection camera

$$\delta a_o = \frac{(\delta S')(S')a_o}{(8R)^2} = \frac{(\delta S')(S)a_o}{23 \times 10^4} \qquad (9a)$$

(2) for the Debye-Scherrer camera

$$\delta a_o = \frac{(\delta S')(S')a_o}{(4R)^2} = \frac{(\delta S')(S)a_o}{3.6 \times 10^4} \; . \qquad (9b)$$

δa_o is the standard error, a_o the extrapolated lattice con-

stant, R is the camera radius, $\delta S'$ is the error in measuring a given line, and S' is the distance between the pair of lines that lies closest to $\theta = 90°$. The derivation of these equations is given in Appendix I. Of these terms only $\delta S'$ is unknown, a value of $\pm$ 0.2 mm was assigned to $\delta S'$. The results obtained from several different patterns of lanthanum sesquicarbide in the two phase regions above and below the sesquicarbide composition indicate that this value for $\delta S'$ would give a standard error within which nine of ten observations would fall.

The lattice parameters for the tetragonal rare earth dicarbides and hexagonal lanthanum metal were calculated by Cohen's (1935) least-squares method. Since there were approximately 25 such determinations, the procedure was programmed so that the calculations were made by the International Business Machine "650" computer. The standard error of the lattice parameters were also calculated by the "650" using the method described by Jette and Foote (1935).

Results

Debye-Scherrer patterns of the various rare earth-carbon alloys revealed the existence of a new rare earth carbide (triyttrium carbide) and confirmed the existences of the reported rare earth carbides (the cerium sesquicarbide and the dicarbides of lanthanum, cerium, neodymium, praseodymium

and samarium). Furthermore, these x-ray studies showed that other rare earths form some or all of these carbide structures.

The triyttrium carbide type structure was shown to exist in the rare earth-carbon systems of samarium, gadolinium, terbium, dysprosium, holmium, erbium, thulium, ytterbium and lutetium. The lattice constants of the carbon-rich side of these carbides are shown in Table 12. This phase was not observed in the lanthanum-, cerium-, praseodymium-, and neodymium-carbon systems. The equilibrium lanthanum-carbon phase system is discussed later; both equilibrium and quenching studies of lanthanum-carbon alloys indicated the presence of only two compounds, the sesqui- and di-carbides. The results of an x-ray study of several cerium-, praseodymium-

Table 12. Lattice constants of the carbon-rich side of the tri-rare earth carbides

Rare earth	Lattice constant (Å)	Rare earth	Lattice constant (Å)
samarium	5.172 ± 0.010	erbium	5.034 ± 0.001
gadolinium	5.126 ± 0.005	thulium	5.016 ± 0.004
terbium	5.107 ± 0.002	ytterbium	4.993 ± 0.001
dysprosium	5.079 ± 0.005	lutetium	4.965 ± 0.001
holmium	5.061 ± 0.002	yttrium	5.102 ± 0.002
	yttrium (yttrium-rich side)	5.127 ± 0.001	

and neodymium-carbon alloys (Table 13) show that the tri-rare earth carbide does not exist in these three systems under the described conditions. It should be pointed out that these results indicate that the cerium monocarbide reported by Brewer and Krikorian (1956) was undoubtedly a solid solution of carbon in cerium. Their lattice constant, a_o = 5.130 Å, is identical to the value found for the cerium metal saturated with carbon. From the description of their work, it is understood how they misinterpreted the existence of the monocarbide. Also, this study does not confirm the existence of the silvery cerium monocarbide reported by Warf (1956).

The plutonium sesquicarbide type structure was found in the lanthanum-, cerium-, praseodymium-, neodymium-, samarium-, gadolinium-, terbium-, dysprosium- and holmium-carbon systems. The lattice parameters and x-ray densities are recorded in Table 14. The lattice parameter for the cerium compound agrees well with the value reported by Brewer and Krikorian (1956), $a_o = 8.455 \pm 0.008$ Å. The other rare earths and yttrium do not form this structure. However, it appears that these rare earths and yttrium form a sesquicarbide; the structure probably has a lower symmetry than either hexagonal or tetragonal. This complex powder pattern was first observed in the yttrium system in several alloys near the sesquicarbide composition. The sesquicarbides of

Table 13. X-ray study of some cerium-, praseodymium-, and neodymium-carbon alloys[a]

Composition of alloy		Phases present
%C	%R.E.	
		Cerium
	100	f.c.c. Ce, a_o = 5.1612[b]
1.1	98.9	f.c.c. Ce, a_o = 5.133
2.78	97.22	theoretical composition of Ce_3C
2.8	97.2	f.c.c. Ce, a_o = 5.130; b.c.c. Ce_2C_3, a_o = 8.448
7.89	92.11	theoretical composition of CeC
7.9	92.1	f.c.c. Ce, a_o = 5.130; b.c.c. Ce_2C_3, a_o = 8.449
11.39	88.61	theoretical composition of Ce_2C_3
12.0	88.0	b.c.c. Ce_2C_3, a_o = 8.4476; b.c.t. CeC_2 (only a few weak lines)
14.63	85.37	theoretical composition of CeC_2
14.6	85.4	b.c.t. CeC_2, a_o = 3.878, c_o = 6.488
19.0	81.0	b.c.t.CeC_2, a_o=3.878, c_o=6.488; free c(determine by chemical analysis)
20.45	79.55	theoretical composition of CeC_3

[a]All alloys were examined in the quenched form (as arc-melted) as well as in the annealed condition.

[b]Spedding et al., (1956).

Table 13. (Continued)

Composition of alloy %C	%R.E.	Phases present
		Praseodymium
	100	hex. Pr, a_o = 3.6725, c_o = 11.835[b]
4.0	96.0	hex. Pr; b.c.c. Pr_2C_3
		Neodymium
	100	hex. Nd, a_o = 3.6579, c_o = 11.799[b]
2.0	98.0	hex. Nd; b.c.c. Nd_2C_3
2.7	97.3	hex. Nd; b.c.c. Nd_2C_3

Table 14. Lattice constants and x-ray densities for some rare earth sesquicarbides

Rare earth	Lattice constant, a_o		X-ray density[a]
	Lanthanum rich side (Å)	Carbon rich side (Å)	(gm/cm^3)
Lanthanum[b]	8.8034 ± 0.0004	8.8185 ± 0.0004	6.079
Cerium	8.4476 ± 0.0004[c]		6.969
Praseodymium	8.5731 ± 0.0005	8.6072 ± 0.0006	6.621
Neodymium	8.5207 ± 0.0011	8.5478 ± 0.0016	6.902
Samarium	8.3989 ± 0.0012	8.4257 ± 0.0012	7.477
Gadolinium	8.3221 ± 0.0005	8.3407 ± 0.0006	8.024
Terbium	8.2434 ± 0.0005	8.2617 ± 0.0007	8.335
Dysprosium	8.198 ± 0.002		
Holmium		8.176 ± 0.003	8.892

[a]Computed from lattice constant of the carbon rich side and assuming the stoichiometry to be R_2C_3.

[b]Density at the theoretical composition of La_2C_3 is 6.081 gm/cm^3.

[c]No solid solubility exhibited.

holmium, erbium, thulium and lutetium appear to be isostructural with the yttrium compound. The holmium sesquicarbide is dimorphic. Ytterbium also forms an intermediate carbide, but it does not appear to be isostructural with the plutonium or the yttrium type sesquicarbides.

The dicarbides of the rare earths and yttrium are all isostructural with the calcium carbide type compound. The lattice parameters, c/a ratios and x-ray densities for these compounds are listed in Table 15. The values obtained in this research for the dicarbides of lanthanum, cerium, prase-

Table 15. The lattice constants, c/a ratios and x-ray densities of the rare earth dicarbides

Rare earth	Lattice constants a_o (Å)	c_o (Å)	c/a ratio	x-ray density gm/cm^3
Lanthanum	3.934 ± 0.002	6.572 ± 0.001	1.671	5.319
Cerium	3.878 ± 0.001	6.488 ± 0.002	1.673	5.586
Praseodymium	3.855 ± 0.002	6.434 ± 0.004	1.669	5.728
Neodymium	3.823 ± 0.001	6.405 ± 0.003	1.675	5.970
Samarium	3.770 ± 0.001	6.331 ± 0.003	1.679	6.434
Gadolinium	3.718 ± 0.001	6.275 ± 0.003	1.688	6.939
Terbium	3.690 ± 0.002	6.217 ± 0.005	1.685	7.176
Dysprosium	3.669 ± 0.001	6.176 ± 0.003	1.683	7.450
Holmium	3.643 ± 0.001	6.139 ± 0.002	1.685	7.701
Erbium	3.620 ± 0.001	6.094 ± 0.003	1.683	7.954
Thulium	3.600 ± 0.002	6.047 ± 0.007	1.680	8.175
Ytterbium	3.637 ± 0.004	6.109 ± 0.010	1.680	8.097
Lutetium	3.563 ± 0.001	5.964 ± 0.006	1.674	8.728
Yttrium	3.664 ± 0.001	6.169 ± 0.004	1.684	4.528

odymium, neodymium and samarium agree well with those values reported by von Stackelberg, see Table 3.

Several additional cerium- and lanthanum-carbon alloys were examined in an attempt to confirm the existence of the cerium tricarbide reported by Warf (1956) and Wells (1950). Microscopic examination and chemical and x-ray analysis show that alloys near the tricarbide composition (either quenched or slow cooled from the molten state) contain only free carbon and the rare earth dicarbide. The photomicrograph of the carbon-lanthanum dicarbide region is shown in Figure 37.

The x-ray diffraction data for all these carbides are shown in Appendix II.

Hydrolytic Studies

Hydrolytic studies of some of these rare earth carbides were undertaken to supplement the x-ray data. The compounds examined were typical examples of the three different carbides (R_3C, R_2C_3 and RC_2) found in the rare earth series. The triyttrium, lanthanum sesqui- and lanthanum di-carbides were chosen as being typical examples of the three structures. Since the carbon atoms are far apart in the triyttrium carbide, this compound might be expected to liberate only pure methane and hydrogen upon hydrolysis. The sesquicarbide and dicarbide with carbon atoms close together might be expected to form acetylene and other unsaturated and saturated hydro-

carbons. However, they should not be expected to form methane, since this would indicate a cleaving of the carbon to carbon bond. The presence or absence of hydrogen should give some idea as to the valence of the metal ion in these compounds. Ytterbium dicarbide was also examined because its lattice parameters appear abnormal (Table 15), which indicates that it might exhibit some divalent character in this compound, and the relative amounts of the products liberated might verify this observation.

The carbides, except the triyttrium compound, react quite readily with water at room temperature. If the triyttrium carbide is added to 0.1 to 1.0 N hydrochloric acid solution the reaction appears to have about the same reactivity as the other carbides do with water. The gases liberated upon hydrolysis were analyzed both qualitatively and quantitatively by a mass spectrometer. The amount of hydrogen gas liberated could not be obtained very accurately, however, the order of magnitude could be determined by this method. The results are shown in Table 16.

Discussion

The tri-rare earth carbides

Interstitial compounds which have non-metallic atoms occupying only some of the octahedral or tetrahedral holes are not uncommon. The nitrides of tungsten, molybdenum,

Table 16. Results of the hydrolytic study of some rare earth carbides[a]

Gas liberated	Compound			
	Y_3C (%)	La_2C_3 (%)	LaC_2 (%)	YbC_2 (%)
acetylene, C_2H_2	--	50.7[b]	70.2[b]	71.3[b]
ethylene, C_2H_4	--	4.5	8.4[b]	17.3[b]
ethane, C_2H_6	--	15.7[b]	12.2[b]	7.3[b]
propadiene, propyne } C_3H_4	--	1.9	--	--
cyclopropane, propylene } C_3H_6	--	1.3	--	--
propane, C_3H_8	--	0.3	--	--
1,2-butadiene, 1,3-butadiene, ethyl acetylene, dimethyl acetylene } C_4H_6	--	7.2[b]	2.0	0.6
butene-1, cis-butene-2, trans-butene-2 } C_4H_8[c]	--	4.6	2.0	2.9
n-butane, C_4H_{10}[c]	--	0.9	0.5	0.4

[a]Results are within ± 20 per cent of the amount reported unless otherwise stated.

[b]Results are within ± 5 per cent of the amount reported.

[c]The analysis of the data from the mass spectrometer indicates that branched chained hydrocarbons having the general formulas C_4H_8 and C_4H_{10} probably are not present in the hydrolytic products.

Table 16. (Continued)

Gas liberated	Compound			
	Y_3C (%)	La_2C_3 (%)	LaC_2 (%)	YbC_2 (%)
methane	31.9	--	--	--
hydrogen	68.1	13.0[d]	4.8[d]	nil
total	100.0	100.1	100.1	99.8

[d]Results are within ± 50 per cent of the amount reported.

manganese and iron; the hydrides of zirconium, titanium and palladium; and the carbides of tantalum, niobium, molybdenum and tungsten have been known for some time to have these types of structures. The lower carbide of niobium has been reported by Umanskij (1940) to exist over a wide range of solid solubility, 16.7 at % (Nb_5C) to 33 at % (Nb_2C). This carbide has a face-centered cubic structure and appears to be quite similar to the tri-rare earth carbides, except that the niobium compound has a greater range of solid solubility. The other carbides (tantalum, tungsten and molybdenum) are all hexagonal and exhibit only a small range of solid solubility (about two or three atomic per cent). If the heavy metal atoms form a face-centered cubic lattice, it is classified according to the Strukturbericht notation as L_1', the Fe_4N type. If the metal atoms form a hexagonal closest-parked lattice it is classified as L_3', the interstitial A_3 type. Therefore, the tri-rare earth carbides are of the L_1' type.

Figure 8 shows that the lattice parameters of the various tri-rare earth carbides lie on a straight line when plotted against the atomic number. The lattice parameter of the yttrium compound lies between the values for terbium and dysprosium carbides. The fact that these lattice parameters lie on a straight line is somewhat unique, since many such plots of different compounds in general form a cusp at gadolinium (for example see Figures 9 and 11). A comparison of the radii derived from the metal to metal distances in the tri-rare earth carbides with the metallic radii (Table 17) shows that the metal to metal distances are expanded on an average of 1.3 per cent by the addition of carbon to the metal to form the lower carbide. A notable exception is that of ytterbium which undergoes a contraction of 9.02 per cent. It should be interesting to see how this increase will affect the various physical properties, i.e., magnetic properties, resistivity, Hall coefficients, etc. The trigadolinium carbide, as gadolinium metal, is ferromagnetic and it appears to have a higher Curie point than the metal.

Further examination of this rare earth carbide shows that if the carbon atoms occupied two adjacent octahedral holes the carbon to carbon bond distance would be equal to $\frac{1}{2}\sqrt{2}\,a_o$. The smallest bond distance would be observed in lutetium, 3.51 Å, the largest in samarium, 3.66 Å. With carbon atoms even as close as 3.5 Å there is little chance

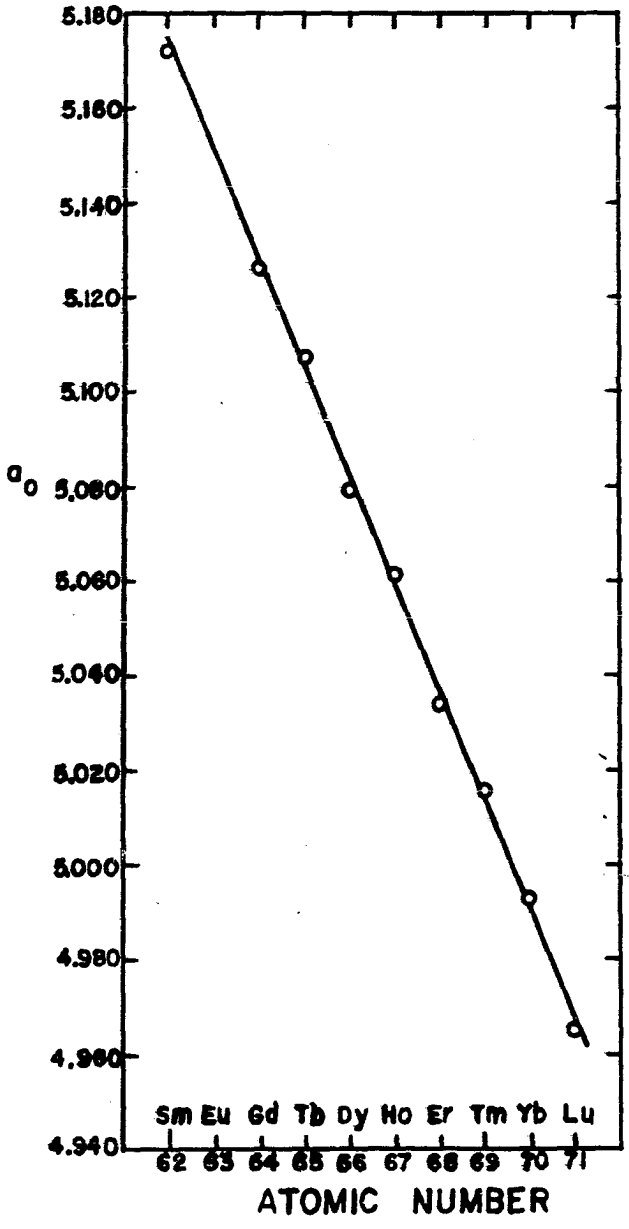

Figure 8. The lattice constants of the tri-rare earth carbides versus the atomic number.

Table 17. Comparison of the radii derived from the metal to metal distances in the tri-rare earth carbide with the metallic radii; and the metal to carbon distances in this carbide

	Radii[a] calculated from the carbide (Å)	Metallic[b] radii (Å)	Per cent change	Metal to[c] carbon distance (Å)
samarium	1.829	1.802	1.50	2.586
gadolinium	1.812	1.802	0.55	2.563
terbium	1.806	1.782	1.35	2.554
dysprosium	1.796	1.773	1.30	2.540
holmium	1.789	1.766	1.30	2.530
erbium	1.780	1.757	1.31	2.517
thulium	1.773	1.746	1.55	2.508
ytterbium	1.765	1.940	-9.02	2.496
lutetium	1.755	1.734	1.21	2.482
yttrium	1.804	1.801	0.17	2.551
yttrium (yttrium-rich side)	1.813	1.801	0.67	--

[a]Equal to $\frac{1}{2}\sqrt{2}\,a_o$.

[b]Calculated from the lattice constants of the metals, Spedding et al., (1956).

[c]Equal to $\frac{1}{2}\,a_o$.

that they would combine upon hydrolysis and form some C_2H_x molecule. Therefore, this compound should be expected to yield only methane and hydrogen gases when attacked by water or dilute acids. The results shown in Table 16 reveal that this is true.

The existence of this tri-rare earth carbide in most of the rare earth-carbon systems and not in the systems of the first four lanthanides is not completely understood. For atoms to occupy the octahedral holes the ratio of the radii of the large atoms to small atoms must lie between 0.414 and 0.732. If the ratio is smaller than 0.414, then the zinc sulfide (sphalerite) structure is more stable, i.e., the smaller atoms will occupy the tetrahedral holes. If the ratio were greater than 0.732, then the cesium chloride (body-centered cubic) structure would be preferred. Examination of the ratio of the radius of carbon (0.771 Å) to the metallic radius of the various rare earths (Table 17) show that they all lie well within this range. But if the metallic radius were subtracted from the corresponding metal to carbon distance (Table 17), then one would obtain a value for the carbon radius in this compound. The calculated radius obtained from these nine carbides, excluding ytterbium, varied from 0.784 to 0.748; the mean was 0.763. Using the mean value to compute the radius ratios, the following values were obtained: 0.406, 0.418, 0.417, 0.419, 0.423, 0.424, and 0.440

for lanthanum, cerium, praseodymium, neodymium, samarium, yttrium and lutetium, respectively. Only the radius ratio for lanthanum is less than the critical value of 0.414, but the values of cerium, praseodymium, and neodymium are just slightly greater (within 1.2 per cent). The value for samarium is more than 2 per cent above the critical ratio. It is possible that the size effect does determine whether or not this compound will be formed. Also, the fact that the first four rare earth metals[1] are hexagonal closest-packed with a double c-axis while the others have a normal c-axis (Spedding et al., 1956) may be significant.

The rare earth sesquicarbides

The existence of the rare earth sesquicarbides from lanthanum to holmium increases the known number of plutonium sesquicarbide type compounds from four[2] to twelve. Some interesting comparisons can be pointed out among the rare earth compounds.

In Figure 9 the lattice parameters of the rare earth sesquicarbides are plotted against the atomic number. One

---

[1]Cerium begins to form the hexagonal closest-packed structure with a double c-axis at 15 ± 5°C (McHargue et al., 1957).

[2]The neptunium compound has been reported to exist, but no lattice parameters were reported (Sheft and Fried, 1953).

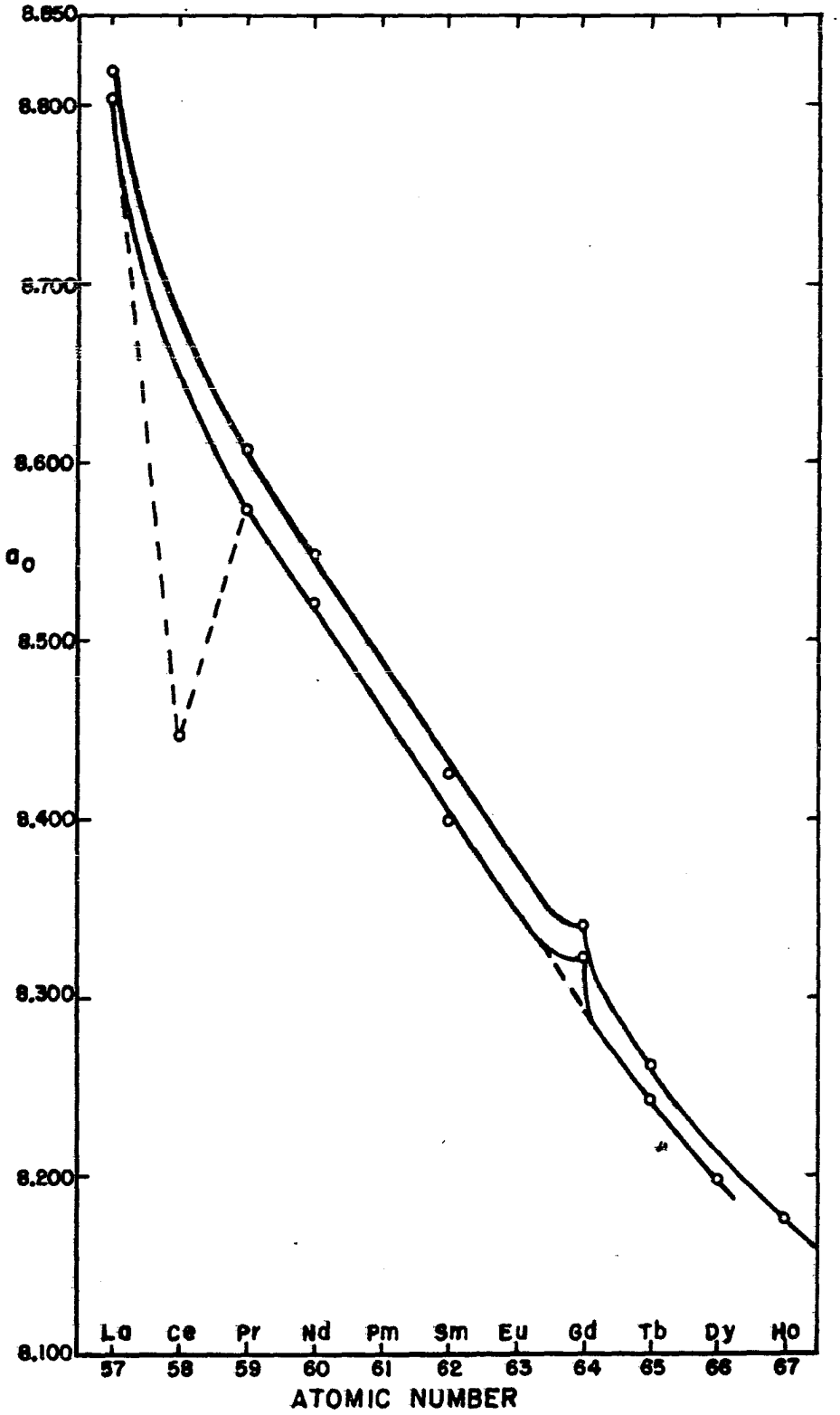

Figure 9. The lattice parameters of the rare earth sesquicarbide versus the atomic number.

notes that the lattice parameter of the cerium compound lies between the values for neodymium and samarium compounds. This may indicate that cerium is partially or wholly tetravalent in this compound. The characteristic cusp is, as usual, found at gadolinium. The density of these rare earth sesquicarbides versus the atomic number gives a straight line, except for cerium (Figure 10). The fact that the last four heavy rare earths do not form this crystal type might indicate that the plutonium sesquicarbide type compounds may be size dependent. If this were true, then the metal atom must have an ionic radius greater than 0.88 or 0.89 Å to form this structure.

Comparing the results of the hydrolytic studies (Table 16) of the lanthanum di- and sesqui-carbides it is noted that the amount of acetylene liberated is approximately 1.4 times larger for the dicarbide, while the amount of hydrogen is smaller by about 2.5 times. It is also significant that the C_3H_x homologs are formed only from the sesquicarbide. The relative amounts of hydrogen liberated can be explained if one assumes that $C_2^=$ anions are formed and the extra lanthanum valence electrons contribute to the conduction band. For the sesquicarbide the number of conducting electrons per lanthanum atom is 1.5, and 1.0 for the dicarbide. Therefore, the amount of hydrogen liberated should be greater for the sesquicarbide, and this is what is observed. The relative

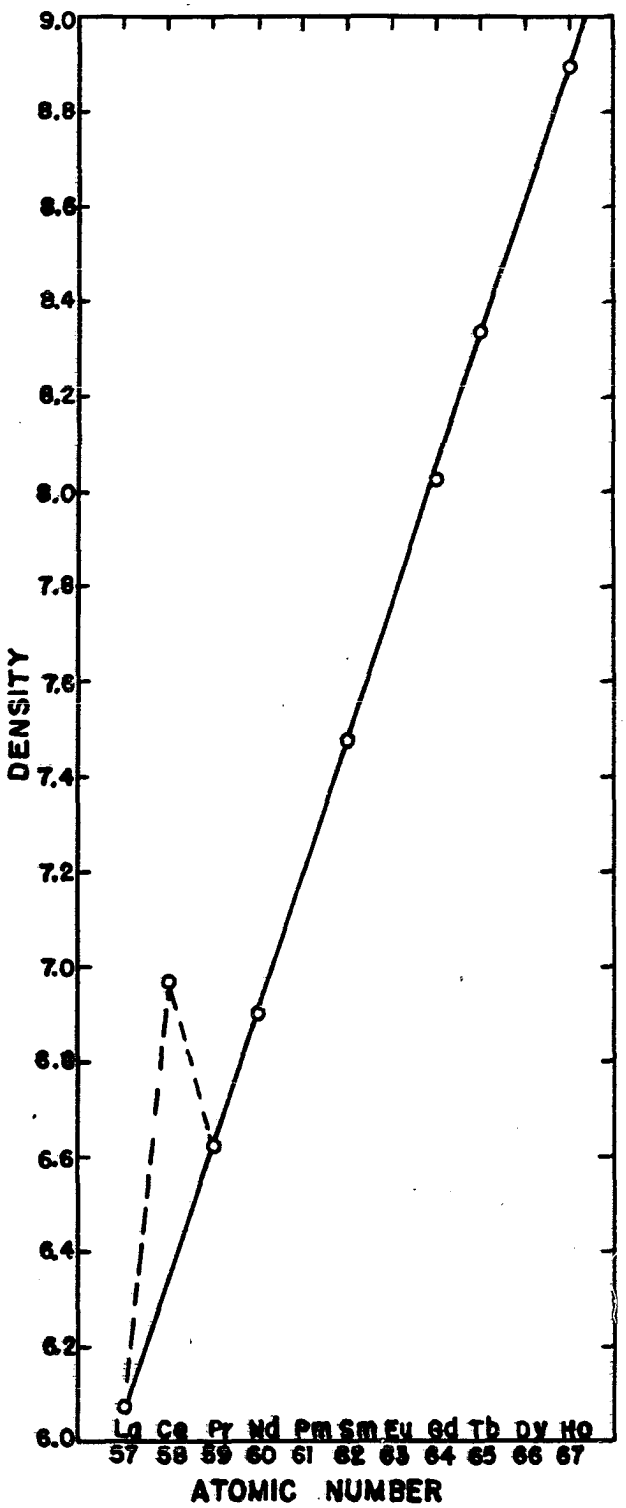

Figure 10. Density of the rare earth sesquicarbides versus the atomic number.

amounts of acetylene liberated can be explained by the number of $C_2^=$ groups per lanthanum atom. There is 1.0 group per lanthanum for the dicarbide and 0.75 for the sesquicarbide, and therefore, the dicarbide is expected to liberate more acetylene, which it does. The formation of C_3H_x homologs is not nearly as easily explained, but it may be significant that the carbon to carbon distance is slightly greater for the sesquicarbide than for the dicarbide (1.32 to 1.28 Å).

The rare earth dicarbides

A plot of the lattice parameters for these dicarbides versus the atomic number is shown in Figure 11, and the densities as a function of the atomic number are given in Figure 12. The lattice parameters of the yttrium dicarbide lie between dysprosium and holmium. The cusp, again, appears at gadolinium, but only for the "c_o" values. Ytterbium dicarbide appears to have an abnormal lattice parameter, which lies between holmium and erbium. This might indicate that the ytterbium is partially or wholly divalent in this compound. Hydrolytic studies of this material show a slight increase of acetylene and the absence of hydrogen as compared to the lanthanum dicarbide, which might be expected for a metal having a valence less than three.

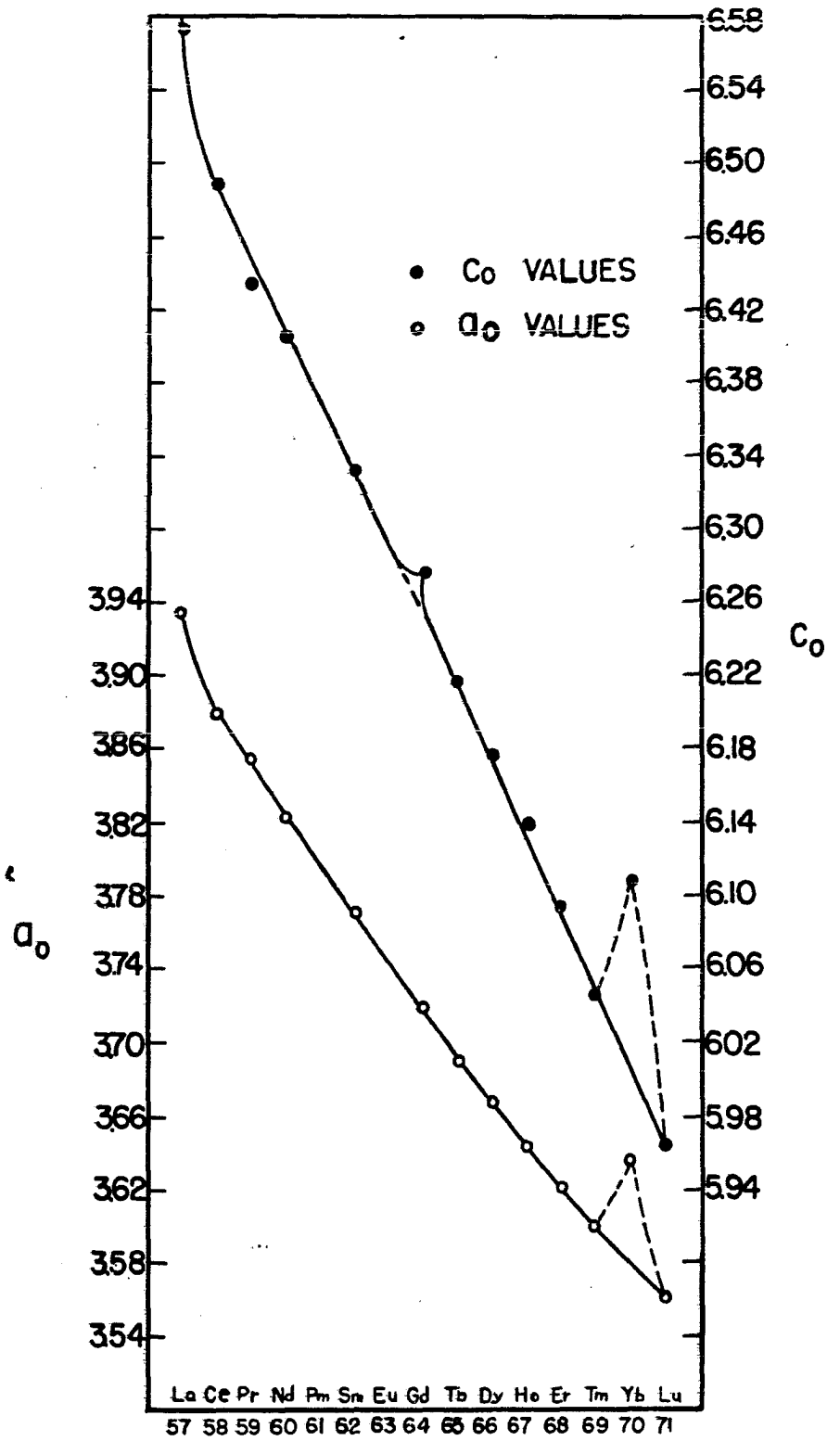

Figure 11. Lattice constants of the rare earth dicarbides versus the atomic number.

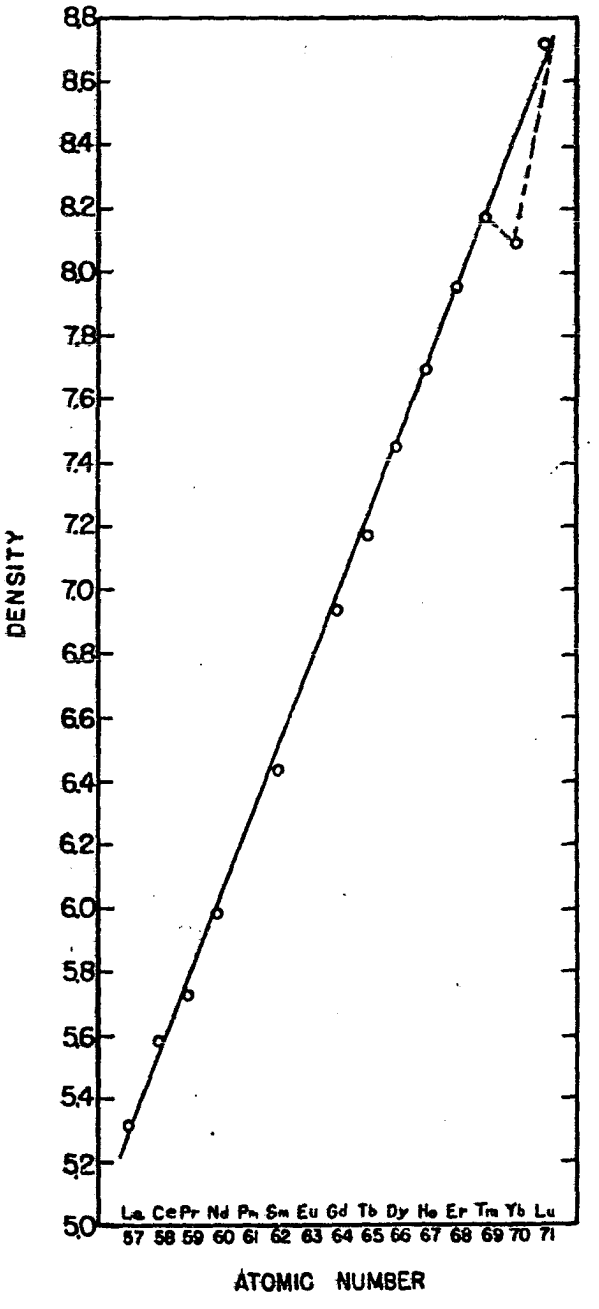

Figure 12. Densities of rare earth dicarbides versus the atomic number.

THE LANTHANUM-CARBON EQUILIBRIUM DIAGRAM

Apparatus and Methods

Three types of furnaces were used in this study for determining liquidus and solidus lines. For low temperature thermal analysis a tantalum wound resistance furnace was employed. At intermediate temperatures (1000-2000°C) a tantalum tube furnace was used and at high temperatures (greater than 2000°C) an induction furnace was employed.

Low temperatures

Figure 13 shows the details of the furnace and arrangement of the sample, thermocouple and shielding used for thermal analysis of lanthanum-carbon alloys having between zero and seven per cent carbon. The quartz tube was connected to a vacuum system by sealing the $\frac{71}{60}$ joint with Apiezon W wax. A vacuum tight seal between the copper electrical leads and the quartz tube was accomplished using Apiezon W wax. A vacuum between 10^{-6} and 10^{-5} mm Hg was maintained at all times during a run by a two stage glass diffusion pump (GF-20W, Distillation Products Industries) backed by a mechanical pump (Duo-Seal, 1400B, M.W. Welch Manufacturing Co.) A cold trap (containing liquid nitrogen) was used to prevent any pump oil from reaching the furnace and sample. The vacuum was measured by a cold cathode gage (Model No.

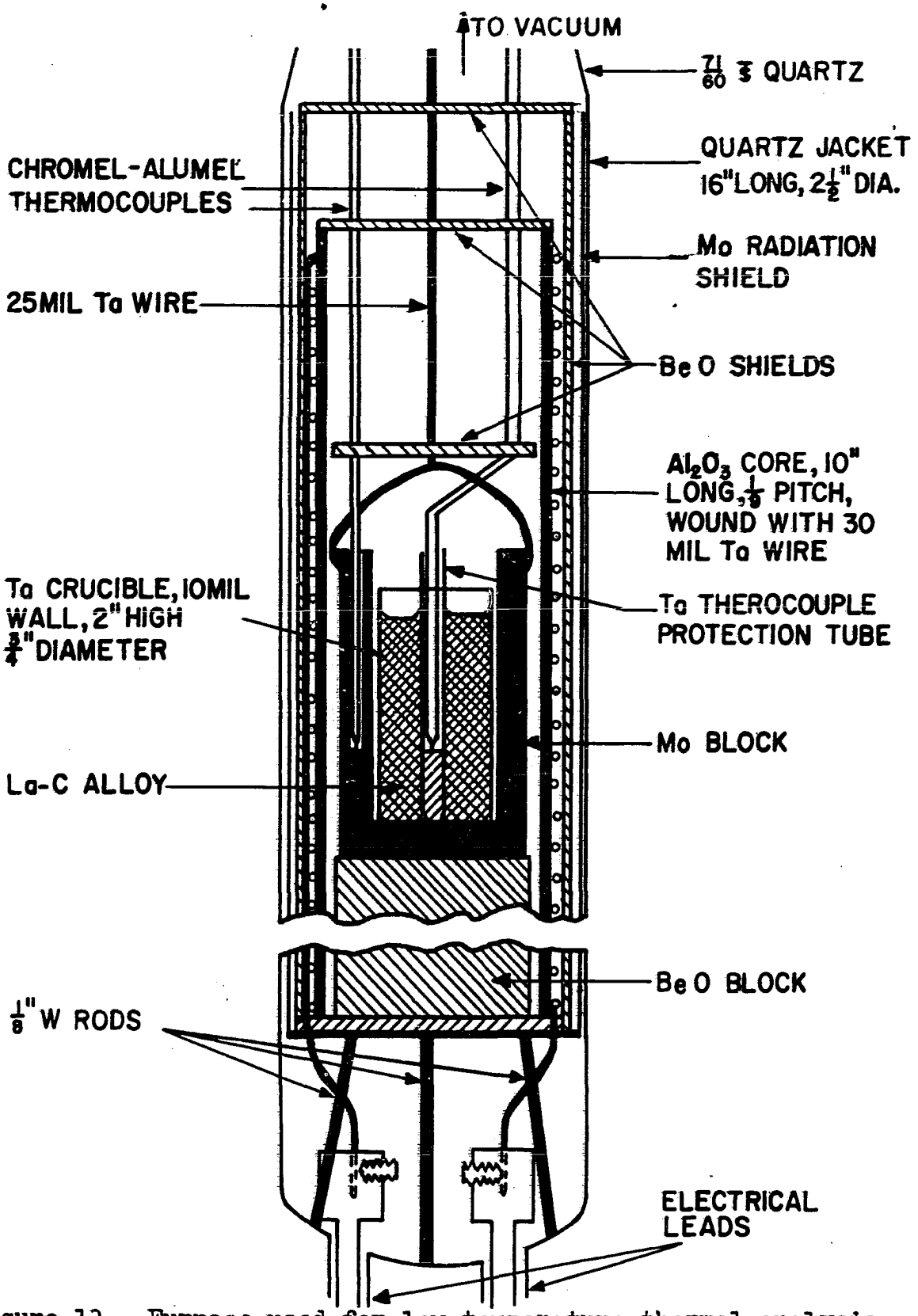

Figure 13. Furnace used for low temperature thermal analysis.

100-A, Miller Laboratories). The entire quartz tube was placed in a water jacket, and constant flow of water kept the Apiezon seals from softening. The two thermocouples, the molybdenum isothermal block containing the sample and the three top beryllia radiation shields were suspended from the main part of the vacuum system so that, when the quartz tube containing the furnace and side radiation shields was removed from the vacuum system there was little difficulty in changing the samples for thermal analysis. A chromel-alumel thermocouple was placed in the molybdenum block and connected to a recorder so that it was possible to tell if there were any large changes in the heating or cooling rates. Before any thermal analyses were made on the lanthanum-carbon alloys the chromel-alumel thermocouple in the sample was checked using secondary standards (tin, lead, zinc, aluminum and copper) calibrated by the National Bureau of Standards. The thermocouple was also checked against the freezing points of silver and copper-silver eutectic. After the thermal analyses were finished the thermocouple was again checked against the aluminum and copper standards and no appreciable difference in the emf (less than 0.04 mv or 1°C) between the two calibration runs was noted. Cooling and heating curves of the standards and various lanthanum-carbon alloys were taken by measuring and recording the emf every 30 seconds. The power was fed into the furnace using two

variable transformers, connected in series; the first was set at a given power output and the second was varied from zero to a hundred per cent using a two rpm Holtzer-Cabot motor. The motor was geared down such that it required 200 minutes to cover the full scale, thus heating and cooling rates between 1.5 and 2.0°C per minute were easily attained. Heating curves were taken after the alloys were annealed at 810 to 830°C for three to four hours.

The alloys were prepared by arc melting according to the procedure described previously, except that the lanthanum and carbon were used in the form of large solid chunks (30-50 gm lanthanum, 1-10 gm carbon) instead of filings. The arc melted alloys were prepared for thermal analysis by melting the arc melted buttons in a tantalum crucible using induction heating. After thermal analysis the alloys were examined microscopically and chemically analyzed. Spectrographic analysis indicated that no tungsten or tantalum and little or no copper (the maximum amount of copper detected was 0.01 per cent) was picked up during arc melting or thermal analysis. The mean result of three carbon determinations gave the composition for the alloy.

Intermediate temperatures

A tantalum tube furnace (shown in Figure 14) was built to determine solidus and liquidus points between 1000 and 2000°C. This furnace was connected to a high vacuum system,

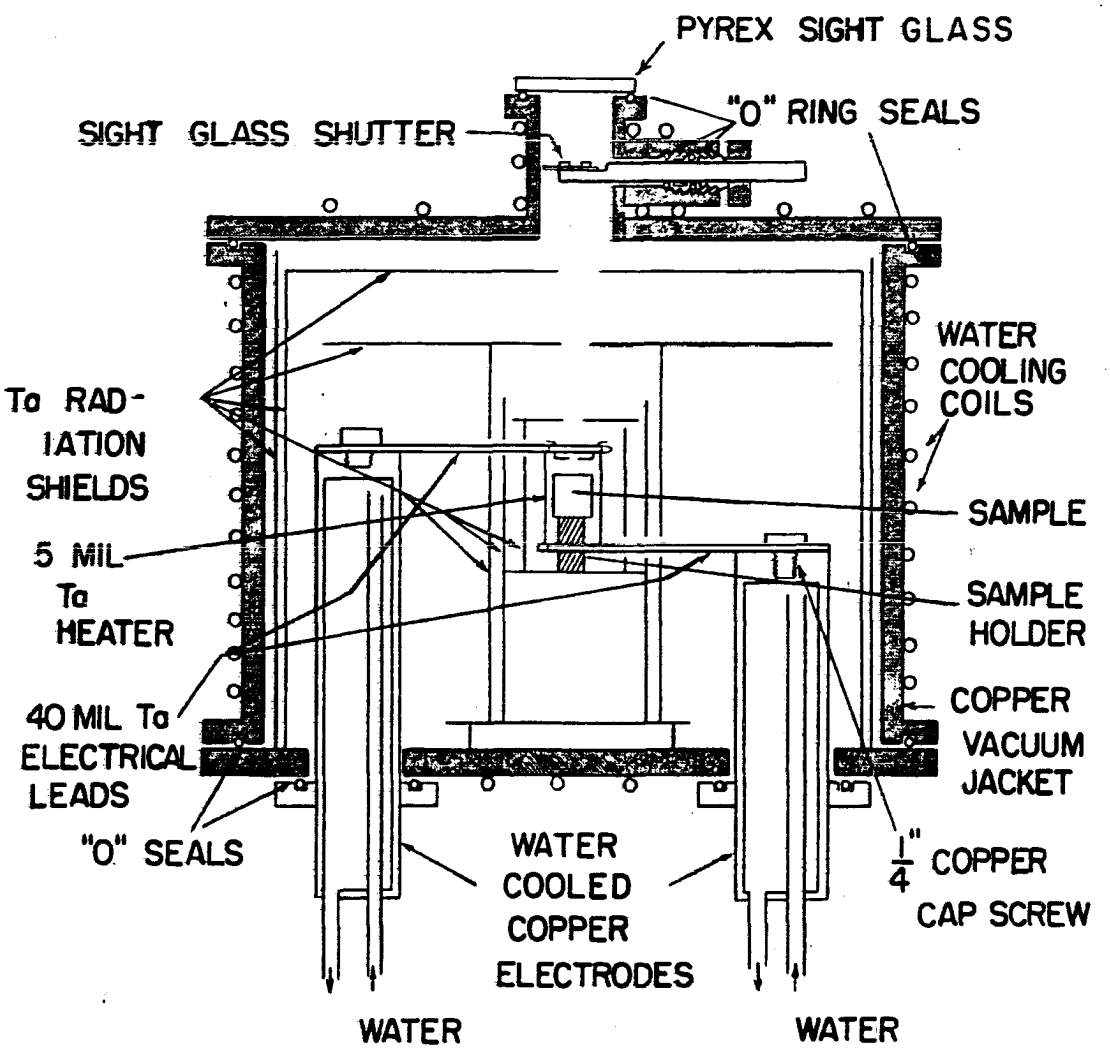

Figure 14. Tantalum tube furnace.

identical to that described above. This system was operated at a pressure between 10^{-6} and 10^{-5} mm Hg during all runs. Although the furnace was quite small (7/8 inch high and 1/2 inch diameter), it was sufficiently large to carry out most operations. A ten kilowatt step-down transformer served as the power supply for this tube furnace. The voltage into the transformer was controlled using two variable transformers connected in series, one was set at a given output, the other was varied from zero to one hundred per cent.

A knowledge of the temperature distribution in the furnace is quite important in the method used for determining the liquidus points. If the differences in temperature were too large, the results would be meaningless. The temperature distribution in the furnace was measured using an optical pyrometer, sighting into a series of holes drilled into a graphite block. The hole depth was always greater than five times the diameter in order to assure black-body conditions. All temperature measurements were made under equilibrium conditions. The results showed that below 1400°C there is about 6-8°C difference between the center of the furnace and 2/3 the distance from the center to the top of the furnace. At 1700°C this difference is 12 to 15°C. The radial distribution remained about the same over all temperatures measured. The center was about 5 to 6°C colder than the point 2/3 the distance from the center to the tantalum heater. However,

in order to make these measurements the two top shields nearest the top of the furnace had to be removed. Therefore, these differences represent a maximum, and probably, are not realized in an experimental run.

The optical pyrometer was first calibrated with a National Bureau of Standards standard light source. However, since it is necessary to sight into the furnace through a pyrex window, the optical system was calibrated against metals with accurately known melting points. The metals used were 99.99 per cent pure silver, copper (calibrated by the National Bureau of Standards) and 99.9 per cent pure nickel. The correction for the sight glass was applied using the following equation:

$$\frac{1}{T_o} - \frac{1}{T_t} = -K \quad , \tag{11}$$

where T_o and T_t are the observed and true temperatures in degrees Kelvin and K is the correction constant. For a clean window the value of K is $(38.9 \pm 0.5) \times 10^{-7}$. The error, $\pm 0.5 \times 10^{-7}$, is the maximum error and it is negligible, since at 2000°C it only amounts to an error of $\pm$ 1°C. The correction factor was assumed to be constant for all temperatures, even above the nickel point.

The liquidus points were determined by the diffusion and saturation method. This procedure involves heating

lanthanum metal at a given temperature above its melting point in a graphite crucible. This temperature is maintained for a length of time sufficient to permit carbon to saturate the lanthanum metal. The carbon content of the center portion of the billet represents the liquidus composition for that temperature. Because graphite is quite porous to lanthanum metal the carbon crucible (1/2 inch high and 3/8 inch in diameter with 1/16 inch walls) had to be placed inside a tantalum crucible to retain the lanthanum. After the samples were held at temperature, the power to the furnace was turned off, and the samples were essentially quenched because of small heat capacity of the furnace. At 2000°C, the cooling rate was 1300°C per minute for the first 1/2 minute interval, at 1000°C it is about 200°C per minute.

The solidus points were obtained using a modified version of Pirani and Alterthum's (1923) method; instead of using the sample as the heater, the specimen was heated by the tantalum tube furnace (Figure 13). A small hole 20 to 30 mil in diameter was drilled with a 20 mil tungsten wire using an ultrasonic drill. The hole depth was at least five times the hole diameter, so that black body conditions were assured. Heating rates of approximately 8°C per minute were used. The temperature at which the first formation of liquid occurred was taken to be the solidus point.

The master alloys were prepared by arc melting 30-40 gm billets. The procedure as previously described was slightly modified because it was quite difficult to obtain a homogeneous alloy with more than six or seven per cent carbon. After a sample was arc melted, inverted and remelted, it was removed from the furnace, crushed into chunks about one cm along an edge, returned to the furnace and arc melted. This procedure was repeated until no visible pieces of carbon were seen on the freshly broken surfaces. The specimens for thermal analysis or x-ray studies were broken off the master alloy when needed. The samples were always chemically analyzed after thermal and x-ray analysis.

The tantalum tube furnace described above was also used for annealing samples for periods of time up to 48 hours. Cooling rates of 6-12°C per minute were used to bring annealed specimens to room temperature.

High temperatures

The vacuum chamber and furnace arrangement used for attaining high temperatures are shown in Figure 15. The vycor standard taper was sealed to a vacuum system using Apiezon T grease. The system was pumped down to a pressure of ten microns of mercury and argon gas was added to increase the pressure to one or two mm of mercury, so that the melting points could be determined without the presence of a gaseous

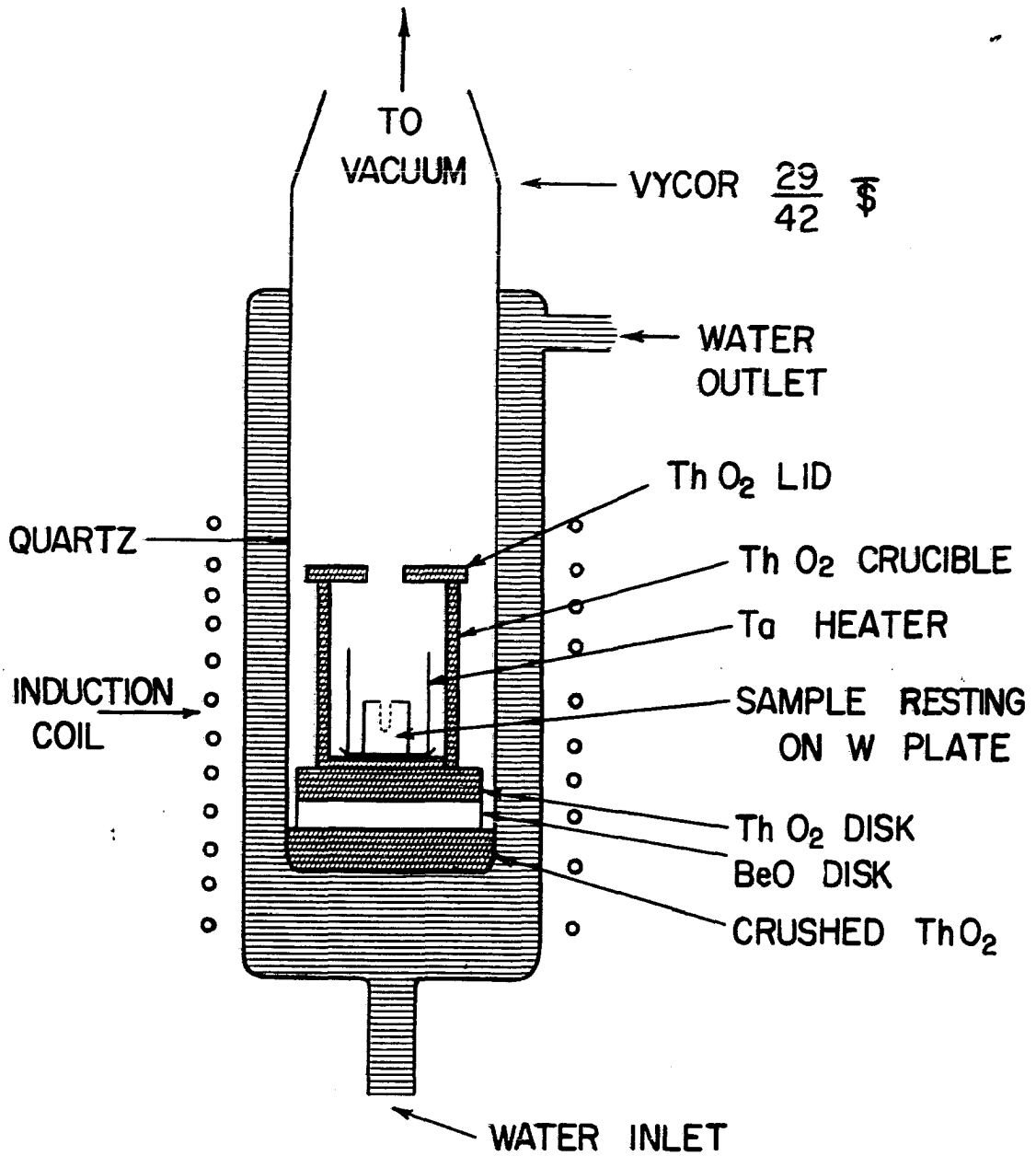

Figure 15. Furnace for determining high temperature solidus points.

discharge caused by the high frequency induction furnace. The heating rate was much faster in this procedure, but near the melting points the rates were reduced to about 15°C per minute. The temperature correction for the sight glass was also applied to the melting points of these alloys. The power for the induction coil was supplied from a 10 KW electronic tube high frequency converter (Model PO-10, Ecco High Frequency Corp.).

An attempt was made to obtain some liquidus points above 2000°C, but in each case the lanthanum and carbon react quite violently and most of the metal was ejected out of the crucible. This was true whether or not the alloy was heated up rapidly or slowly. Using carbon-lanthanum alloys instead of pure lanthanum, the same thing occurred. This may have been due to the oxide coating on the alloy.

Preparation of alloys for microscopic examination

Since all lanthanum-carbon alloys and pure lanthanum tarnish when the usual wet polishing procedures are used, the samples are polished using carbon tetrachloride or absolute alcohol as the coolant. The samples were mounted in one inch diameter bakelite mounts. Rough grinding was followed by polishing the specimen on 320, 500 and 600 grit emery papers. The final polishing step was carried out using diamond paste (National Bureau of Standards grade 1-medium)

on "Microcloth". Samples with a carbon content greater than two or three per cent were not etched, since any etching tarnished the specimen. The various phases in the microstructure were quite easily distinguished without etching. Before microscopic examination of alloys containing more than five per cent carbon, the specimens were generally covered with a low viscosity oil to prevent air oxidation. This oxidation tends to reduce the sharpness of the picture. Low carbon alloys (below two or three per cent carbon) were etched using either a five per cent nital solution or a solution consisting of 15 per cent concentrated nitric acid in glacial acetic acid. The samples were examined microscopically and photographed on an American Optical Metallograph Model 2400.

Determination of solvus lines

Solvus lines were determined by x-ray and microscopic methods. The x-ray technique was based on Vegard's Law. An attempt was made to determine the solubility of carbon in lanthanum metal at various temperatures (room temperature, 175, 380, 555 and 670°C) but the results were so erratic no conclusions could be drawn. The microscopic method was used instead to determine the approximate solvus lines. However, the x-ray method was applied quite successfully to determine the room temperature solid solubility limits of the sesqui-

carbide. The alloys were annealed between 1000 and 1400°C for two to ten hours and slow cooled at 5 to 8°C per minute above 800°C and at 8 to 12°C per minute below 800°C. The alloys were crushed in a dry box for back reflection and Debye-Scherrer x-ray analysis. The lattice constants of the lanthanum sesquicarbide in the two phase regions above and below this compound are reported as weighted averages. The weights were assigned from the standard error of each individual determination, i.e. the smaller the error the greater the weight. The slope of the line through the points in the one phase region was determined by a least squares treatment.

The quenching apparatus used in conjunction with the microscopic method is shown in Figure 16. The system was evacuated by the diffusion and mechanical pumps described previously. Silicon diffusion pump oil was used as the quenching medium. There was a slight increase in the silicon content of the alloys after quenching (from 0.01 to 0.1 per cent) and therefore, the alloys were only used for one quench.

A quantitative microscopic method was used to determine the phase boundary of the lanthanum rich side of the lanthanum sesquicarbide. Areal analysis of quenched alloys was carried out using a point count method. This technique involved superimposing a grid on a negative photomicrograph and count-

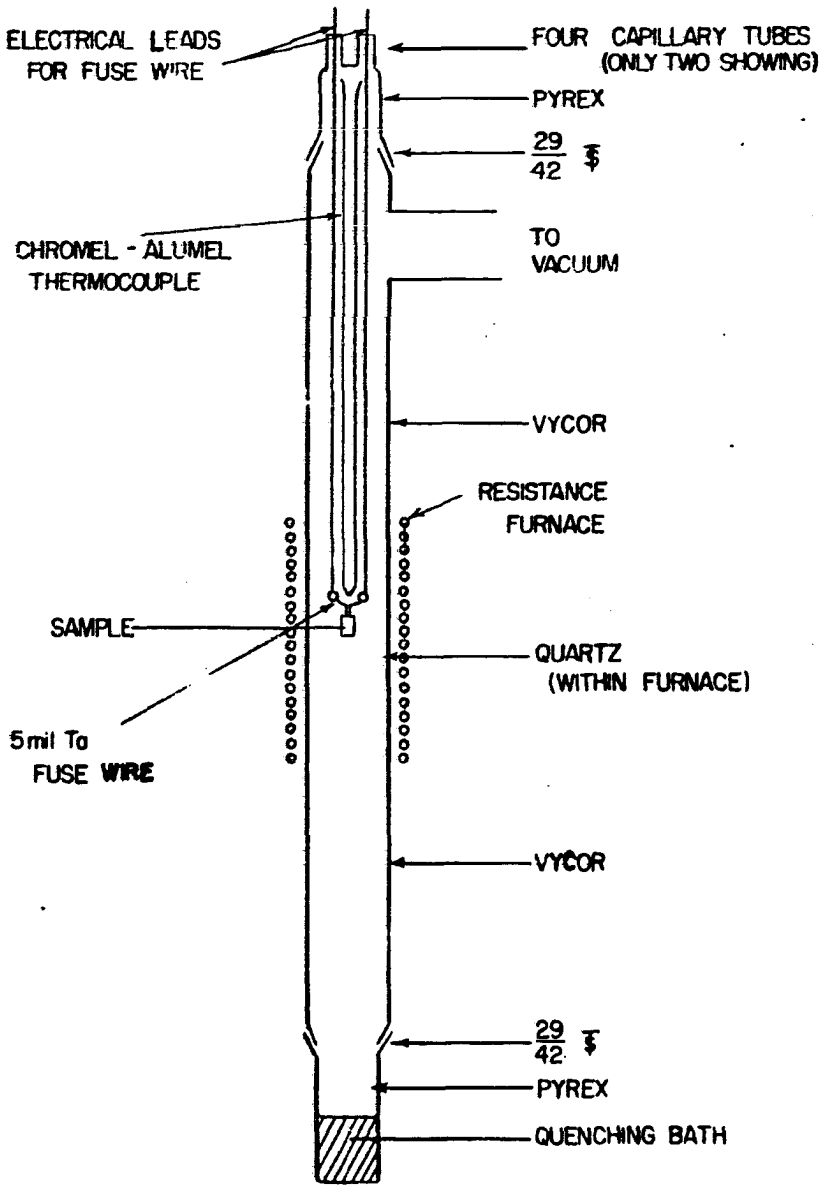

Figure 16. Quenching apparatus.

ing the number of intersections for each phase present. The grid size was 0.1 inch. In general about 10,000 points (intersections) were used for each alloy examined. The relative areas occupied by the different phases is proportional to the volumes of these phases, if the microsection is representative of the whole alloy. The weight percentages of the various phases can be calculated by multiplying the relative volumes by their respective densities.

Results

The equilibrium phase diagram of the lanthanum-carbon system as constructed from thermal, metallographic and x-ray data is shown in Figure 17. The details of the system at low carbon compositions are shown in Figure 18.

The thermal data obtained by heating and cooling curves are given in Table 18. The heating and cooling curves are shown in Figure 19. The eutectic temperature of 806 $\pm$ 2°C was obtained as a mean value from seven determinations, where $\pm$ 2°C is the probable error. The maximum error is $\pm$ 4°C. Although Pirani and Alterthum's method is not very accurate below 900°C, this method was used on two low carbon alloys and the eutectic temperature was observed at about 800°C, (Table 20). Two photomicrographs showing the lanthanum-lanthanum sesquicarbide eutectic are given in Figures 28 and 29. The former shows the lanthanum side of the eutectic,

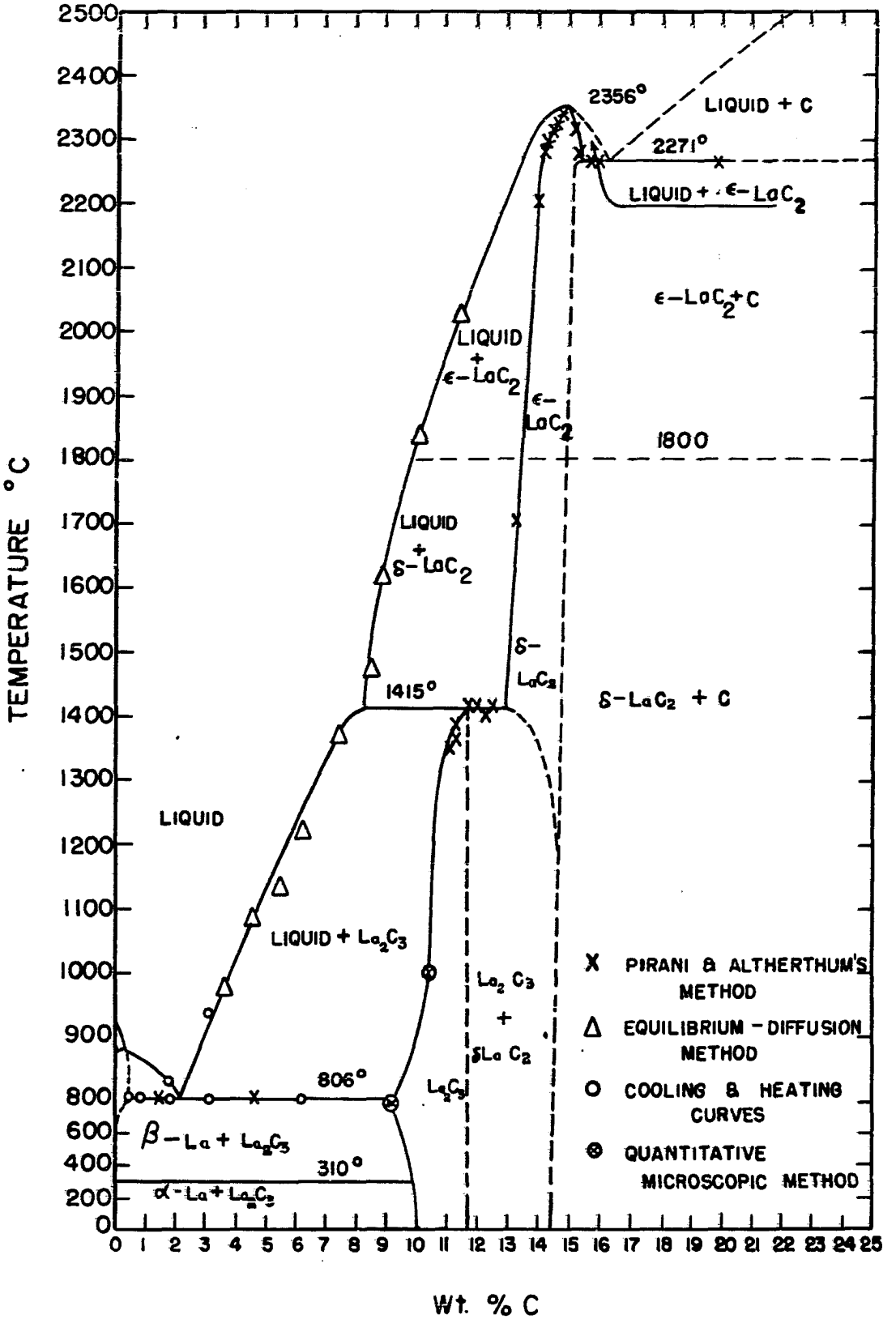

Figure 17. The lanthanum-carbon equilibrium diagram.

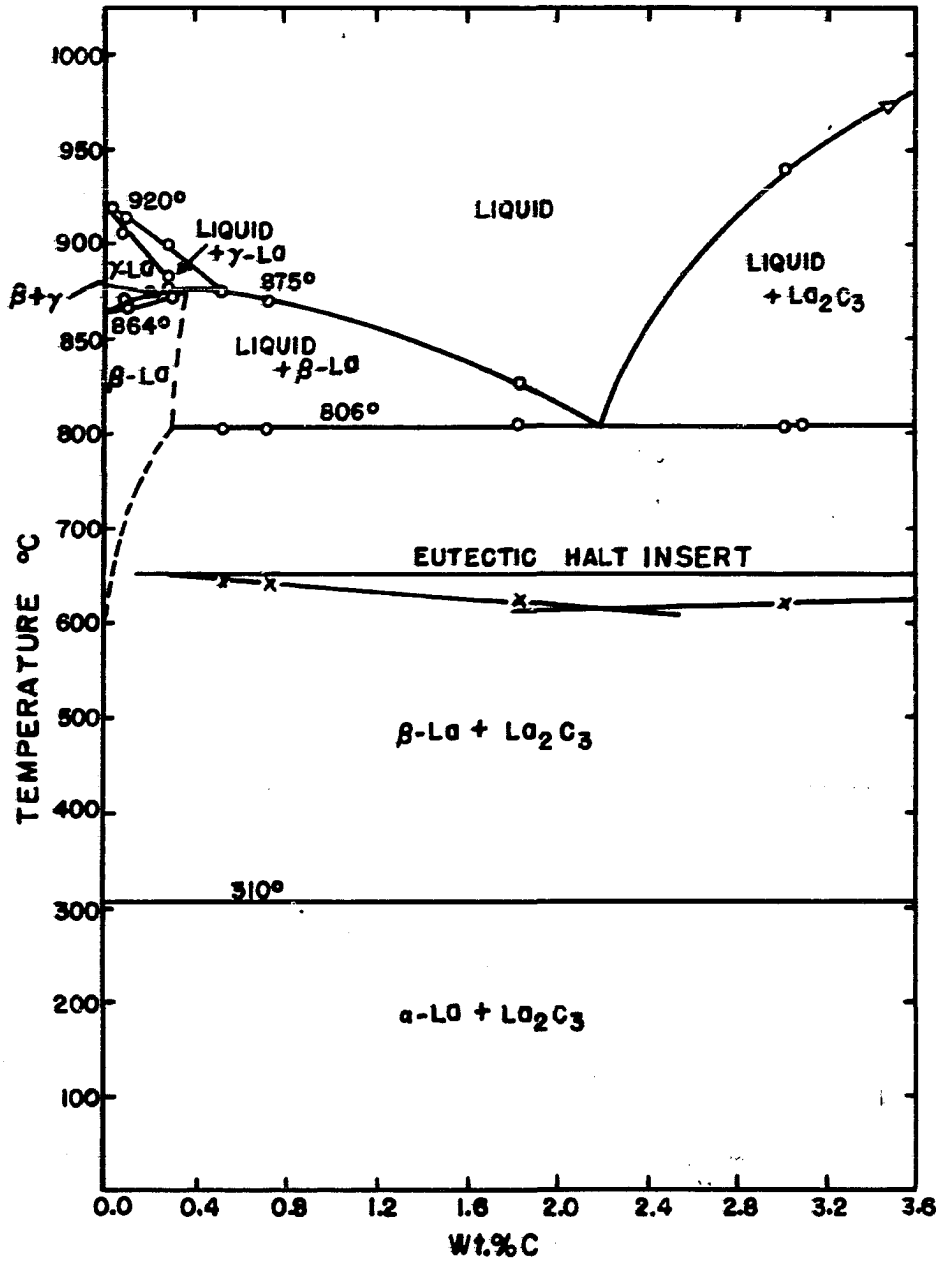

Figure 18. The lanthanum-carbon equilibrium diagram at low carbon compositions.

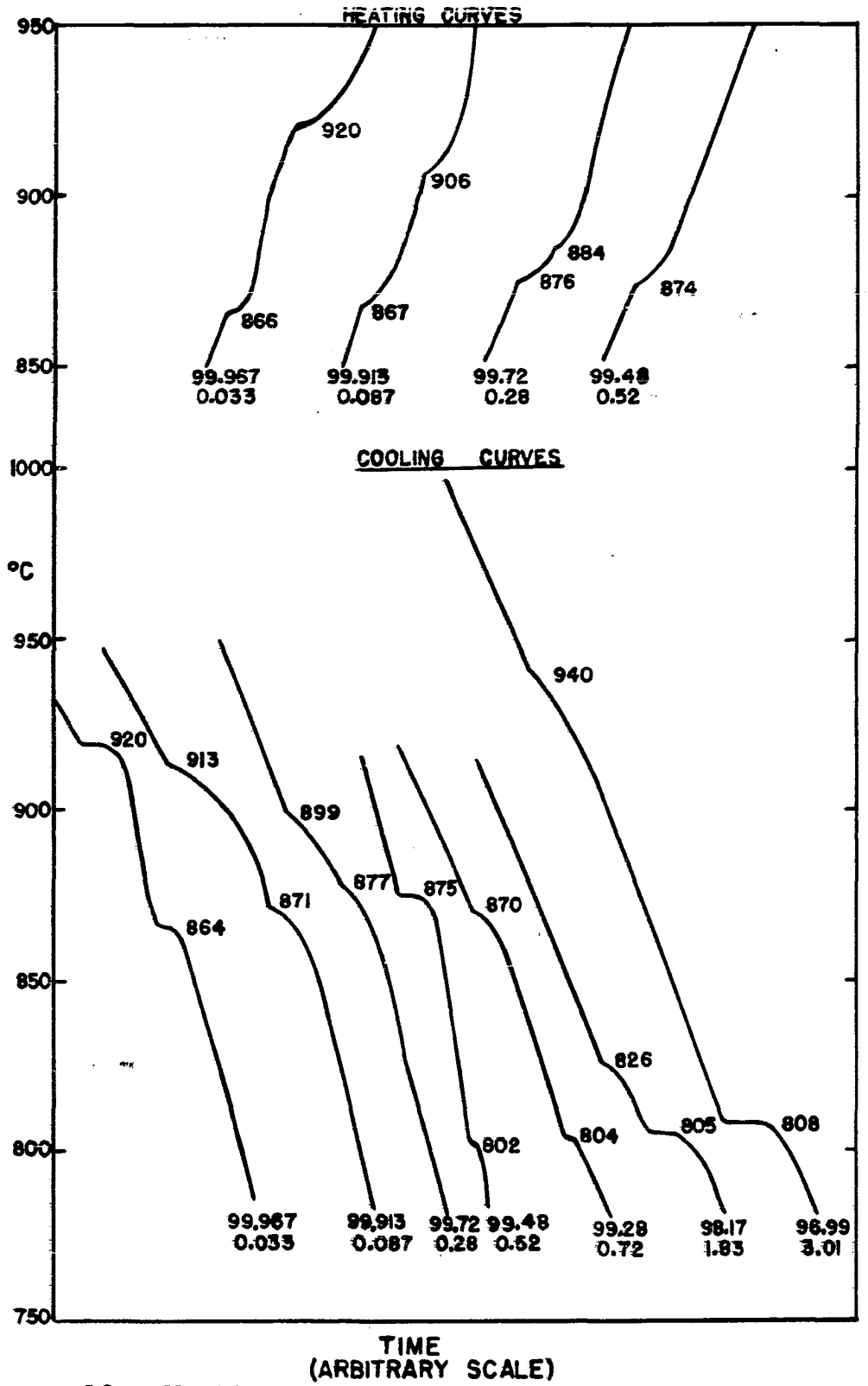

Figure 19. Heating and cooling curves of some lanthanum carbon alloys.

Table 18. Thermal data obtained from heating and cooling curves

%C	%La	Liquidus (°C)	Solidus (°C)	$\gamma \rightarrow \beta$ (°C)	$\beta \rightarrow \gamma$ (°C)	Eutectic (°C)
0.033	99.967	919	919	866	864	--
0.087	99.913	913	906	871	867	--
0.28	99.72	899	884	877	876	--
0.52	99.48	875	874	875	874	802
0.72	99.28	870	--	--	--	804
1.83	98.17	826	--	--	--	805
3.01	96.99	940	--	--	--	808[a]
3.09	96.91	--	--	--	--	807
6.05	93.95	--	--	--	--	806

[a]Mean value of two determinations

while the latter is near the eutectic composition. The eutectic halt is shown in Figure 18 just below the eutectic horizontal. Applying this principle the composition of the eutectic was confirmed, and the solid solubility limit of carbon in lanthanum was found to be 0.30 ± 0.05 per cent C at the eutectic temperature.

The results of the liquidus and solidus determinations by the methods previously described are shown in Tables 19 and 20. The peritectic temperature of lanthanum sesquicarbide is 1415 ± 3°C. The probable error for four determinations is ± 2°C and the uncertainty in applying the correction factor

Table 19. Equilibrium carbon content of lanthanum heated in contact with graphite

Temperature (°C)	Time at temperature (min.)	Carbon (%)
972 ± 6	20	3.49
1081 ± 11	15	4.44
1124 ± 7	15	5.26
1217 ± 11	15	6.12
1368 ± 8	15	7.15
1468 ± 6	15	8.23
1614 ± 8	15	8.70
1835 ± 8	12	9.92
2021 ± 13	12	11.22

Table 20. Melting points of lanthanum-carbon alloys

Melting point (°C)	Carbon content (%)
800 ± 15	1.4
810 ± 10	4.4
1365	10.99
1389	11.10
1383	11.12
1412	11.49
1417	11.91
1417	12.0
1413	12.38

Table 20. (Continued)

Melting point (°C)	Carbon content (%)
1700	13.07
2204	13.85
2309	14.02
2316	14.07
2324	14.35
2338	14.46
2347	14.46
2278	15.03
2321	15.11
2270	15.55
2265	15.6
2270	19.66

for the sight glass at this temperature is less than one degree, but nevertheless, one is added, to give a total value for the probable error of ± 3°C. Figures 33 and 34 show to some extent the peritectic reaction (liquid + δ-LaC_2 ⟶ La_2C_3) in a 10.5 per cent and a 12.9 per cent carbon-lanthanum alloy, respectively. The former was cooled from 1600 to 1375°C at a rate of 5-8°C per minute and then furnace cooled to room temperature, while the latter was furnace

cooled from 1700 to 25°C. The light area in the primary phase is lanthanum dicarbide which did not have sufficient time to react with the liquid to form the sesquicarbide. The gray area in both the primary and secondary phases is lanthanum sesquicarbide, while the dark area in the secondary phase is the lanthanum-lanthanum sesquicarbide eutectic. The mean temperature of the lanthanum dicarbide-carbon eutectic was found to be 2271 ± 5°C, where ± 5 is the probable error for four determinations. The uncertainty in using the correction factor for the absorption of light by the sight glass at these high temperatures is about ± 10°C. This gives a value of 2271 ± 15°C for the eutectic temperature. The lanthanum dicarbide-carbon eutectic is shown in Figure 37. The melting point of lanthanum dicarbide was obtained by extrapolation of the observed melting points of alloys near the theoretical composition, Figure 20. The extrapolated value is 2356 ± 25°C where the uncertainty, ± 25°C, is due to the errors in extrapolating (± 15°) and in applying the temperature correction (± 10°).

From the data in Table 21 the solid solubility limits of lanthanum sesquicarbide at room temperature are obtained by a plot of "a_o" versus the carbon concentration, Figure 21. The carbon composition of the lanthanum sesquicarbide ranges from 9.98 to 11.58 per cent (56.2 to 60.2 atomic per cent) carbon. The theoretical composition is 11.48 per cent carbon.

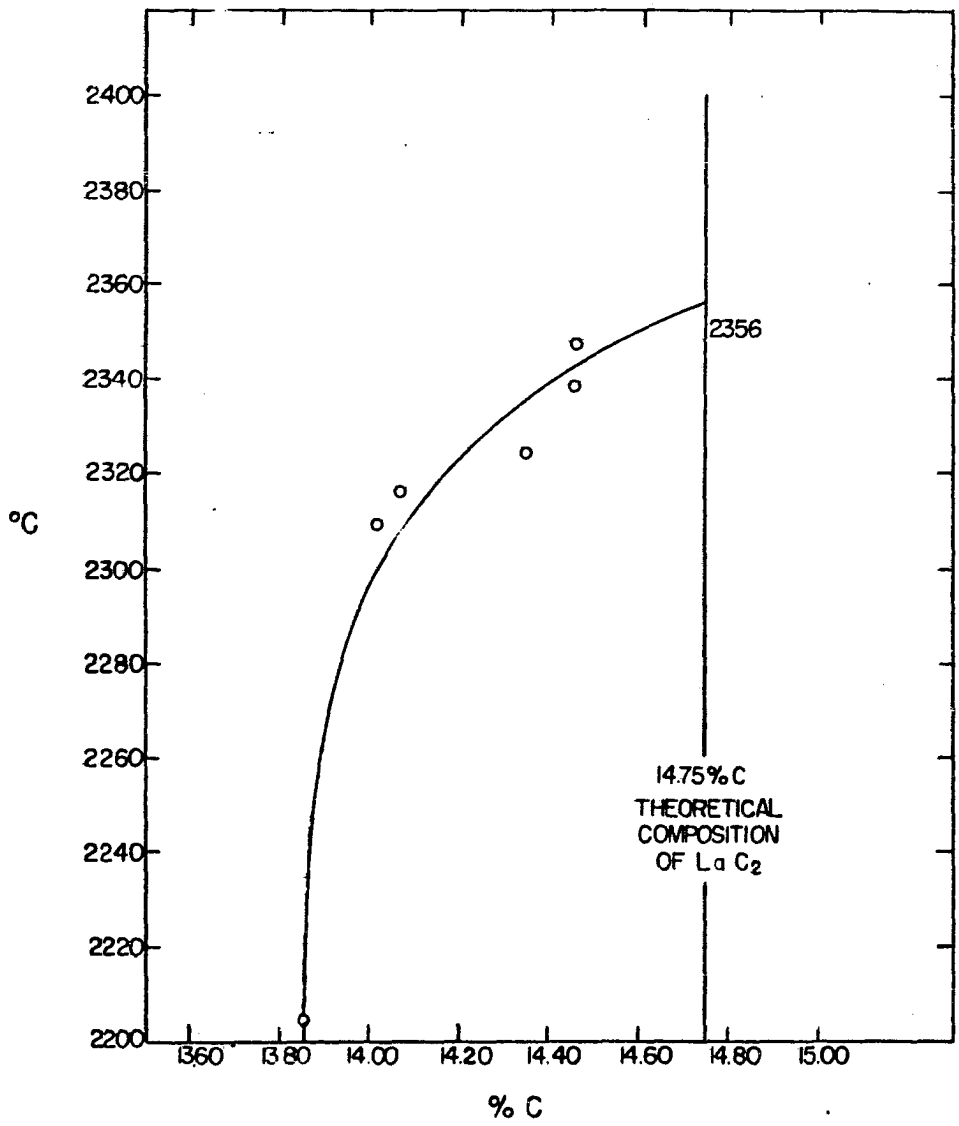

Figure 20. The melting points of alloys near the lanthanum dicarbide composition.

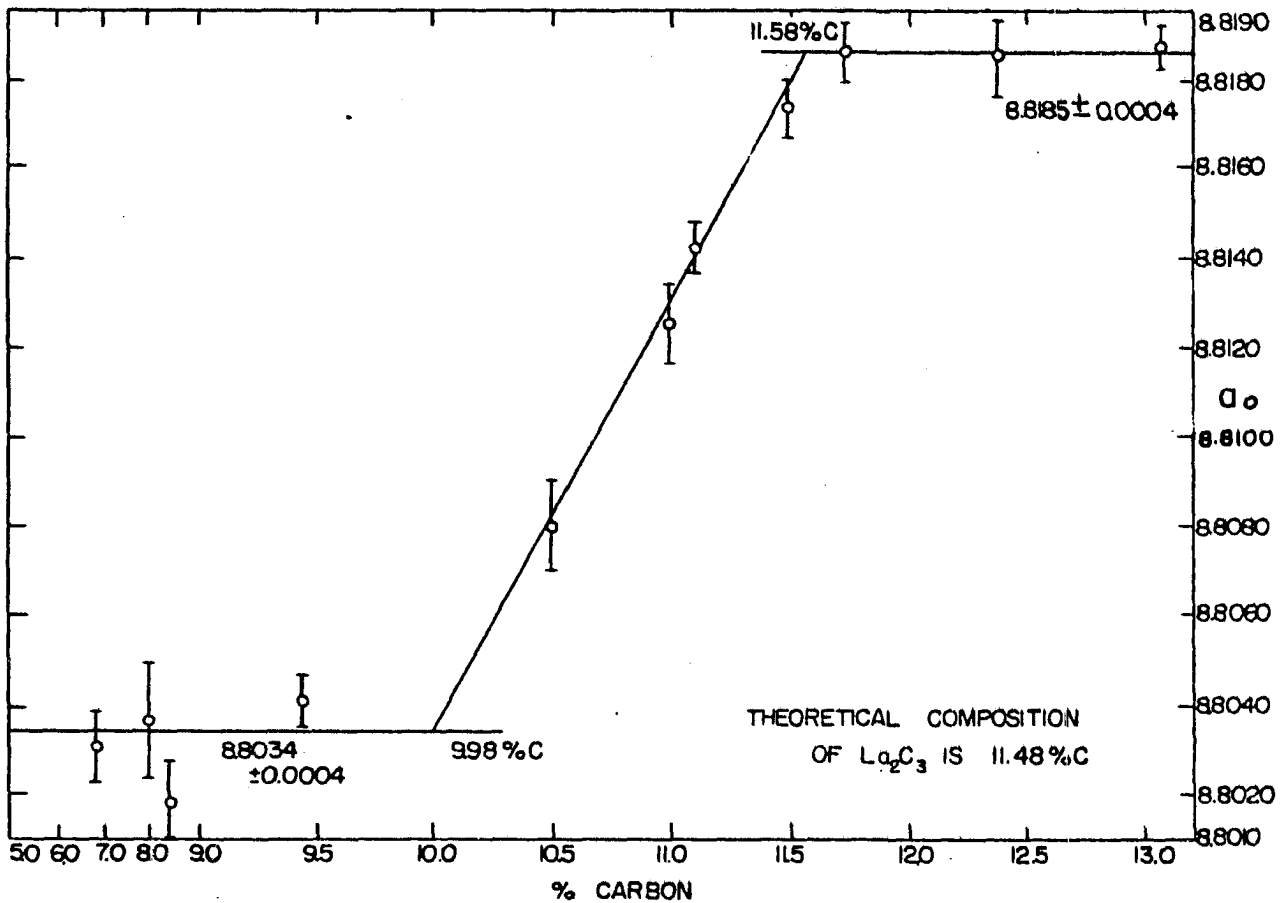

Figure 21. Variation of the lattice parameter of lanthanum sesquicarbide with the carbon concentration at room temperature.

Table 21. The lattice parameter of lanthanum sesquicarbide at various compositions

Lattice constant (Å)	Standard error of lattice constant x 10^4	Carbon content (%)
8.8031	8	6.81
8.8037	13	7.96
8.8018	10	8.33
8.8041	6	9.43
8.8080	10	10.49
8.8125	9	10.99
8.8142	6	11.10
8.8173	6	11.49
8.8185	7	11.74
8.8184	9	12.38
8.8186	5	13.07

Examination of several alloys around the dicarbide composition indicated that the lattice parameters vary slightly with composition, as shown in Table 22.

It appears that a_o is more sensitive to the carbon concentration than c_o. The maximum amount of combined carbon in these alloys was found to be 14.43 per cent carbon. This fact and the above data indicate that the range of solid solubility of this compound at room temperature is quite small, probably about 0.2 or 0.3 per cent carbon. The final

Table 22. The lattice parameters of lanthanum dicarbide at various compositions

Carbon content	Lattice constants			
	a_o (Å)	Standard error x 10^4	c_o (Å)	Standard error x 10^4
13.89	3.9322	5	6.5716	8
14.23	3.9342	22	6.5715	36
14.61	3.9373	9	6.5722	12

values reported for the lattice parameters of the lanthanum dicarbide were the averages of these three results, i.e. $a_o = 3.934 \pm 0.002$ and $c_o = 6.572 \pm 0.001$ Å.

Quantitative microscopic analysis was used to determine the solid solubility limits of the lanthanum-rich side of the lanthanum sesquicarbide at 800 and 1000°C. The data are shown in Table 23. The relative volumes of the two phases present as obtained from areal analysis are assigned the symbols A_v and B_v. At 800° A_v is the amount of the lanthanum-lanthanum sesquicarbide eutectic present in the alloy; the carbon content of this phase is 2.20 per cent carbon. At 1000° A_v is the amount of the liquid lanthanum phase, saturated with carbon, present in the alloy; the equilibrium concentration of carbon in this liquid phase is 3.87 per cent carbon. B_v is the percentage of the lanthanum sesquicarbide phase (lanthanum-rich side) present in the alloy. The volume percentages are converted to corresponding weight per-

Table 23. Results from quantitative microscopic analysis

Temperature (°C)	Alloy number	Composition of alloy (%C)	A_v[a] (V%)	B_v[b] (V%)	A_w[c] (W%)	B_w[d] (W%)	L[e] (%C)	Mean L (%C)
800	68A	7.61	22.44	77.56	22.75	77.25	9.20	
	68B	6.36	37.67	62.33	38.09	61.91	8.92	9.20 ±0.23
	72A	7.33	29.17	70.83	29.54	70.46	9.48	
1000	71	7.98	31.03	68.97	31.42	68.58	9.86	
	80A	7.62	38.82	61.18	39.25	60.75	10.04	10.32 ± 0.46
	80B	9.40	21.18	78.82	21.48	78.52	10.91	

[a]At 800° A_v is the volume per cent of the lanthanum-lanthanum sesquicarbide eutectic present in the alloy, as obtained from areal analysis. At 1000° A_v is the volume per cent of the liquid lanthanum phase, saturated with carbon, present in the alloy, as obtained from areal analysis.

[b]B_v is the volume per cent of the lanthanum sesquicarbide phase, lanthanum-rich side, as obtained from areal analysis.

[c]A_w is the weight per cent of the lanthanum phase, saturated with carbon, as calculated from A_v.

[d]B_w is the weight per cent of the lanthanum sesquicarbide phase, lanthanum-rich side, as calculated from B_v.

[e]L is the percentage of carbon in the lanthanum sesquicarbide phase at the lanthanum-rich end.

centages, A_w and B_w, by multiplying by the densities of lanthanum and lanthanum sesquicarbides (6.190 and 6.081 gm/cm^3, respectively). The percentage of carbon in the lanthanum sesquicarbide phase at the lanthanum-rich end is assigned the symbol L; and it may be calculated by the following equations:

at 1000°C

$$L = \frac{(100)(\%C_{alloy}) - (A_w)(3.87)}{B_w} , \qquad (12a)$$

and at 800°C

$$L = \frac{(100)(\%C_{alloy}) - (A_w)(2.20)}{B_w} \qquad (12b)$$

The mean values of L are 10.32 $\pm$ 0.46 and 9.20 $\pm$ 0.23 at 1000 and 800°C, respectively. Typical photomicrographs of some quenched alloys from which quantitative microscopic measurements were made are shown in Figures 30 and 31; the photomicrograph in Figure 32 shows an alloy quenched from 850°C. In Figure 31 the dark spots in the primary phase are material that was liquid which is present at the annealing temperature because of the decrease in solubility of lanthanum in lanthanum sesquicarbide with increasing temperature (Figure 17). Since these liquid pockets did not have sufficient time to diffuse to the secondary phase during annealing, they were frozen in the primary phase on quenching.

The approximate concentration of carbon in solid lanthanum at various temperatures was determined by quenching several low carbon alloys. Examination of the photomicrographs shown in Figures 24 to 27 indicates that at 775°C the solid solubility limit lies between 0.14 and 0.30 per cent carbon and at 695°C the limit appears to be slightly less than 0.14 per cent carbon.

The lower transition in lanthanum (α to β) does not give a thermal arrest on either heating or cooling curves, but Barson et al. (1957) have shown that this lower transition can easily be observed by dilatometric measurements. The thermal expansion of a three per cent carbon alloy was measured on the same apparatus used by Barson and co-workers. The results are shown in Figure 22. For comparison the curve for lanthanum containing 0.02 per cent carbon[1] (Barson, et al., 1957) is also shown in Figure 22. Only the heating curves are shown, but it is apparent that the transition begins at 310 ± 5°C for both the alloy and pure lanthanum. The transition temperature on cooling is lowered and the β to α transformation appears to be quite sluggish (Barson et al., 1957).

A high temperature modification of lanthanum dicarbide has been reported by Bredig (1953). An investigation was

---

[1]This alloy will be referred to as "pure lanthanum".

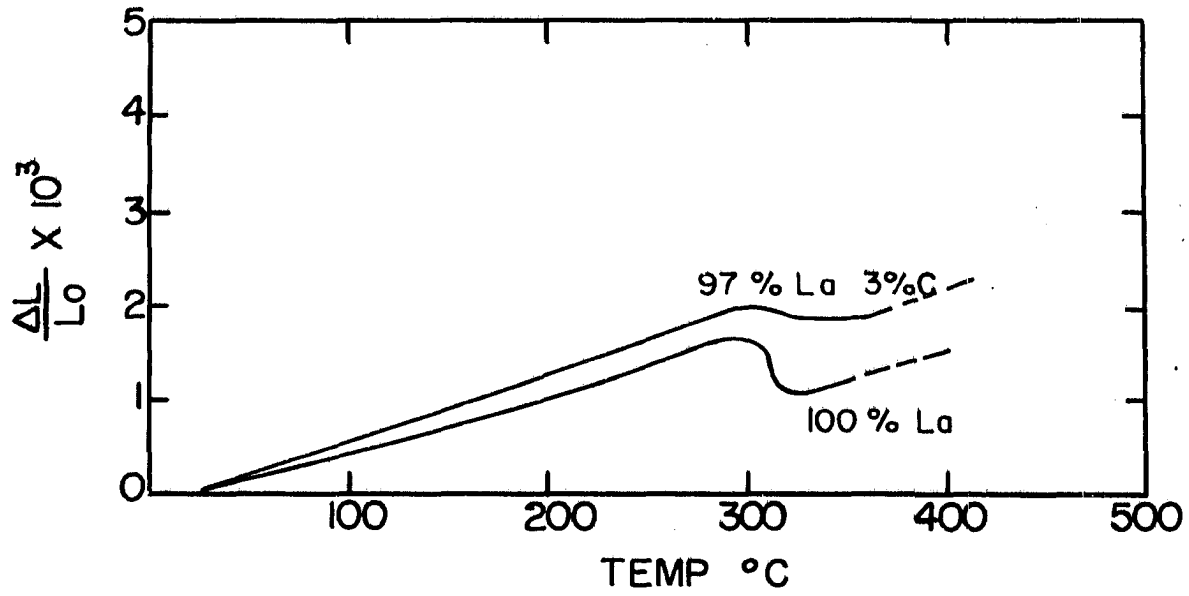

Figure 22. Thermal expansion of pure lanthanum and a 3 per cent carbon - 97 per cent lanthanum alloy.

made to verify the existence of this high temperature phase by electrical resistance measurements. The description of the apparatus and method was reported by Chiotti (1954). The temperatures were measured with an optical pyrometer. The sample was prepared by arc melting several chunks of lanthanum dicarbide into a rod 2.5 inches long; the cross sectional area varied from about 0.5 cm^2 at the ends to approximately 0.3 cm^2 at the center of the rod. The probes, approximately 0.75 inch apart, were fastened to the bar by arc melting the surface of the lanthanum dicarbide and allowing it to wet the tantalum wire, thus assuring good contacts. The data are given in Table 24, and the results are shown in Figure 23. The resistivity cannot be accurately calculated, since the cross-sectional area and length of the specimen cannot be accurately measured. But in order to observe a transition by this method, only the change in resistance is needed, and since the resistivity is proportional to the number of divisional units, D, read from the recorder, the results are given in terms of D. The transition temperature was observed to occur at 1800°C. This temperature is only accurate within $\pm$ 100°C because of the temperature gradient along the sample and the lack of black-body conditions. This result agrees with the transition temperature reported by Bredig, 1750°C.

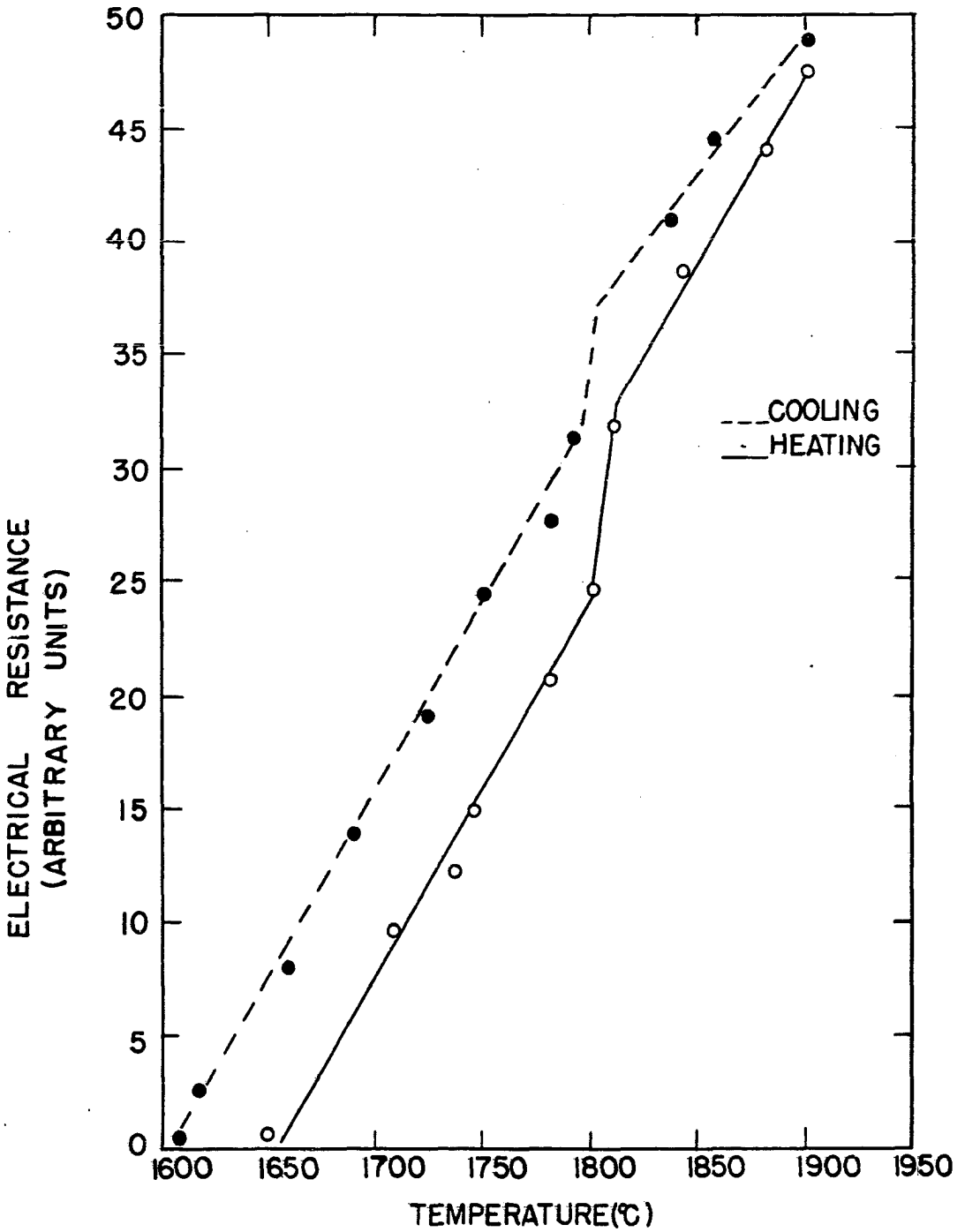

Figure 23. High temperature electrical resistance of lanthanum dicarbide.

Table 24. High temperature electrical resistance data of lanthanum dicarbide

Temperature	D[a,b]	Temperature	D[a,b]
1650	0.8	1900	49.2
1710	9.8	1855	44.6
1735	12.4	1835	41.1
1745	15.0	1790	31.5
1780	20.8	1780	27.9
1800	25.0	1750	24.6
1810	32.0	1725	19.3
1840	39.0	1690	14.0
1880	46.2	1660	8.2
1900	47.8	1620	2.7
		1610	0.5

[a]D (the number of divisional units read from the recorder) is related to the resistivity by the following equation:

$$\rho = 3.161 \times 10^{-6} \left(\frac{A}{L}\right) D \ .$$

[b]The values of D are relative; the correct number of scale divisions can be obtained by adding 355.8 to a given value of D.

Photomicrographs of various regions of the lanthanum-carbon system are shown in Figures 24 to 37. Figures 24 to 34 and 37 have been noted in the text. Figures 35 and 36 show two alloys of compositions between 12 and 14 per cent carbon. Figure 35 indicates the existence of two phases at

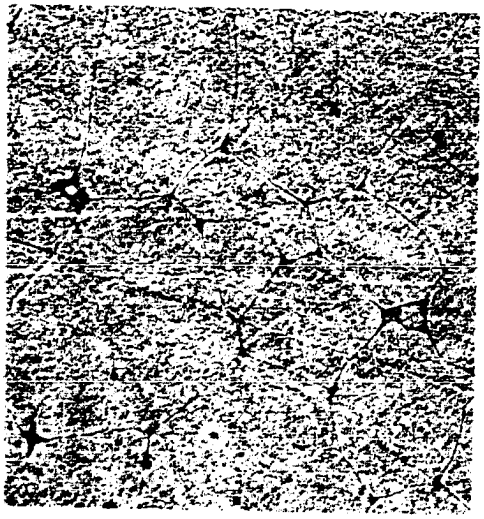

Figure 24. 0.14 per cent C, quenched from 775°, etched with 5 per cent nital. X200.

Figure 25. 0.30 per cent C, quenched from 775°, etched with 5 per cent nital. X200.

Figure 26. 0.14 per cent C, quenched from 695°, etched with 5 per cent nital. X200.

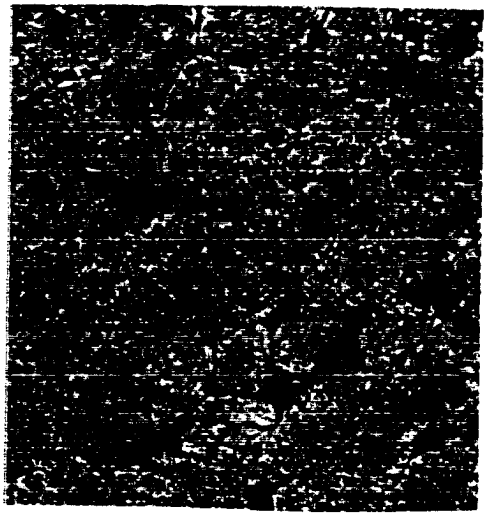

Figure 27. 0.30 per cent C, quenched from 695°, etched with 5 per cent nital. X200.

Figure 28. 1.4 per cent C, quenched from the liquid state, etched with 5 per cent nital. X200.

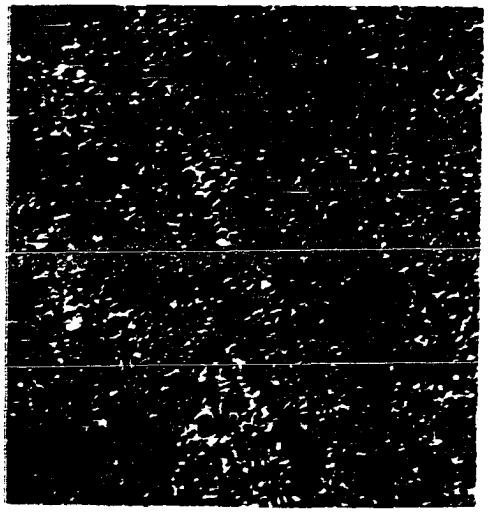

Figure 29. 2.0 per cent C, furnace cooled, etched with 5 per cent nital. X100.

Figure 30. 7.33 per cent C, quenched from 800°, used in areal analysis, unetched: dark area---La-La_2C_3 eutectic, light area---La_2C_3. X200.

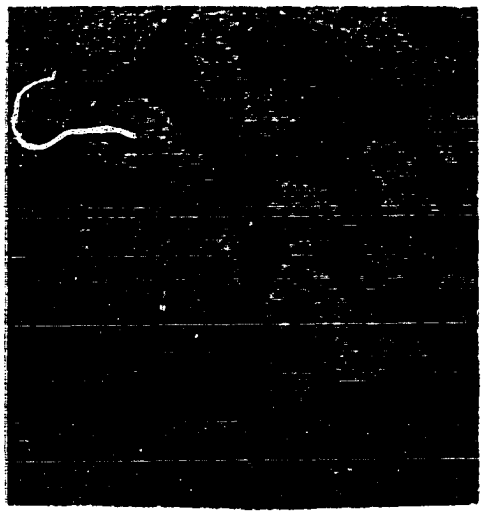

Figure 31. 7.62 per cent C, quenched from 1000°, used in areal analysis, unetched: dark area---La-La_2C_3 eutectic, light area---La_2C_3. X200.

Figure 32. 9.4 per cent C, quenched from 850°, unetched: dark area---La-La_2C_3 eutectic, light area---La_2C_3. X200.

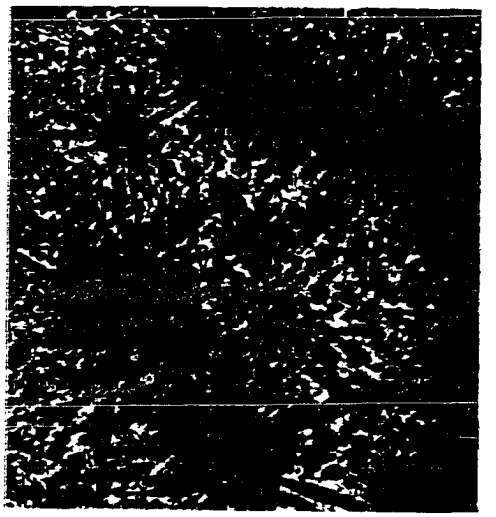

Figure 33. 10.5 per cent C, cooled from 1600 to 1375° at 5-8°C per min, furnace cooled from 1375 to 25°. X200. (See text for explanation, p. 97).

Figure 34. 12.9 per cent C, furnace cooled from 1695 to 25°. X200. (See text for explanation, p. 97).

Figure 35. 12.6 per cent C, quenched from 1400 ± 25°. X500. (See text for explanation, p. 109).

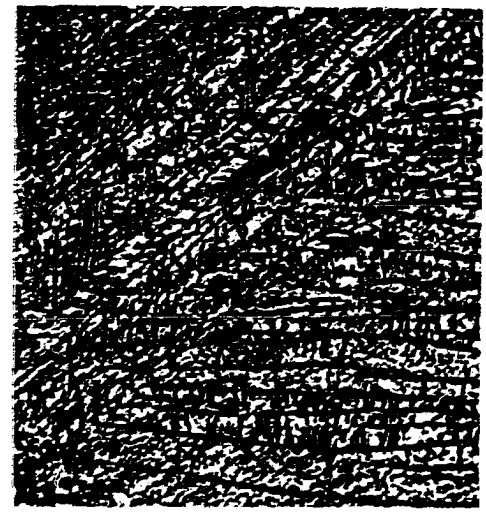

Figure 36. 13.5 per cent C, furnace cooled after annealing at 1385 ± 25°: dark area (precipitate) ---La_2C_3, light area--- LaC_2. X200.

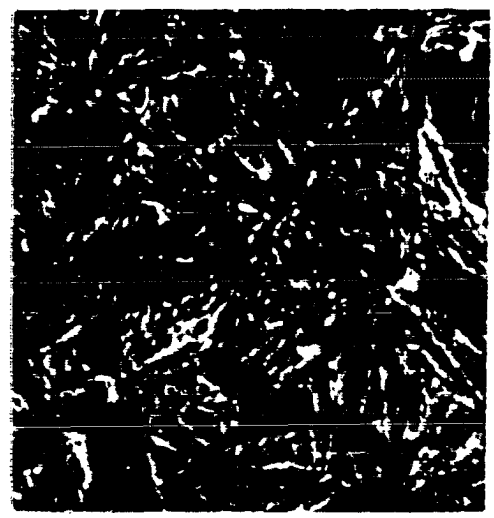

Figure 37. 20 per cent C, as arc melted (quenched), dark area---C, light area---LaC_2. X200.

1400 ± 25 °C in an alloy containing 12.6 per cent carbon. On quenching, the lanthanum sesquicarbide precipitated out of the dicarbide phase, indicating a decrease of solubility of the sesquicarbide in the dicarbide. The black area in the grain boundary is the lanthanum-lanthanum sesquicarbide eutectic, the gray material between the black area and the primary phase is lanthanum sesquicarbide. The photomicrograph shown in Figure 36 indicates that at 1385 ± 25°C and 13.5 per cent carbon the material consists of one phase, the dicarbide, and upon furnace cooling the sesquicarbide precipitated out.

Miscellaneous Properties

Electrical resistivity

The electrical resistivity of the lanthanum sesqui- and di-carbides were measured at room temperature by the DC potentiometric method. A constant current source of 100 ± 0.01 ma was employed in addition to a precision potentiometer, galvanometer and a standard one ohm resistance. The resistivity, ρ, was calculated from the following equation

$$\rho = \frac{RA}{L}, \qquad (13)$$

where R is the resistance of the specimen, A the cross-sectional area and L is the length. The specimens were pre-

pared by arc melting the alloys in the shape of rods five cm long, and about 0.3 cm^2 in cross-sectional area. Since these rods are not of a uniform shape the average cross-sectional area was obtained by measuring the volume of alcohol displaced by that portion of the rod between the two probes that are used to measure the voltage drop along the sample. The volume of the alcohol displaced is equal to the volume of the sample between the probes. The cross-sectional area was obtained by dividing this volume by the distance between probes.[1] The room temperature resistivities for lanthanum

---

[1]It should be pointed out that the use of this value of the cross-sectional area as obtained by the above method in Equation 13 is valid if the area between the probes is approximately constant. If, however, the area changes from one section of the rod to another, the use of this value of A in Equation 13 is in slight error, because the total resistance in this case is given by the sum of the resistances of the various sections, that is

$$R_T = \rho\left(\frac{L_1}{A_1} + \frac{L_2}{A_2} + \ldots\ldots\frac{L_n}{A_n}\right). \qquad (14)$$

But in the above method it was assumed that

$$R_T = \rho\,\frac{L_T}{A_M}\ , \qquad (15)$$

where L_T is the total length between probes and A_M is the mean cross-sectional area. And it is obvious that

$$\frac{L_T}{A_M} \neq \frac{L_1}{A_1} + \frac{L_2}{A_2} + \ldots\ldots\frac{L_n}{A_n}\ . \qquad (16)$$

However, the error introduced by this assumption is small and probably less than two or three per cent of the value reported.

sesqui- and di-carbides are 144 x 10^{-6} and 68 x 10^{-6} ohm-cm, respectively. The error in measuring the cross-sectional area, length and voltage drop is estimated to give an uncertainty of ± 15 per cent of the value reported for the sesquicarbide and ± 17 per cent for the dicarbide.

Chemical behavior

The rate of oxidation of lanthanum and some lanthanum carbon alloys in air at room temperature has been discussed previously and the results were given in Figure 2.

The reactivity of the two lanthanum carbides with several reagents was examined. Acids containing some water will react quite readily with both of these materials to form hydrocarbons and hydrogen. Concentrated acids (nitric, sulfuric and acetic) behave quite differently than the diluted ones. Concentrated nitric reacts to liberate nitrogen dioxide and to form a black residue, probably amphorous carbon. Concentrated sulfuric has very little effect; only after about 24 hours the sample turns black indicating that some reaction is occurring. Glacial acetic acid decomposes and disintegrates the samples quite slowly forming lanthanum acetate, which is insoluble in glacial acetic acid, and probably liberating hydrocarbons.

It was discovered that rare earth carbides could be stored for 24 hours and longer in a bottle of absolute alco-

hol, provided the lid was tightly closed. The inertness of alcohol to these carbides, enables one to transport samples to and from various pieces of equipment with little or no oxidation of the sample.

Several refractory substances were examined to see if a suitable crucible material could be found for the rare earth carbides. Carbon and tantalum carbide, TaC, crucibles were tested, but both were quite porous and the lanthanum or lanthanum-carbon alloys leaked out. Molybdenum and tungsten were examined; the reaction between the lanthanum-carbon alloys and molybdenum began between 1100 and 1500°C, while for tungsten it commenced between 1700 and 2300°C. In both cases the R_2C compound of molybdenum and tungsten was formed, and the lanthanum-carbon alloys picked up about 0.1 per cent molybdenum or tungsten. It appears that both these metals would serve as suitable crucible materials at low temperatures, but fabrication problems are such that it makes their use inconvenient. Tantalum was found to extract some of the carbon from the various lanthanum-carbon alloys regardless of the temperature or composition of the alloy, provided the alloy was molten when in contact with the tantalum. X-ray and metallographic data indicated that the TaC compound was always formed when the tantalum was in contact with these alloys, and that the reaction appears to stop or slow down after a certain thickness is attained. This reaction should

cause no difficulties provided the center sections of the melts are used for carbon analysis.

Hardness measurements and mechanical properties

The hardness measurements of some lanthanum-carbon alloys were made on a Rockwell Hardness Tester (Wilson Mechanical Instrument Division). The results of these measurements are given in Table 25; Figure 38 shows the variation of the hardness with the carbon content for both quenched and furnace cooled alloys. In both cases there is initially a rapid increase, up to about 0.1 per cent carbon, above this concentration the hardness increases at a much slower rate. Examination of the lanthanum-carbon phase diagram, reveals that this sudden increase of hardness is probably due to the phenomenon called "precipitation hardening". Several attempts were made to measure the hardness of the two lanthanum carbides, but these alloys were so brittle that they broke into several pieces when the load was applied.

Pure lanthanum and lanthanum-carbon alloys containing less than 0.2 per cent carbon are soft and tend to gum up saw blades and files, much like pure lead. The higher carbon content alloys machine, file and saw about the same as ordinary brass; however, alloys containing more than five per cent carbon are quite pyrophoric, behaving about the same as pure cerium.

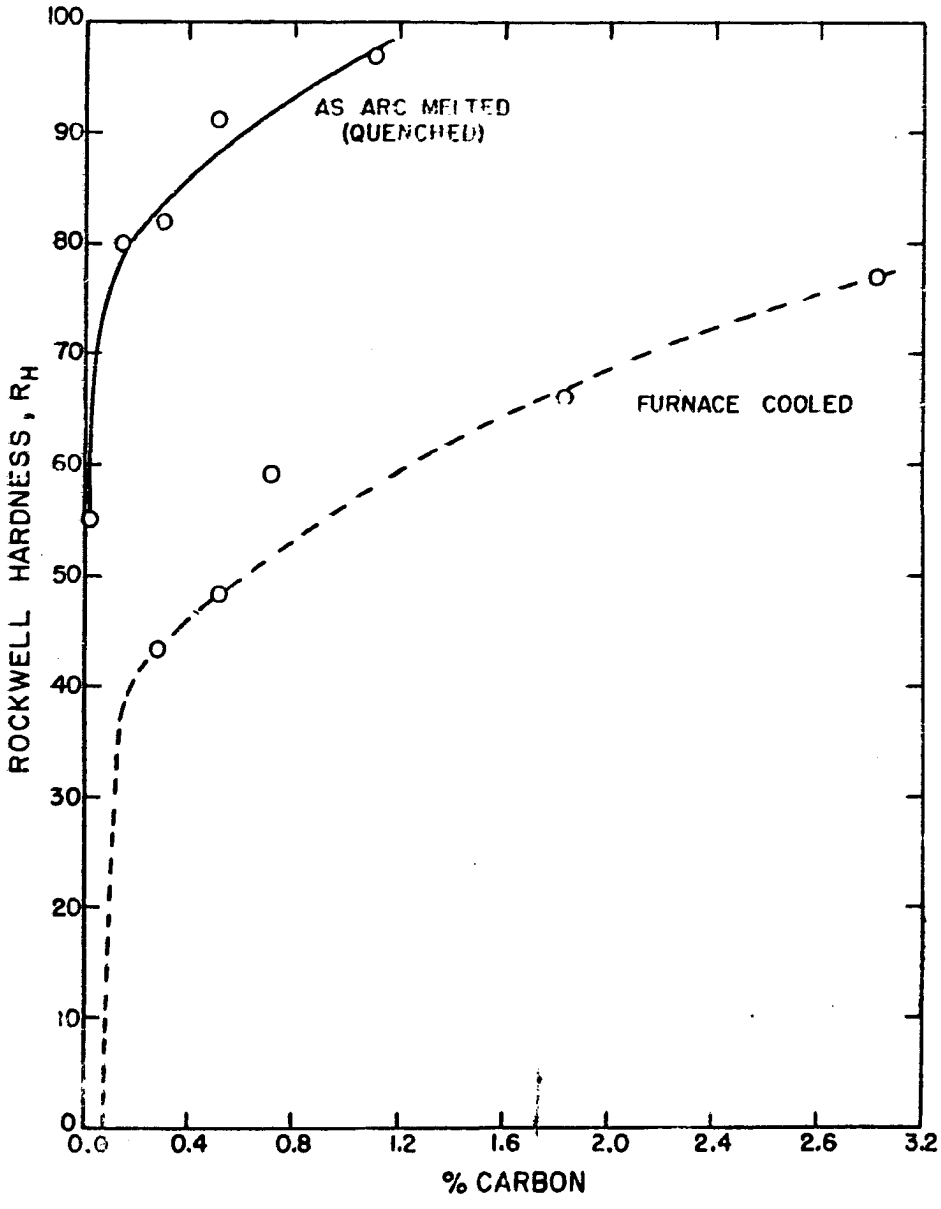

Figure 38. The hardness of several lanthanum-carbon alloys versus the carbon content.

Table 25. Rockwell hardness of some lanthanum-carbon alloys

	Carbon content (%)	Hardness R_H
Furnace cooled		
	0.09	< 0
	0.28	45.8
	0.52	48.2
	0.72	59.3
	1.83	65.9
	3.09	77.1
Quenched		
	0.02	55
	0.14	80
	0.30	82
	0.51	91
	1.10	97

Effect of carbon on the oxygen content

The oxygen content in several lanthanum-carbon alloys was determined by a spectroscopic method described by Fassel and Tabeling (1956). The alloys were filed down to samples weighing 100 ± 10 mg in a dry box filled with helium, and then stored in vacuo by sealing in pyrex tubes until the samples were ready to be analyzed. The alloys were briefly

exposed to air twice, once when transferred from the dry box to the pyrex storage tubes and secondly, when the tubes were broken open and the specimens were placed into the vacuum chamber containing the arc source of the spectrograph. The results, which are consistent with one another within ± 10 per cent of the value reported, are shown in Table 26. The

Table 26. Results of oxygen analysis of lanthanum and some carbon-lanthanum alloys

Carbon content (%)	Oxygen content (ppm)
0.02	1000
0.09	490
0.48	390
0.72	493
1.35	445
3.09	840

actual oxygen content may be in error as much as ± 50 per cent of the reported value. However, these data show that the oxygen content is reduced by about half by the addition of even a small amount of carbon. This value appears to be approximately constant up to 1.5 per cent carbon, but at 3.1 per cent the oxygen content has increased to nearly the amount in pure lanthanum. This increase is believed to be

due to oxygen pick up on the surface while these alloys were exposed to air during transfer operations.

Discussion

A study of the lanthanum-carbon system by thermal, metallographic, x-ray, dilatometric and electrical resistivity methods has shown the existence of two compounds (lanthanum sesquicarbide and lanthanum dicarbide) and the effect of carbon on lanthanum metal.

The sesquicarbide is body-centered cubic and shows a range of solid solubility (from 9.98 to 11.58 per cent carbon at room temperature). This compound melts incongruently at 1415 $\pm$ 3°C, and at room temperature it has an electrical resistivity about 2 1/2 times that of pure lanthanum.

The tetragonal structure of the dicarbide reported by von Stackelberg was confirmed in this study, and a transition at about 1750°C reported by Bredig was also observed. This compound melts congruently at 2356 $\pm$ 25°C and at room temperature it has an electrical resistivity about equal to that of pure lanthanum.

The addition of carbon to lanthanum lowers the melting point of lanthanum about 115°C, raises the higher (β - γ) transformation about 10°C and appears to have no effect on the lower (α - β) transformation. The addition of carbon appears to lower the oxygen content in the metal and improve

the machinability; however the tendency to oxidize is increased.

Two eutectics are formed in the system. The first occurs at 2.2 per cent carbon and melts at 806 ± 2°C, while the second occurs between lanthanum dicarbide and carbon with a melting point of 2271 ± 15°C.

It is interesting to make some comparisons between the lanthanum-carbon system and some other metal-carbon systems that might be expected to be comparable in some degree (i.e. systems between carbon and the alkaline earth metals, aluminum, rare earth and actinide metals). Of these systems only the thorium and uranium-carbon phase diagrams have been reported in detail. At low carbon concentrations a eutectic is formed in the lanthanum-carbon system, but the addition of carbon raises the liquidus temperature of the thorium and uranium systems. In addition to being isostructural, the sesquicarbides of lanthanum and uranium are formed on cooling by similar processes: the uranium compound is formed by a peritectoid reaction ($UC + UC_2 \longrightarrow U_2C_3$), while in the lanthanum case it is formed by a peritectic reaction of liquid (of approximately the theoretical composition, LaC) and lanthanum dicarbide. The eutectic which occurs between lanthanum dicarbide and carbon is similar to that which occurs in the thorium-carbon system. All three of these dicarbides are very high melting compounds; the melting points are

2356, 2475 and 2655°C for the lanthanum, uranium and thorium dicarbides, respectively. It is interesting to note, that at high temperatures the mono- and di-carbides of thorium and uranium are mutually soluble (Wilhelm and Chiotti, 1950 and Mallett et al., 1952), indicating that they might have similar structures at these high temperatures. Since the monocarbides of uranium and thorium are face-centered cubic and since a high temperature face-centered cubic form has been reported for both the calcium and lanthanum dicarbides (Bredig, 1942 and 1953), the mutual solubility would appear to be quite reasonable if the uranium and thorium dicarbides undergo the same sort of transformation as do the calcium and lanthanum dicarbides. Since the rare earths, samarium to lutetium, form a face-centered cubic carbide, R_3C, which is structurally quite similar to the face-centered cubic thorium and uranium monocarbides, and since the rare earth and uranium dicarbides are isostructural at room temperature one might expect the tri-rare earth carbide to be mutually soluble with the corresponding rare earth dicarbide at high temperatures. Also one might wonder whether those rare earth-carbon systems that have three carbide compounds will behave like lanthanum at low carbon contents and form a eutectic, or react like thorium and uranium and have a rising liquidus curve. Furthermore, one might wonder whether the

other rare earth sesquicarbides are formed by a peritectic or by a peritectoid reaction.

This research has introduced several new questions and opened some new avenues of research. Future studies should prove quite fruitful and may add much more information to the present concepts of alloying behavior and to the general knowledge of metal carbides.

SUMMARY

A study of the rare earth-carbon systems has been made. The existence of the reported rare earth dicarbides and the cerium sesquicarbide have been confirmed. The existence of the tetragonal calcium carbide, CaC_2, type structure for the other rare earth dicarbides (except promethium and europium) has been shown. The lattice constants of these compounds decrease in a regular fashion, except for the ytterbium dicarbide, whose lattice parameters lie between those of the holmium and erbium compounds. The body-centered cubic plutonium sesquicarbide, Pu_2C_3, type structure has been found to exist in all the rare earths from lanthanum to holmium (except promethium and europium). The lattice constants decrease in a normal manner, except for the cerium compound, whose lattice parameters are smaller than would be expected. It appears that the heavy rare earths holmium to lutetium and also yttrium form another type structure, not yet determined. A new rare earth carbide has been found, the tri-rare earth carbide, it is similar to the face-centered cubic sodium chloride type structure, except that it is deficient in carbon. In the case of yttrium it was found to have a range of composition varying from $YC_{0.25}$ to $YC_{0.40}$. This compound has been found to exist in the rare earth-carbon systems of samarium to lutetium (except europium), and the lattice parameters decrease in a regular manner. No x-ray

evidence was found for the existence of this lower carbide in the lanthanum-, cerium-, praseodymium- and neodymium-carbon systems.

Hydrolytic studies showed that the tri-rare earth carbides are methanides, while the sesqui- and di-carbides form primarily acetylene plus some other saturated and unsaturated hydrocarbons.

A thorough study of the lanthanum-carbon system was made and equilibrium diagram has been constructed from thermal, metallographic, x-ray, dilatometric and electrical resistance data. The lanthanum sesquicarbide shows a range of solid solubility, melts incongruently at 1415°C, and has an electrical resistivity at room temperature about 2 1/2 times that of pure lanthanum. The existence of a high temperature modification of the lanthanum dicarbide has been verified by electric resistance measurements. This compound was found to melt at 2356°C, and at room temperature it has an electrical resistivity about equal to that of pure lanthanum. Two eutectics have been found, one at 2.2 per cent carbon, melting at 806°C and the second occurs between lanthanum dicarbide and carbon with a melting point of 2271°C. The addition of carbon to lanthanum lowers the melting point about 115°C, raises the higher transformation about 10°C and appears to have no effect on the lower transformation. The addition of carbon to lanthanum appears to reduce the oxygen

content, increase machinability and increase the tendency to oxidize.

LITERATURE CITED

Atoji, M., K. A. Gschneidner, Jr., A. H. Daane, R. E. Rundle and F. H. Spedding, (1957). Submitted for publication to the J. Am. Chem. Soc. (ca. 1958).

Baenziger, N. C., J. R. Holden, G. E. Knudson and A. J. Popov, (1954). J. Am. Chem. Soc. 76, 4734.

Barson, F., S. Legvold and F. H. Spedding, (1957). Phys. Rev. 105, 418.

Barton, R., (1956). Unpublished Ph.D. Thesis, Iowa State College Library, Ames, Iowa.

Bertaut, F. and P. Blum, (1952). Compt. rend. 234, 2621.

Bommer, H., (1939). Z. anorg. Chem. 241, 273.

Bradley, A. J. and A. H. Jay, (1932). Proc. Phys. Soc. (London) 44, 563.

Bredig, M. A., (1942). J. Phys. Chem. 46, 801.

_____, (1953). Oak Ridge National Laboratory Report No. ORNL-1260, 106.

Brewer, L. and O. Krikorian, (1956). J. Electrochem. Soc. 103, 38.

Bühring, H. J., (1875). J. prakt. Chem., Ser. 2: 12, 215.

Chiotti, P., (1954). Rev. Sci. Instr. 25, 876.

Cohen, M. U., (1935). Ibid. 6, 68.

Cromer, D. T., (1957). J. Phys. Chem. 61, 753.

Daane, A. H., D. H. Dennison and F. H. Spedding, (1953). J. Am. Chem. Soc. 75, 2272.

_____, R. E. Rundle, H. G. Smith and F. H. Spedding, (1954). Acta Cryst. 7, 532.

Damiens, M. A., (1918). Ann. Chim., Ser. 9: 10, 137.

Delafontaine, M., (1865). Arch. Phys. Nat., Ser. 2: 22, 30.

Dennison, D. H., (1957). Private communication. Information on the melting and transformation temperatures of some rare earth fluorides. Ames Laboratory, Iowa State College, Ames, Iowa.

Fassel, V. A. and R. W. Tabeling, (1956). Spectrochim. Acta 8, 201.

Fried, S. and W. H. Zachariasen, (1956). In Finniston, H. M. and F. P. Howe, eds. "Progress in Nuclear Energy, Series 5: Metallurgy and Fuels" 1, 757: London, Pergamon Press, Ltd.

Goldschmidt, V. M., (1954). "Geochemistry": Oxford, England, Clarendon Press.

Haefling, J., (1957). Private communication. Information on the solubility of some rare earth metals in uranium and uranium in some rare earth metals: information on the lanthanum-, yttrium- and neodymium-iron systems. Ames Laboratory, Iowa State College, Ames, Iowa.

Hagg, G. (1931). Z. phys. Chem. 12B, 33.

Hanak, J., (1957). Private communication. Information on the melting and boiling points of europium metal. Ames Laboratory, Iowa State College, Ames, Iowa.

Holley, C. E., Jr., R. N. R. Mulford, F. H. Ellinger, W. C. Koehler and W. H. Zachariasen, (1955). J. Phys. Chem. 59, 1226.

Hunt, E. B. and R. E. Rundle, (1951). J. Am. Chem. Soc. 73, 4777.

Iandelli, V. A. and E. Botti, (1937). Atti accad. Lincei, Classe sci. fis. mat. nat. 26, 233.

"International Tables for X-Ray Crystallography", (1952). 1: Birmingham, England, Kynoch Press.

Jepson, J. O. and P. Duwez, (1955). Trans. Am. Soc. Metals 47, 543.

Jette, E. R. and F. Foote, (1935). J. Chem. Phys. 3, 605.

Klemm, W. and G. Winkelmann, (1956). Z. anorg. Chem. 288, 87.

Korst, W. L. and J. C. Warf, (1956). Acta Cryst. 9, 452.

Litz, L. M., A. B. Garrett and F. C. Croxton, (1948). J. Am. Chem. Soc. 70, 1718.

Lock, J. M., (1957). Proc. Phys. Soc., Ser. 449B: 70, 476.

Lohberg, K., (1935). Z. phys. Chem. 28B, 402.

Mallett, M. W., A. F. Gerds and H. R. Nelson, (1952). J. Electrochem. Soc. 99, 197.

_____, _____ and D. A. Vaughan, (1951). Ibid. 98, 505.

McHargue, C. J., H. L. Yakel, Jr. and L. K. Jetter, (1957). Fourth International Congress, International Union of Crystallography, Montreal, Canada. Abstracts of Communications, No. 13.3: 104.

Moissan, H., (1896a). Compt. rend. 122, 357.

_____, (1896b). Ibid. 123, 148.

_____, (1896c). Bull. Soc. Chim., Ser. 3: 15, 1293.

_____, (1896d). Ann. Chim. Phys., Ser. 7: 9, 302.

_____, (1900a). Compt. rend. 131, 595.

_____, (1900b). Ibid. 131, 924.

_____, (1901). Ann. Chim. Phys., Ser. 7: 22, 110.

Mosander, C. G., (1827). Pogg Ann. 11, 406.

Mott, W. R., (1918). Trans. Am. Electrochem. Soc. 34, 255.

Mulford, R. N. R. and C. E. Holley, Jr., (1955). J. Phys. Chem. 59, 1222.

Muthmann, W., H. Hofer and L. Weiss, (1902). Liebig's Ann. 320, 260.

Nelson, J. B. and D. P. Riley, (1945). Proc. Phys. Soc. (London) 57, 160.

Pauling, L., (1947). J. Am. Chem. Soc. 69, 542.

_____ and M. D. Shappell, (1930). Z. Krystallogr. 75, 129.

Pettersson, O., (1895). Bericht 28, 2419.

Pirani, M. and H. Alterthum, (1923). Z. Elektrochem. 29, 5.

Post, B., D. Moskowitz and F. W. Glaser, (1956). J. Am. Chem. Soc. 78, 1800.

Rundle, R. E., N. C. Baenizger, A. S. Wilson and R. A. McDonald, (1948). Ibid. 70, 99.

Sheft, I. and S. Fried, (1953). Ibid. 75, 1236.

Smidt, F., (1957). Private communication. Information on the crystal structure of yttrium nitride. Ames Laboratory, Iowa State College, Ames, Iowa.

Spedding, F. H. and A. H. Daane, (1954). J. Metals 6, 504.

_____ and J. E. Powell, (1954). Ibid. 6, 1131.

_____, A. H. Daane and K. W. Herrmann, (1956). Acta Cryst. 9, 559.

_____, S. Legvold, A. H. Daane and L. D. Jennings, (1957). In Gorter, C. J., ed. "Progress in Low Temperature Physics" 2, 368: Amsterdam, Netherlands, North-Holland Publishing Co.

von Stackelberg, M., (1930). Z. phys. Chem. 9B, 437.

_____, (1931). Z. Elektrochem. 37, 542.

Sterba, J., (1902). Compt. rend. 134, 1056.

_____, (1904). Ann. Chim. Phys., Ser. 8: 2, 209.

Sturdy, G. E. and R. N. R. Mulford, (1956). J. Am. Chem. Soc. 78, 1083.

Templeton, D. H. and G. F. Carter, (1954). J. Phys. Chem. 58, 940.

_____ and C. H. Dauben, (1953). J. Am. Chem. Soc. 75, 6069.

Trombe, F., (1944). Compt. rend. 219, 182.

Umanskij, J., (1940). Z. Fiz. Khim. SSSR 14, 332. (Original not available for examination; abstracted in "Structure Reports" 8, 48 (1940-41).

Vickery, R. C., (1953). "Chemistry of the Lanthanons" New York, Academic Press Inc., Publishers.

Warf, J. C., (1956). Paper presented at the Am. Chem. Soc. Northwest Regional Meeting, Seattle, Washington. (Abstract) Chem. and Eng. News 34, 3446.

Wells, A. F., (1950). "Structural Inorganic Chemistry", 2nd ed. London, England, Oxford University Press.

Wilhelm, H. A. and P. Chiotti, (1950). Trans. Am. Soc. Metals 42, 1295.

Zachariasen, W. H. (1926). Z. phys. Chem. 123, 134.

_____, (1948). J. Chem. Phys. 16, 254.

_____, (1951). Acta Cryst. 4, 231.

_____, (1952). Ibid. 5, 17.

Zalkin, A. and D. H. Templeton, (1953). J. Am. Chem. Soc. 75, 2453.

ACKNOWLEDGMENT

The writer wishes to express his appreciation to Drs. F. H. Spedding and A. H. Daane, who gave helpful advice and counsel during the progress of this investigation. Acknowledgment is also due to Dr. P. Chiotti who gave counsel on several metallurgical problems. The writer wishes to thank Mr. N. Driscoll who gave much assistance in measuring films, performing calculations and conducting experiments. The author is grateful to Mr. H. Born for performing the dilatometric analysis, Mr. W. Gordon for the oxygen analyses, Dr. H. Svec and Mr. J. Capellan for the gas analysis of the hydrolytic products from the rare earth carbides and Mr. D. Rowland for assistance in conducting the high temperature resistivity measurements. Acknowledgment is made to Messrs. D. H. Dennison, C. Habermann and G. Wakefield who supplied most of the rare earth metals used in this research. The author also wishes to thank the analytical groups of the Ames Laboratory for performing analyses on the carbide samples.

APPENDICES

APPENDIX I: DERIVATION OF THE FORMULAS USED TO CALCULATE THE STANDARD ERROR OF LATTICE CONSTANTS FOR CUBIC MATERIALS

Back Reflection Camera

The increase in precision of the lattice constant for a cubic material with increasing θ is shown by differentiating the Bragg equation with respect to θ:

$$n\lambda = 2d \sin\theta \,, \tag{17}$$

$$0 = 2\frac{\delta d}{\delta \theta}\sin\theta + 2d\cos\theta \,, \tag{18}$$

$$\frac{\delta d}{d} = -\frac{\cos\theta}{\sin\theta}\,\delta\theta = -\cot\theta\,\delta\theta \,. \tag{18a}$$

Since

$$d = \frac{a_o}{\sqrt{h^2 + k^2 + l^2}} \,, \tag{19}$$

then

$$\frac{\delta a_o}{a_o} = \frac{\delta d}{d} = -\cot\theta\,\delta\theta \,. \tag{20}$$

The relationship of θ with S' (the distance between a given pair of lines of the back reflection diffraction pattern) and R (the camera radius) is given below with the aid of Figures 39 and 40. From Figure 39

$$S' = 4\beta R \,, \tag{21}$$

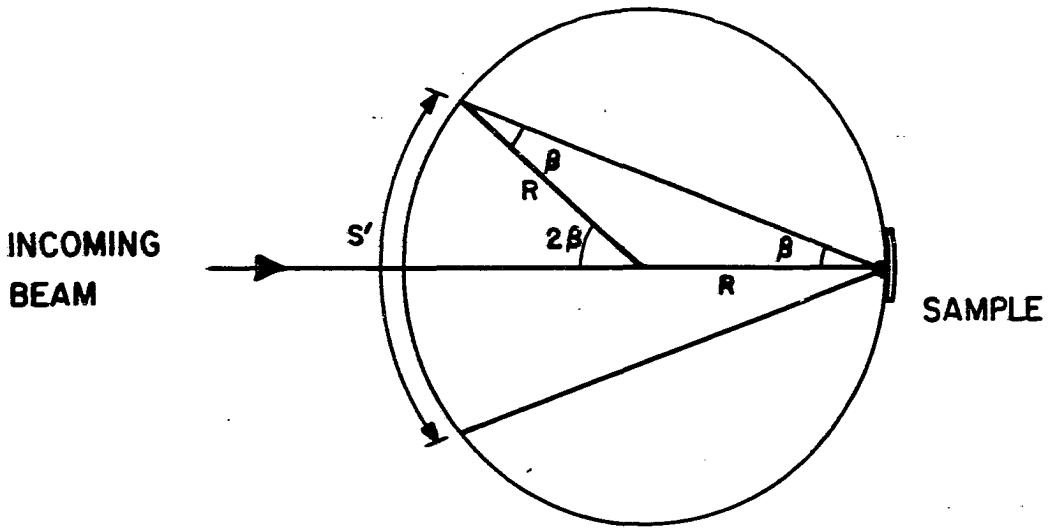

Figure 39. Geometry of the back reflection camera.

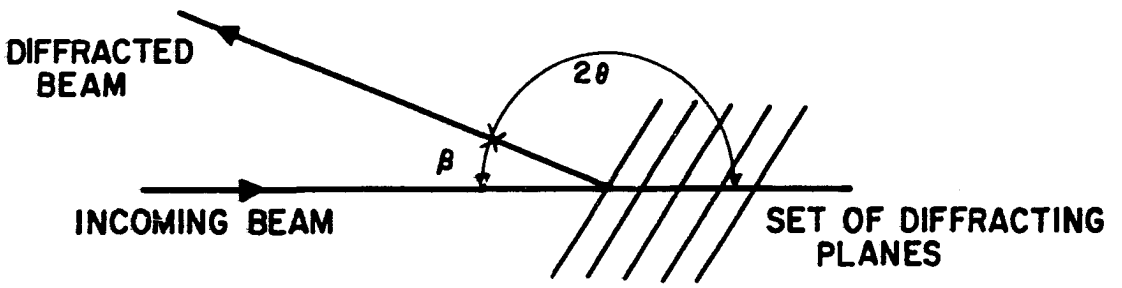

Figure 40. Geometrical relationship between β and θ.

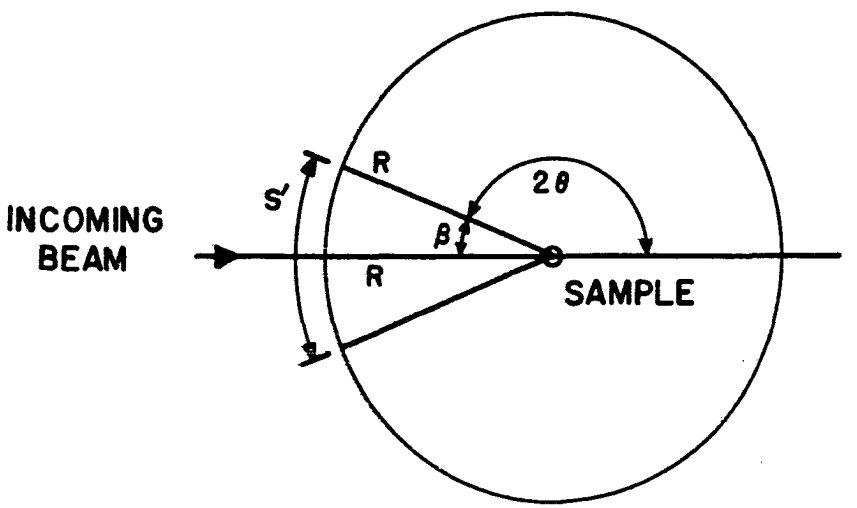

Figure 41. Geometry of the Debye-Sherrer camera.

and from Figure 40

$$\beta = \pi - 2\theta \ . \tag{22}$$

Substituting for β in Equation 21, we have

$$S' = 4R(\pi - 2\theta) \ , \tag{23}$$

and rearranging

$$\theta = \frac{4\pi R}{8R} - \frac{S'}{8R} \ , \tag{24a}$$

$$\theta = \frac{\pi}{2} - \frac{S'}{8R} \ . \tag{24b}$$

Differentiating Equation 24b with respect to θ:

$$1 = \frac{\delta S'}{\delta \theta}\left(\frac{1}{8R}\right) \ , \tag{25a}$$

or

$$\delta\theta = - \frac{\delta S'}{8R} \ . \tag{25b}$$

Substituting θ and $\delta\theta$ into Equation 20, then

$$\frac{\delta a_o}{a_o} = \frac{\delta S'}{8R} \cot\left(\frac{\pi}{2} - \frac{S'}{8R}\right) \ , \tag{26}$$

and

$$\frac{\delta a_o}{a_o} = \frac{\delta S'}{8R} \tan\left(\frac{S'}{8R}\right) \ . \tag{27}$$

Since $\frac{S'}{\delta R}$ is small then $\tan\left(\frac{S'}{\delta R}\right) \approx \frac{S'}{\delta R}$, and the final form becomes

$$\delta a_o = \frac{(\delta S')(S')a_o}{(\delta R)^2} \quad . \tag{28}$$

Substituting the value for R (60.00 mm) in Equation 28, the above equation becomes

$$\delta a_o = \frac{(\delta S')(S')a_o}{23 \times 10^4} \quad . \tag{29}$$

Debye-Scherrer Camera

The case for the Debye-Scherrer camera is quite similar except for the relationship between S' and β. From Figure 41 it is seen that

$$S' = 2\beta R \quad . \tag{30}$$

Following the same reasoning as in the case of the back reflection camera, Equations 22 to 28, the final form becomes

$$\delta a_o = \frac{(\delta S')(S')a_o}{(4R)^2} \quad . \tag{31}$$

Substituting the value for R (57.295 mm) into Equation 31 we have

$$\delta a_o = \frac{(\delta S')(S')a_o}{3.6 \times 10^4} \quad . \tag{32}$$

APPENDIX II: X-RAY DIFFRACTION DATA FOR THE RARE EARTH CARBIDES, INTERPLANAR SPACINGS

Table 27. The tri-rare earth carbides, carbon-rich side

hkl	Sm	Gd	Tb	Dy	Ho
111	2.964	2.964	2.932	2.893	2.886
200	2.605	2.584	2.554	2.520	2.510
220	1.816	1.817	1.798	1.775	1.778
311	1.569	1.555	1.541	1.511	1.522
222	1.493	1.491	1.474	1.456	1.459
400	———	———	1.285	1.263	1.264
331	1.185	1.182	1.173	1.158	1.153
420	1.156	1.153	1.143	1.128	1.128
422	1.064	1.058	1.044	1.039	1.031
511, 333	0.99721	0.98613	0.98352	0.97732	0.97270
440	———	.90317	———	———	.89248
531	.87513	.86602	.86400	.86370	.85345
600, 442	.86075	.85374	.85022	.84432	.84210
620	———	———	.80749	.80358	.80053
533	———	———	———	———	———
622	———	———	———	***	***
	***	***	***		

hkl	Er	Tm	Yb	Lu	Y
111	2.906	2.904	2.871	2.848	2.942
200	2.514	2.490	2.489	2.469	2.549
220	1.778	1.756	1.762	1.746	1.804
311	1.517	1.513	1.505	1.492	1.538
222	1.452	1.433	1.440	1.430	1.472
400	1.260	1.248	1.247	1.241	1.278
331	1.153	1.149	1.144	1.138	1.170
420	1.125	1.116	1.115	1.109	1.141
422	1.026	1.028	1.017	1.011	1.040
511, 333	0.96816	0.96509	0.95881	0.95365	0.98067
440	.88798	.88385	.88083	.87696	.89973
531	.84932	.84749	.84327	.83820	.86082
600, 442	.83776	.83293	.83168	.82689	.84973
620	.79512	.79246	.78925	.78440	.80591
533	***	***	***	***	***

Table 28. The rare earth sesquicarbides, the carbon-rich side

hkl	La	Ce	Pr	Nd	Sm
211	3.581	3.427	3.523	3.469	3.509
220	3.108	2.962	3.039	3.003	2.982
310	2.781	2.663	2.712	2.670	2.650
321	2.343	2.249	2.300	2.275	2.253
400	2.195	2.112	———	2.129	2.111
332	1.877	1.794	1.834	1.818	1.793
422	1.794	1.718	1.756	1.742	1.718
510, 431	1.724	1.652	1.684	1.670	1.654
521	1.608	1.539	1.572	1.556	1.538
440	1.558	———	———	———	———
530	1.510	1.446	———	1.463	1.451
611, 532	1.429	1.368	1.395	1.384	1.369
620	1.392	1.335	1.356	1.348	1.333
541	1.358	1.301	1.327	1.318	1.301
631	1.298	1.245	1.266	1.258	1.243
444	1.271	1.217	1.239	1.233	1.216
710, 543	1.246	1.194	1.216	1.208	1.193
721, 633	1.198	1.147	1.170	1.161	1.148
642	1.177	1.127	1.147	1.141	1.126
730	1.158	1.108	1.130	———	1.104
732, 651	1.119	1.072	1.092	———	1.069
800	1.100	1.055	1.076	———	1.053
741	1.084	1.039	1.058	1.051	1.034
653	1.052	1.008	———	1.018	1.005
822, 660	1.037	0.99479	1.015	1.006	0.99112
831, 750, 743	1.024	.98175	0.99821	0.99253	.97839
752	0.99778	.95597	———	.96700	———
840	.98503	———	———	———	———
910	.97114	.93217	———	.94600	———
921, 761, 655	.95040	.91115	.92615	.92124	.90796
664	.93903	.90039	.91696	.91085	.89784
930, 851, 754	.92919	.89049	.90737	.90078	.88744
932, 763	.90945	.87131	.88851	.88083	.86844
844	.89926	.86165	———	.87219	.85955
941, 853	.89003	.85302	———	.86516	.85043

Table 28. (Continued)

hkl	La	Ce	Pr	Nd	Sm
10.11,772	.87333	.83571	.85190	.84613	.83413
10.20,862	.86462	.82802	.84379	.83814	.82610
950, 943	.85661	.82031	.83596	.83051	.81834
10.31,952, 765	.84074	.80488	.82052	.81492	.80332
871	.82560	.79109	———	.80034	———
10.33,961	.81189	.77761	.79226	.78682	———
10.42	.80497	———	.78432	———	***
11.10,954 873	.79832	***	.77928	***	
11.21,10.51, 963	.78550		———		
880	.77935		***		
11.30,970	.77333 ***				

hkl	Gd	Tb	Dy[a]	Ho
211	3.404	3.343	3.336	3.326
220	2.936	2.899	2.891	2.866
310	2.618	2.593	2.584	2.553
321	2.221	2.198	2.183	2.172
400	2.073	2.058	———	———
332	1.771	1.756	1.738	1.732
422	1.698	1.678	1.668	1.664
510, 431	1.632	1.615	1.603	1.599
521	1.518	1.503	1.493	1.490
440	———	———	———	———
530	1.427	1.412	1.400	———
611, 532	1.350	1.337	1.327	1.322
620	1.314	1.300	1.293	———
541	1.285	1.272	1.260	1.259
631	1.226	1.214	1.205	———
444	1.203	1.189	1.179	———
710, 543	1.178	1.166	1.157	———
721, 633	1.135	1.122	1.113	1.109
642	———	1.102	1.095	1.092
730	———	1.084	1.074	1.074

[a]Data for the dysprosium-rich side of dysprosium sesquicarbide.

Table 28. (Continued)

hkl	Gd	Tb	Dy[a]	Ho
732, 651	1.058	1.046	1.040	1.038
800	1.041	1.031	1.024	1.020
741	1.026	1.016	———	1.004
653	0.99550	0.98667	0.97732	0.97692
822, 660	.98175	.97218	.96294	.96281
831,750, 743	.96867	.95918	———	.94849
752	.94400	.93406	———	———
840	———	———	———	———
910	.92113	———	———	.90212
921,761, 655	.89840	.89066	.88194	.88161
664	.88842	.87999	———	.87034
930,851, 754	.87872	.86995	———	.86060
932, 763	.85963	.85133	.84453	.84222
844	.85147	.84275	.83571	———
941, 853	.84190	.83474	.82734	.82471
10.11, 772	.82555	.81787	———	———
10.20, 862	.81797	.81003	.80362	.80157
950, 943	.81026	.80230	.79620	———
10.31,952, 765	.79538	.78760	.78153	.77908
871	.78119	———	***	***
	***	***		

Table 29. The rare earth dicarbides

hkl	La	Ce	Pr	Nd	Sm	Gd	Tb
101	3.373	3.300	3.304	3.264	3.215	3.171	3.162
002	3.278	3.204	3.218	3.179	3.146	3.106	3.099
110	2.776	2.722	2.718	2.685	2.645	2.609	2.600
112	2.122	2.072	2.075	2.054	2.032	2.008	1.994
200	1.967	1.929	1.926	1.902	1.879	1.850	1.842
103	1.910	1.878	1.866	1.855	1.834	1.814	1.802
211	1.691	1.669	1.663	1.643	1.622	1.599	1.591
202	1.684	1.656	1.652	1.637	1.615		1.585
004	1.640	1.614	1.621	1.598	1.578	1.563	———
114	1.412	1.392	1.382	1.374	1.357	1.343	1.333
220	1.388	1.366	1.361	1.349	1.330	1.313	1.304
213	1.369	1.349	1.340	1.332	1.314	1.297	1.291
301	1.282	1.260	1.255	1.244	1.227	1.210	1.204
222							———
204	1.260	1.242	1.232	1.225	1.212	1.195	
105	1.244	1.226	1.217	1.211	1.197	1.186	1.176
310				1.207	1.188	1.172	1.164
312	1.166	1.145	1.138	1.129	1.116	1.097	1.091
303	1.124	1.108	1.100	1.092	1.076	1.062	1.056
006	1.093	1.080	———	1.067	———	1.046	1.049
321	1.074	1.059	1.053	1.044	1.030	1.017	1.010
224	1.060	1.045	———	1.031	———	1.009	0.99980
215	1.053	1.037	1.030	1.023	1.011	1.002	.99197
116	1.017	1.004	0.99650	0.99154	0.97933	0.97192	.96118
314	0.99043	0.97599	.96971	.96306	.95160	.94238	.93106
400	———	.96881	———	.95353	———	———	———
323	.97467	.96105	.95523	.94753	.93317	.92529	.91624
206	———	.94284	.93597	.93040	.91956	.91338	———

Table 29. (Continued)

hkl	La	Ce	Pr	Nd	Sm	Gd	Tb
411	} .94192	.92963	} .92283	} .91531	} .90317	} .89184	.88603
402		.92876					———
305	} .92604	} .91327	} .90678	} .90039	} .88958	.88169	———
330						.87638	.86995
107	.91085	.90058	.89367	.88878	.87805	.87139	.86508
332	.89266	.87922	.87236	.86632	.85509	.84473	.83889
420	.88126	.86710	.86090	.85381	.84203	.83145	.82527
413	.87513	.86188	.85596	.84980	.83751	.82785	———
226	.85933	.84925	.84229	.83677	———	.81880	———
422	.84987	.83770	.83162	.82515	.81859	.80433	.79734
404	———	.83263	.82655	———	———	———	———
325	.83997	.82773	.82179	.81641	.80536	.79719	.78916
217	.82877	.81717	.81100	.80622	.79613	.78874	.78075
316	} .82237	} .81090	} .80463	.80025	} .79028	———	———
008				———		———	———
334	.80920	.79617	.79067	.78520	———	***	***
118	.78819	.77759	———	———	***		
501	.78128	***	***	***			
422	.77294						
	***						

hkl	Dy	Ho	Er	Tm	Yb	Lu	Y
101	3.131	3.106	3.097	3.085	3.101	3.035	3.144
002	3.060	3.037	3.027	3.019	3.021	2.929	3.076
110	2.571	2.552	2.547	2.533	2.547	2.505	2.587
112	1.975	1.963	1.952	1.945	1.950	1.919	1.982
200	1.827	1.812	1.807	1.798	1.792	1.779	1.829

Table 29. (Continued)

hkl	Dy	Ho	Er	Tm	Yb	Lu	Y
103	1.785	1.774	1.771	1.755	1.767	1.730	1.789
211	1.573	1.563	1.561	1.575	1.559	1.532	1.578
202			1.556	1.548		1.526	
004	1.530	1.530	1.521	1.510	1.520	1.487	1.541
114	1.318	1.313	1.307	1.298	1.298	1.278	1.323
220	1.293	1.283	1.278	1.271	1.278	1.257	1.293
213	1.277	1.269	1.264	1.256	1.266	1.241	1.279
301	1.190	1.186	1.180	1.173	1.182	1.161	1.195
222							
204	1.177	1.172	1.165	1.158	———	1.142	1.180
105	1.163	1.160	1.153	1.146	1.155	1.126	1.168
310	1.155	1.149	1.142	1.138	1.145		1.157
312	1.082	1.076	1.072	1.063	———	1.053	1.084
303	1.048	1.042	1.036	1.030	1.038	1.019	1.050
006	———	1.019	1.014	0.99851	1.016	———	———
321	1.000	0.99493	0.99029	.98462	0.99309	0.97310	1.002
224	———	———	.97920	.98257	———	.96193	———
215	0.98230	.97826	.97218	.97362	.97481	.95341	0.98420
116	.95341	.94872	.94354	.93733	.94541	———	.95512
314	.92465	.91925	.91409	.90995	.91768	.89850	.92626
400	.91686	———	.90472	.90058	———	———	.91522
323	.90985	.90434	.89888	.89458	.90356	.88393	.91035
206	.89385	.89066	.88463	.87999	.88673	.86625	.89662
411	.88789	———	.86758	.86309	.87139	.85423	.87956
402		.87244		———		———	.87889
305	———	.86363	.85771	.84857	———	———	.86789
330	.86340	.85911	.85288	.84640	.85625	.83915	.86332

Table 29. (Continued)

hkl	Dy	Ho	Er	Tm	Yb	Lu	Y
107	.85509	.85302	.84593	.83966	.84781	———	.85705
332	.83168	.82455	.82115	.81701	.82324	.80829	.83132
420	.81952	.81497	.80929	.80536	———	.79649	.81921
413	.81601	.81184	.80570	.80165	.81058	.79260	0.81571
226	———	———	———	.79003	———	———	.80617
422	.79240	.78736	.78237	———	.78464	***	.79206
404	———	———	———	———	———		———
325	.78522	.77917	———	***	***		.78464
		***	***				
217	.77717						.77647
316	———						***
	***						